M

MACHINE VISION

See *Visible and Thermal Images for Fruit Detection*

MACHINE VISION IN AGRICULTURE

John Billingsley
University of Southern Queensland, Toowoomba, QLD, Australia

Definition

Machine vision: Visual data that can be processed by a computer, including monochrome, color and infra red imaging, line or spot perception of brightness and color, time-varying optical signals.
Agriculture: Horticulture, arboriculture and other cropping methods, harvesting, post production inspection and processing, livestock breeding, preparation and slaughter.

Introduction

The combination of low-cost computing power and applications that target its use for entertainment has led to a readily available platform for analyzing vision signals in a variety of ways. Applications are many and various, but some of the most potentially significant ones are found in agriculture.

Sorting by color

For some decades, a simplified form of machine vision has been used for sorting produce (Tao et al., 1995). Tomatoes may be picked green for ripening in the shed. When their color is changing, they ride a conveyor that has pockets for individual fruit. These holders can be tripped by a computer signal, to eject the tomato at one of many packing stations corresponding to the degree of ripeness, as defined by color.

A very similar system is used for grading apples, as seen in Figures 1 and 2.

Fragments of nut shell can be detected when pecan nuts are shelled, once again by detection of the color. Kernels fall through the inspection area at a speed of around one meter per second. In an early system, light that was reflected from the kernel was split between two photocells that detected the intensity of different wavelengths. The ratio enabled color to discriminate between nut and shell. More recent versions incorporate laser scanning. As the nut falls further, a jet of air is switched to deflect any detected shell into a separate bin.

Detection of weeds

Color discrimination can also be used in the field to discriminate between plants and weeds for the application of selective spraying (Åstrand and Baerveldt, 2002; Zhang et al., 2008). It is possible for the color channels of the camera to include infra-red wavelengths, something that can be achieved by removing the infra-red blocking filter from a simple webcam. Figure 3 is a low-resolution frame-grab showing one stage in the detection of a grass-like weed, "panic," during trials in sugar cane. The computer has marked pixels determined to be "weed" in yellow.

Quality assessment

True machine vision concerns shape information. One example is the assessment of fodder quality. From a webcam image of a sample handful of hay, the stem-widths can be measured and a histogram displayed. Color can also be determined by comparison of the video signal against that from the image of a calibration card. This makes an objective standard possible, to achieve agreement between vendor and purchaser (Dunn and Billingsley, 2007).

Shape information can also be used to monitor the growth of a crop, measuring stem length between nodes automatically (McCarthy et al., 2008).

Jan Gliński, Józef Horabik & Jerzy Lipiec (eds.), *Encyclopedia of Agrophysics*, DOI 10.1007/978-90-481-3585-1,

Machine Vision in Agriculture, Figure 1 Apples moving towards washing and grading.

Machine Vision in Agriculture, Figure 2 A conveyor automatically ejects each apple at the correct station.

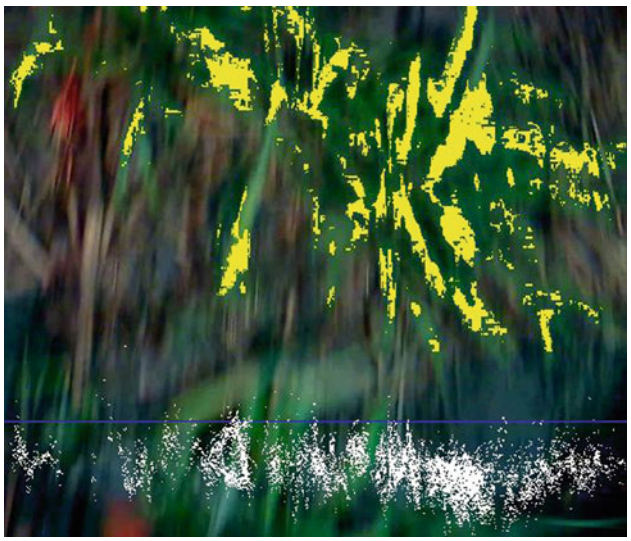

Machine Vision in Agriculture, Figure 3 A frame-grab from the computer-processing of image data to locate weeds.

Livestock identification

A more detailed version of shape information, in the form of an s-psi profile, has been used to discriminate between animals of different species passing a checkpoint while they approach a watering place. Now the image represents the profile of the animal as seen against a background. A blue background simplifies discrimination for producing a silhouette. From this a boundary can be found by edge-tracing, which yields a sequence of incremental

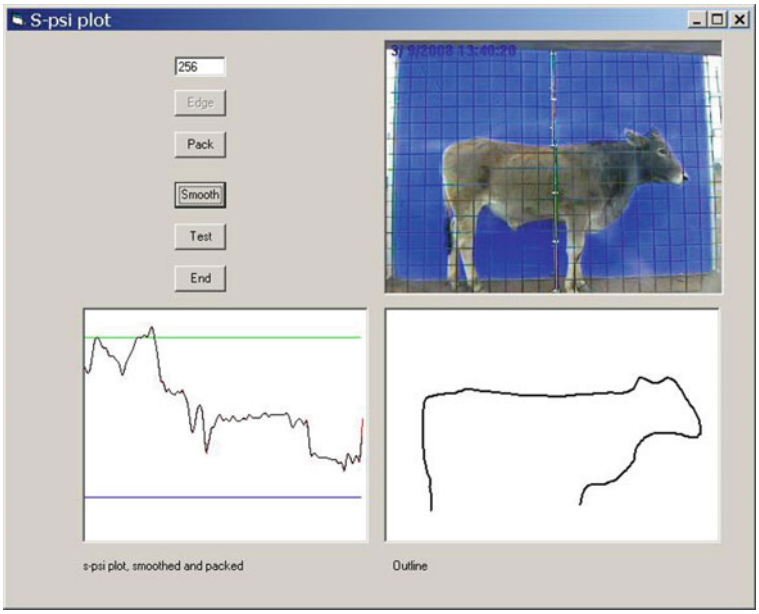

Machine Vision in Agriculture, Figure 4 S-psi plot of the outline of a steer.

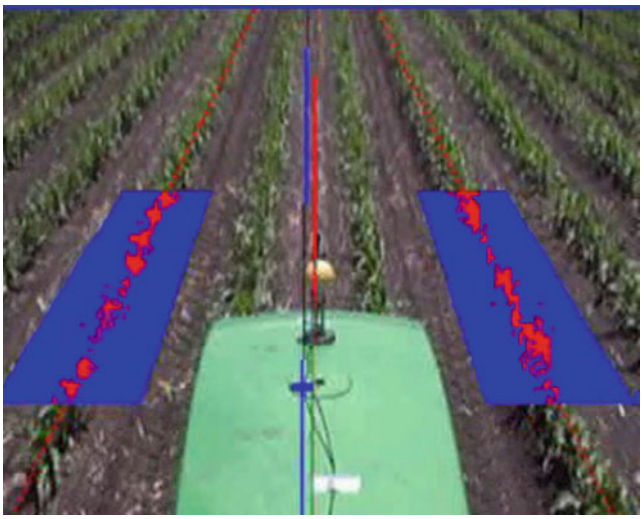

Machine Vision in Agriculture, Figure 5 Frame-grab from the video image that is steering a tractor at speed.

vectors that form a "Freeman chain." These in turn deliver a sequence of tangent angles, to be plotted against the distance travelled around the circumference of the silhouette, as seen in Figure 4.

From the original megabyte image, some 256 bytes of data now define the shape of the animal in view, for correlating against a set of templates to separate sheep from goats or camels from cattle. A gate is then driven to exclude or to draft the animals. This work is being refined to assess the condition of cattle as they pass a point where their RFID tag can be read, to monitor their progress towards "harvesting."

Picking

Many attempts have been made over the years to use machine vision to detect and locate fruit for automatic picking. Although positive research results have been reported, operational speeds are generally low and there has been very limited commercial success. It has been suggested that the growing availability of broadband communication can make it possible for "armchair pickers" to tele-operate picking machinery, with the aid of real-time imaging.

Machine guidance

Vision guidance has been applied with great technical success to tractors (Billingsley and Schoenfisch, 1996). Within each received image, the software locates the rows of crop and assesses the control action needed to bring the vehicle back on course. The algorithms were developed in the early 1990s, when computing power was much less plentiful. The result is a robust strategy that can time-share with GPS analysis and other signal processing.

Within the field of view, "keyholes" are defined that will each contain the image of a single row. Within each keyhole, plant images in the form of green pixels are regarded as data points through which to construct a regression line. For the next image, the keyholes are moved to be centered on these regression lines. The set of two or three keyholes move at once to indicate the vanishing point, from which the heading error and the lateral displacement can be deduced. These signals then give a steering command to bring the tractor back on track, to

an accuracy of a centimeter or two. A frame-grab from the steering software is shown in Figure 5.

The method is greatly superior to the use of GPS, satellite navigation, since an operation such as cultivating will cut the ground at a point relative to the actual location of the plants, not relative to where the plants are supposed to have been planted.

It is unfortunate that marketing of the system started when enthusiasm for GPS was reaching fever pitch and success has passed it by. Nevertheless research on vision guidance is widespread (Gottschalk et al., 2008).

Conclusions

As sensors and computing power become ever cheaper, the opportunity for farm robotics increases. It would be unwise to make a large machine autonomous, not least for insurance against the damage it might cause. Small robot machines, however, can already be equipped with vision, navigation, detection and communication systems at a very modest price. We may very soon see teams of "Autonomous Robot Farmhands" at work in the field.

Bibliography

Åstrand, B., and Baerveldt, A.-J., 2002. An agricultural mobile robot with vision-based perception for mechanical weed control. *Journal Autonomous Robots*, **13**(1), 21–35.

Billingsley, J., and Schoenfisch, M., 1996. The successful development of a vision guidance system for agriculture. *Computers and Electronics in Agriculture*, **16**(2), 147–163.

Dunn, M., and Billingsley, J., 2007. The use of machine vision for assessment of fodder quality. In *Proceedings of the 14th International Conference on Mechatronics and Machine Vision in Practice*, Xiamen, PRC, 3–5 December 2007, pub IEE ISBN 1-4224-1357-5, pp. 179–184.

Gottschalk, R., Burgos-Artizzu, X. P., Ribeiro, A., Pajares, G., and Sainchez-Miralles, A., 2008. Real-time image processing for the guidance of a small agricultural field inspection vehicle. In *Proceedings Mechatronics and Machine Vision in Practice, 2008*. pp. 493–498

McCarthy, C. L., Hancock, N. H., and Raine, S. R., 2008. On-the-go machine vision sensing of cotton plant geometric parameters: first results. In Billingsley, J., and Bradbeer, R. S. (eds.), *Mechatronics and Machine Vision in Practice*. New York: Springer-Verlag, pp. 305–312.

Tao, Y., Heinemann, P. H., Varghese, Z., Morrow, C. T., and Sommer, H. J., III, 1995. Machine vision for color inspection of potatoes and apples. *Transactions of the ASAE*, **38**(5), 1555–1561.

Zhang, Z., Kodagoda, S., Ruiz, D., Katupitiya, J., and Dissanayake, G., 2008. Classification of bidens in wheat farms. In *Proceedings of Mechatronics and Machine Vision in Practice,* 2008, pp. 505–510.

MACROPORE FLOW

Synonyms

Funnel flow; Preferential flow

See *Bypass Flow in Soil*

MAGNETIC PROPERTIES OF SOILS

Andrey Alekseev
Laboratory Geochemistry and Soil Mineralogy, Institute of Physicochemical and Biological Problems of Soil Science, Russian Academy of Sciences, Pushchino, Moscow Region, Russia

Synonyms

Environmental magnetism; Soil magnetism

Definition

Magnetic properties of soils are dominantly controlled by the presence, volumetric abundance, and oxidation state of iron in soils. Different types of Fe oxides, Fe–Ti oxides, and Fe sulfides are the predominant causes of magnetic soil characteristics. The concentration of magnetic Fe oxides in soils is affected by the parent material and soil-forming factors and processes.

Introduction

Magnetism is a fundamental property of all natural materials. The most important kinds of magnetic properties are those called diamagnetism, paramagnetism, ferromagnetism, ferrimagnetism, and superparamagnetism. The magnetic properties of soils are a subject of investigation started first more than 50 years ago (Le Borgne, 1955). Magnetism of soils have traditionally been investigated in the environmental science and geophysics communities to indicate soil development, paleosols and climate change, pollution, and as tools for archaeological mapping and prospecting (Thompson and Oldfield, 1986; Maher and Thompson, 1999; Evans and Heller, 2003; Maher, 2008).

Soil magnetics

The magnetic characteristics of soil and sediments reflect the amount and quality of ferruginous minerals they contain and are connected with their content, mineralogy, and the grain size. The presence of Fe oxides in different forms and quantities is the predominant cause of the magnetic properties of soils. Iron oxide minerals can be both pedogenic (product of soil formation) and lithogenic (unweathered minerals from the parent material) in origin. Iron is the most common element in the crust of the earth. Iron is not only essential to plant development, but it also participates in the formation of complexes of clay and organic matter, which in turn influence soil structure and fertility. Iron-containing minerals can be found in igneous, metamorphic, and sedimentary rocks. As a rule, clay minerals possess paramagnetic properties. The most widespread minerals of sedimentary rocks and soils quartz, carbonates, feldspars are diamagnetic or weak paramagnetic and also do not bring the appreciable contribution to the magnetic behavior of soils. Hydrated Fe oxides like goethite, which is the most abundant Fe oxide in soils around the world, ferrihydrite, and lepidocrocite play

a minor role in determining the magnetic character of soils. The concentration of (magnetic) Fe oxides in soils is affected by the parent material, soil age, soil-forming processes, biological activity, and soil temperature (Singer et al., 1996). In soils, primary ferromagnetic minerals of detrital origin derive from the disintegration of the bedrock and they reflect its mineralogy. Secondary minerals are formed through complex chemical and biological processes, which also depend on climate and the soil pH, humidity, and organic matter content. These processes operate not only on primary ferromagnetic minerals, but also on the elementary iron contained in many silicates. Depending on the parent material, the physicochemical conditions and the pedogenetic processes, goethite, hematite, maghemite, or magnetite can be formed. Mineralogically, by soil magnetism point of view, the most important ingredients are magnetite (Fe_3O_4), maghemite (γ-Fe_2O_3), and hematite (α-Fe_2O_3). The main properties and pathway of formation of these minerals are discussed in many books and review papers (Thompson and Oldfield, 1986; Cornell and Schwertmann, 2003; Mullins, 1977; Schwertmann, 1988). The nature, content, and grain size of each magnetic phase reflect the physicochemical conditions of the soil. For example, magnetic susceptibility enhancement in topsoil is found in most temperate soils (Le Borgne, 1955; Babanin, 1973; Maher, 1986; Alekseev et al., 1988), except in acidic, podzolic, and waterlogged conditions (Maher, 1998); it can be related to soil conditions at the surface. Magnetic minerals, which occur in very small concentration in most soils, are as fingerprints of pedological processes. At present, several theories are put forward to explain the concentration and distributions of the ferrimagnetic minerals in soils: burning, biotic transformation of hydrous ferric oxides; abiotic transformation of hydrous ferric oxides; residual primary minerals; magnetotactic bacteria; anaerobic dissimilatory bacteria; and atmospheric contamination and pollution. Environmental magnetic studies have revealed that a range of ferrimagnetic minerals can be formed at Earth surface temperatures and pressures within soils and sediments, rather than merely "inherited" from disintegration and weathering of magnetic mineral-bearing igneous rocks. Notably, trace concentrations of nanoscale magnetite can be precipitated in situ in the soil matrix of well-drained, generally oxidizing, near-neutral soils (Maher, 2008). The generally accepted view is that most soils produce secondary nanoscale iron oxides magnetite/maghemite in surface horizons (Maher 1998; Alekseev et al., 2003; Maher et al., 2003; Blundell et al., 2009). The magnetic research techniques are express which allow producing the mass analysis in comparison with other methods. Magnetic methods have many advantages over other techniques: nearly all rocks and soils contain magnetic iron oxides/sulfides, sample preparation and measurement is quick, easy and generally nondestructive, and the methods are sensitive to both concentration and grain-size – particularly for ultrafine grains, which can be difficult to detect by other means.

Magnetic parameter and instrumentation

To describe magnetic properties of soil, different types of magnetization are commonly used.

Magnetic susceptibility – when a low-intensity magnetic field is applied to a material, the net magnetic moment (magnetization, M) is proportional to the applied field strength (H). Therefore, the low-field magnetic susceptibility, which is defined as M/H and expressed per unit volume (κ) or per unit mass (χ), is a material-specific property. Magnetic susceptibility (χ) reflects the total concentration of ferrimagnetic or total concentration of paramagnetic minerals and antiferromagnetic with low content of ferromagnetics. A magnetic susceptibility (χ) is one of most simply obtained magnetization characteristics and rather large set of the data on the application of this parameter for the problems of soil science exists.

Remanent magnetization occurs within ferromagnetic and ferromagnetic minerals and exists in the absence of an applied field.

Viscous remanent magnetization refers to the delay of the secondary magnetic field relative to the primary magnetic field and has been linked to the presence of superparamagnetic grains of iron oxides.

Four laboratory instruments make up the basic requirements for magnetic characterization of environmental samples and soils: a susceptibility bridge (preferably dual frequency); a magnetometer; magnetizing coils; and a demagnetizer. These magnetic techniques are nondestructive and sensitive to trace amounts of magnetic minerals (Thompson and Oldfield, 1986; Maher and Thompson, 1999; Maher, 2008).

The magnetic properties of soils typically have been studied using the following equipment as example: – magnetic susceptibility (χ) – MS 2 Bartington or Kappameter KT-5-9 (field measurements), Kappabridges (2–4) (laboratory measurements); frequency – dependent magnetic susceptibility (χ_{fd}) – MS 2 Bartington; curves of saturation magnetizations (IRM) in magnetic fields with strength up to 1–4 T – Molspin magnetometer and Molspin pulse magnetizer; anhysteretic remanent magnetization (ARM) – complex of the equipment included Molspin demagnetizer and Molspin magnetometer; complete magnetization curves (hysteresis curve) – vibrating sample magnetometer-VSM Molspin (Table 1).

Soil magnetism applications

Present instruments and methods enable very sensitive determination of low concentrations of strong ferrimagnetic minerals in soils. Possible mechanisms of magnetic enhancement of soils due to increased concentrations of secondary ferrimagnetic minerals are discussed above. Herewith, we will outline some examples of application of magnetic study of the soils. Magnetic properties measurements of soils are mostly used for three purposes: to read the climatic signal recorded by palaeosols, to identify pollution in soils, and as tools for archaeological mapping and prospecting.

Magnetic Properties of Soils, Table 1 Magnetic parameters and their interpretation (Thompson and Oldfield, 1986; Maher and Thompson, 1999; Evans and Heller, 2003; Maher, 2008)

χ (10^{-8} m^3 kg^{-1})	Magnetic susceptibility (χ or χ_{lf}) – total concentration of ferrimagnetic or total concentration of paramagnetic minerals and antiferromagnetic by low content of ferrimagnetic
χ_{fd} %-	Frequency-dependent magnetic susceptibility. Is calculated on a difference of measurements at different frequencies (for MS2 460 χ_{lf} and 4,600 Hz χ_{hf} accordingly): $(\chi_{fd})\% = (\chi_{lf} - \chi_{hf})/\chi_{lf} \times 100$ Reflects the presence of ultrafine ferrimagnetic grains. Is especially sensitive to the size of particles in an interval 0.015–0.025 μm
χARM ($10^{-8}m^3kg^{-1}$)	Susceptibility of anhysteretic remanent magnetization (ARM). Maximum intensity of the alternating field used in the instrument Molspin demagnetizer for magnetization −100 mT, with step of decrease of a magnetic field for each cycle 0.016 mT, strength of the constant biasing field −0.08 mT. It is high sensitive to ferrimagnetic with the size of particles in an interval 0.02–0.4 μm. Reflects the presence of fine-grained magnetite (stable single domain grains)
χARM/SIRM (m A^{-1})	The ratio is sensitive to grain-size changes of ferrimagnetics. For superparamagnetic particles the significances in an interval −0.5 to 1.5 are characteristic, for stable single domain particles 1.8–2.0
IRM_{100mT}/SIRM	Allows evaluating the contents of ferrimagnets (magnetite, maghemite). As the majority of ferrimagnetic is fully saturated in fields of 100 mT
SIRM-IRM_{300mT}	Can be used for approximating the total concentration of high coercitivity minerals (hematite + goethite) Remanence acquired in a field of 1T is referred as SIRM (SIRM = $IRM_{1,000mT}$). It is necessary to note that the full saturation for antiferromagnetic phases can be reached at fields strength above 4 T

As example, recently, a quantitative, soil magnetism-based climofunction has been established for the area of the Russian steppe (Maher et al., 2002; Maher et al., 2003). A similar correlation between rainfall and magnetic susceptibility was previously obtained for the Chinese Loess Plateau and explained as a result of pedogenic formation of magnetite and maghemite via oxidation/reduction processes through soil wetness events (Maher and Thompson, 1999).

The pedogenic magnetic response of these well-drained, near-neutral, Russian steppe soils appears strongly correlated with that of the similarly well-drained and buffered modern soils across the Chinese Loess Plateau (and across the wider Northern Hemisphere temperate zone). Such correlation suggests that the rainfall component of the climate system is a key influence on soil magnetic properties in both these regions. This direct coupling of the soil magnetism of modern soils with present-day climate substantiates the use of magnetic climofunctions to make quantitative estimates of past rainfall variations from the magnetic properties of buried palaeosols for both the Russian steppe and the Chinese Loess Plateau.

Applying a soil magnetism climofunction, calculated from a modern-day soil training set, to each set of buried soils enables quantitative estimation of precipitation at each time step when soil burial occurred as for Holocene paleosols or loess-paleosols sequences of Pleistocene (Alekseeva et al., 2007).

Atmospherically deposited ferrimagnetic particles of anthropogenic origin also contribute a great deal to the concentration-dependent magnetic properties of top soils, such as low-field magnetic susceptibility. The highest concentration of anthropogenic ferrimagnetic particles is usually found in humic layers (e.g., Strzyszcz et al., 1996). Practically all industrial fly ashes contain a significant fraction of ferromagnetic particles, the most important sources being fly ashes produced during combustion of fossil fuel (Hanesch and Scholger, 2002; Kapička et al. 2003). Other sources, such as iron and steel works, cement works; public boilers and road traffic also contribute to contamination by anthropogenic ferrimagnetics (Heller et al., 1998; Scholger, 1998; Hoffmann et al., 1999). In contrast to particles of pedogenic origin, anthropogenic ferrimagnetics are characterized by specific morphology and distinct magnetic properties. They are often observed in the form of spherules, with the magnetic phase frequently sintered on aluminum silicates or amorphous silica. Prevailing ferrimagnetic phases are Fe oxides, namely magnetite and maghemite, with Fe ions very often substituted by other cations (Strzyszcz et al., 1996). Application of the comparatively simple technique of measuring magnetic susceptibility enables delineation of areas with concentrations of deposited anthropogenic ferrimagnetics significantly above background values. Magnetic mapping thus represents a rapid, sensitive, and cheap tool for targeting the areas of interest. These studies showed that in polluted areas, the magnetic susceptibility of surface soil layers is considerably higher. Recently, rock-magnetic methods have been applied to modern soils in several environmental studies (for an overview see, e.g., Petrovský and Ellwood, 1999). Measurements of low-field magnetic susceptibility of surface soils have been applied recently around local pollution sources and at a larger, regional scale, areas in Poland and Great Britain and Austria have been investigated (Strzyszcz et al., 1996; Heller et al., 1998; Hanesch and Scholger, 2002; Magiera et al., 2006).

Summary

In a course of soil formation, the change of magnetic properties of soils in comparison with parent material takes place. The amplitude of these changes depends on the factors of soil formation. Generally, the conditions of transformation of iron-containing minerals result in enhancement of the contents of ferric oxides in soils. The analysis of magnetic properties of zonal soils shows that the behavior of soil magnetics in profile reflects genetic properties of soils at the soil type level and

connected with distribution and state of iron minerals in soils and landscapes. Atmospherically deposited ferrimagnetic particles of anthropogenic origin also contribute a great deal to the concentration-dependent magnetic properties of top soils. Magnetic properties measurements of soils are mostly used for three purposes: to read the climatic signal recorded by palaeosols, to identify pollution in soils, and as tools for archaeological mapping and prospecting. The definition of soil magnetism as a genetic parameter, which is able together with other soil properties to be used for diagnostics of soil looks to be useful and important. Magnetic methods have many advantages over other techniques: sample preparation and measurement is quick, easy and generally nondestructive, and the methods are sensitive to both concentration and grain-size – particularly for ultrafine grains, which can be difficult to detect by other means. Hence, magnetic analyses of soils provide an additional, sensitive window on soil iron.

Bibliography

Alekseev, A. O., Kovalevskaya, I. S., Morgun, E. G., and Samoylova, E. M., 1988. Magnetic susceptibility of soils in a catena. *Soviet Soil Science (Pochvovedenie)*, **8**, 27–35.

Alekseev, A. O., Alekseeva, T. V., and Maher, B. A., 2003. Magnetic properties and mineralogy of iron compounds in steppe soils. *Eurasian Soil Science*, **36**, 59–70.

Alekseeva, T., Alekseev, A., Maher, B. A., and Demkin, V., 2007. Late Holocene climate reconstructions for the Russian steppe, based on mineralogical and magnetic properties of buried palaeosols. *Palaeogeography, Palaeoclimatology, Palaeoecology*, **249**, 103–127.

Babanin, V. F., 1973. The use of magnetic susceptibility in identifying forms of iron in soils. *Soviet Soil Science (Pochvovedenie)*, **5**, 487–493.

Blundell, A., Dearing, J. A., Boyle, J. F., and Hannam, J. A., 2009. Controlling factors for the spatial variability of soil magnetic susceptibility across England and Wales. *Earth-Science Reviews*, **95**, 158–188.

Cornell, R. M., and Schwertmann, U., 2003. *The Iron Oxides*. Weinheim: Wiley-VCH.

Evans, M. E., and Heller, F., 2003. *Environmental Magnetism: Principles and Applications of Enviromagnetics*. San Diego: Academic.

Hanesch, M., and Scholger, R., 2002. Mapping of heavy metal loadings in soils by means of magnetic susceptibility measurements. *Environmental Geology*, **42**, 857–870.

Heller, F., Strzyszcz, Z., and Magiera, T., 1998. Magnetic record of industrial pollution in forest soils of Upper Silesia, Poland. *Journal of geophysical research*, **103**, 17767–17774.

Hoffmann, V., Knab, M., and Appel, E., 1999. Magnetic susceptibility mapping of roadside pollution. *Journal of Geochemical Exploration*, **66**, 313–326.

Kapička, A., Jordanova, N., Petrovský, E., and Podrázský, V., 2003. Magnetic study of weakly contaminated forest soils. *Water, Air and Soil Pollution*, **148**, 31–44.

Le Borgne, E., 1955. Susceptibilité magnetique anormale du sol superficiel. *Annales de Geophysique*, **11**, 399–419.

Magiera, T., Stryszcz, Z., Kapička, A., and Petrovský, E., 2006. Discrimination of lithogenic and anthropogenic influences on topsoil magnetic susceptibility in Central Europe. *Geoderma*, **130**, 299–311.

Maher, B. A., 1986. Characterisation of soils by mineral magnetic measurements. *Physics of the Earth and Planetary Interiors*, **42**, 76–92.

Maher, B. A., 1998. Magnetic properties of modern soils and Quaternary loessic paleosols: palaeoclimatic implications. *Palaeogeography, Palaeoclimatology, Palaeoecology*, **137**, 25–54.

Maher, B. A., 2008. Environmental magnetism and climate change. *Contemporary Physics*, **48**, 247–274.

Maher, B. A., and Thompson, R. (eds.), 1999. *Quaternary Climates, Environments and Magnetism*. Cambridge: Cambridge University Press.

Maher, B. A., Alekseev, A., and Alekseeva, T., 2002. Variation of soil magnetism across the Russian steppe: its significance for use of soil magnetism as a paleorainfall proxy. *Quaternary Science Reviews*, **21**, 1571–1576.

Maher, B. A., Alekseev, A., and Alekseeva, T., 2003. Magnetic mineralogy of soils across the Russian steppe: climatic dependence of pedogenic magnetite formation. *Palaeogeography, Palaeoclimatology, Palaeoecology*, **201**, 321–341.

Mullins, C. E., 1977. Magnetic susceptibility of the soil and its significance in soil science: a review. *Journal of Soil Science*, **28**, 223–246.

Petrovský, E., and Ellwood, B. B., 1999. Magnetic monitoring of air-land and water-pollution. In Maher, B. A., and Thompson, R. (eds.), *Quaternary Climates, Environments and Magnetism*. Cambridge: Cambridge University Press.

Scholger, R., 1998. Heavy metal pollution monitoring by magnetic susceptibility measurements applies to sediments of the river Mur (Styria, Austria). *European Journal of Environmental and Engineering Geophysics*, **3**, 25–37.

Schwertmann, U., 1988. Occurrence and formation of iron oxides in various pedoenvironments. In Stuki, J. W., Goodman, B. A., and Schwertmann, U. (eds.), *Iron Oxides in Soils and Clay Minerals*. Dordrecht: Reidel.

Singer, M. J., Verosub, K. L., Fine, P., and TenPas, J., 1996. A conceptual model for the enhancement of magnetic susceptibility in soils. *Quaternary International Journal*, **34–36**, 2443–2458.

Strzyszcz, Z., Magiera, T., and Heller, F., 1996. The influence of industrial immisions on the magnetic susceptibility of soils in Upper Silesia. *Studia Geophysica et Geodaetica*, **40**, 276–286.

Thompson, R., and Oldfield, F., 1986. *Environmental Magnetism*. London: Allen and Unwin.

Cross-references

Clay Minerals and Organo-Mineral Associates
Climate Change: Environmental Effects
Databases of Soil Physical and Hydraulic Properties
Physical Properties for Soil Classification
Mapping of Soil Physical Properties
Mineral–Organic–Microbial Interactions
Nanomaterials in Soil and Food Analysis
Oxidation–Reduction Reactions in the Environment
Parent Material and Soil Physical Properties
Physical (Mechanical) Weathering of Soil Parent Material
Wildfires, Impact on Soil Physical Properties

MAGNETIC RESONANCE IMAGING IN SOIL SCIENCE

Andreas Pohlmeier
ICG-4, Research Centre, Jülich, Germany

Definition

Magnetic resonance imaging (MRI) or magnetic resonance tomography (MRT) is a noninvasive, three-dimensional

(3D) imaging technique for monitoring water content, water fluxes, and tracer transport in porous media. It uses the effect of nuclear magnetic resonance (NMR) of certain atomic nuclei, mostly ^{1}H in H_2O, which is modulated by the chemical and physical environment inside the porous medium. The methods yield finally 2D (slices) or 3D (volume graphics) images of the medium under investigation.

Basics

Magnetic resonance imaging is based upon the physical effect of nuclear magnetic resonance (NMR) of spin bearing atomic nuclei (Callaghan, 1991; Blümich, 2000). The most important NMR active nuclei in soil science applications are ^{1}H, ^{13}C, ^{19}F, ^{31}P, and ^{23}Na, of which mostly ^{1}H with a spin quantum number of $\boldsymbol{I} = ½$ (e.g., in H_2O) is used for imaging purposes leading to a nuclear magnetic moment $\boldsymbol{\mu}$. If placed in an external magnetic field $\boldsymbol{B_0}$ pointing into z-direction of a Cartesian coordinate system, (The direction of the external magnetic field $\boldsymbol{B_0}$ is mostly determined by convention as "z") the nuclear magnetic moment precesses around the axis of $\boldsymbol{B}_0$ with the *Larmor frequency* υ_0:

$$\upsilon_0 = \omega_0/2\pi = -\gamma|B_0|/2\pi \tag{1}$$

The parameter γ, a proportionality constant termed as gyromagnetic ratio, is a basic property of the respective nucleus. For protons its value is $\gamma_H = 2.68 \times 10^8\ T^{-1}\ s^{-1}$, leading to typical values of $\upsilon_0 = 300$ MHz at $|\boldsymbol{B}_0| = 7$ T in stationary superconducting magnets, and $\upsilon_0 = 4.3$ MHz at $|\boldsymbol{B}_0| = 0.1$ T in mobile low-field relaxometers and scanners. Due to the quantum mechanical nature of the nuclear spin for proton magnetic moments, only two states are allowed in an external magnetic field: parallel (↑) and antiparallel orientation (↓). The energy gap between these two states is $\Delta E = h\upsilon_0$, where h is Planck's constant and the two states are populated according to Boltzmann's law: $n\uparrow/n\downarrow = \exp(-\Delta E/kT)$. In practice, it is more convenient not to regard single spins but ensembles of spins, which may be treated semi-classically. If an ensemble is sufficiently large, the x- and y-components of the nuclear magnetic moments precessing around the z-axis cancel mutually, so only the z-component persists. Since the lower energy state is slightly higher populated than the higher state, a macroscopic magnetic moment $\boldsymbol{M}_0$ pointing into z-direction is observable. Now, by absorption of electromagnetic radiation matching exactly the *Larmor frequency,* spins may swap from parallel to antiparallel orientation. Regarding the ensemble, this irradiation by a sufficiently long pulse, termed as 90° *pulse*, leads to a rotation of $\boldsymbol{M}_0$ into the xy-plane, where it precesses again with the Larmor frequency υ_0 around the z-axis. Subsequently, the excess energy of the ensemble is lost by two relaxation mechanisms:

Firstly, the coherence of the magnetic moments in the xy-plane decays with the *transverse* relaxation time T_2, see Equation 2 and radiation is emitted, which is detectable by an external receiver coil. This is the free induction decay (FID).

$$M_{xy} = M_0\exp(-t/T_2), \tag{2}$$

It is composed of two contributions: coherence loss (dephasing) in static inhomogeneities, which is reversible, and irreversible loss due to stochastic motions. The reversible contribution of dephasing can be restored by the creation of a *spin echo* by means of the application of a 180° pulse after a period of $t_E/2$ (cf. Equation 5) after the 90° pulse. What remains is the irreversible part. For details, see textbooks (Callaghan, 1991; Blümich, 2000).

Secondly, the thermal equilibrium is restored, that is, magnetization in the z-direction is reformed again. This is called *longitudinal relaxation* characterized by the relaxation time T_1:

$$M_z = M_0(1 - \exp(-t/T_1)) \tag{3}$$

Pure water possesses relaxation times of about 3 s in high field, but the environment, in which the interesting water molecules are located, reduces T_1 and T_2 considerably. Decisive factors are (1) pore size, (2) pore filling factor, (3) pore geometry, (4) chemical nature of pore walls, (5) dissolved paramagnetic substances and, in case of T_2, (6) diffusive motion in internal magnetic field gradients. By the latter effect T_2 can get much faster than one millisecond, which has implications on imaging capabilities, see below. The investigation of relaxation times is the basis of relaxometric exploration of pore space in geological materials (Dunn et al., 2002), see also the article Proton NMR Relaxometry in Soil Science, Nr of G. Schaumann in the encyclopedia.

Imaging

Magnetic resonance imaging (MRI) is the extension of NMR by adding spatial resolution to the observed NMR signal. In the following a basic spin echo imaging method is presented exemplarily (see Figure 1). According to Equation 1, the precession frequency is proportional to the magnetic field $\boldsymbol{B}_0$. If an additional spatially variable magnetic field (a *gradient* $\boldsymbol{G}_{slice}$) is added to $\boldsymbol{B}_0$ during excitation only one slice is excited according to Equation 4:

$$\upsilon_0 = -\gamma|B_0 + G_{slice} \cdot z|/2\pi. \tag{4}$$

All subsequent detectable signals originate only from this slice leading to the family of the so-called multi-slice imaging sequences, see Figure 1. The next dimension (here: x) is addressed by application of a further gradient $\boldsymbol{G}_{read}$ (orthogonal to $\boldsymbol{G}_{slice}$) during the detection of the signal that encodes the frequency of the received signal with respect to the x-direction. The third dimension is finally encoded by the phase-selective $\boldsymbol{G}_{phase}$, orthogonal to the other two gradients. After its application, the phase of the signal is turned with respect to a reference, and the phase shift is proportional to the position on the y-axis. The real-space image is finally obtained by two-dimensional Fourier transformation. The signal intensity is given by

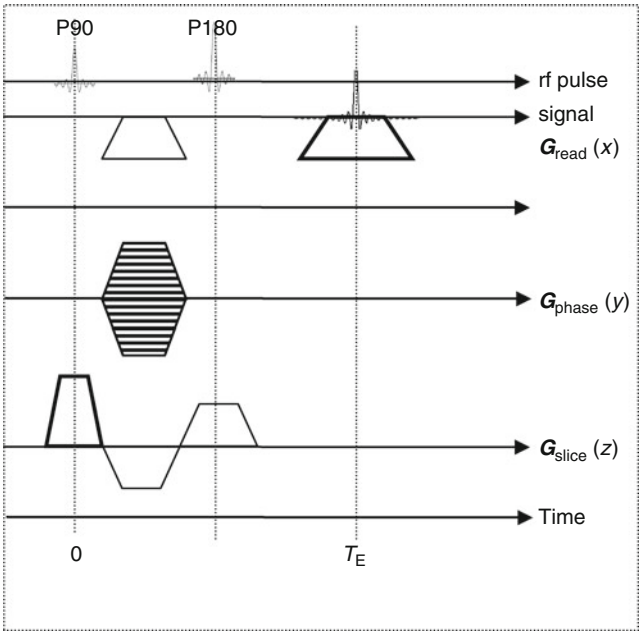

Magnetic Resonance Imaging in Soil Science, Figure 1 Basic spin echo imaging pulse sequence. P90 and P180 mean 90° and 180° pulses of electromagnetic irradiation for excitation of the spin ensemble system and creation of the echo, respectively. The gradients in this example are applied in *x*-, *y*-, and *z*-directions, but can also be applied in other orders.

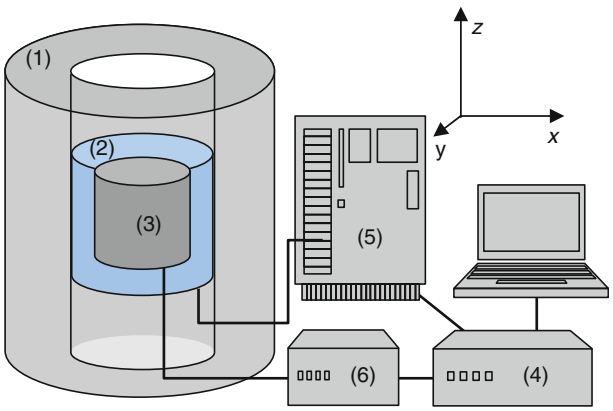

Magnetic Resonance Imaging in Soil Science, Figure 2 Schematic magnetic resonance imaging (MRI) scanner. For details, see text.

$$S(xyz) \propto \rho_0(xyz)(1 - \exp(-t_R/T_1(xyz))) \times \exp(-t_E/T_2(xyz)), \quad (5)$$

where ρ_0 is the spin density, t_R is the repetition time between successive excitation pulses, and t_E is the echo time, that is, twice the period between 90° and 180° pulse, T_1 and T_2 are the longitudinal and transverse relaxation times, respectively. Note that ρ_0 as well as T_1 and T_2 depend on space. The sequence in Figure 1 is only an example of a basic, but still widespread MRI pulse sequence (Spin echo multi slice sequence, also termed as spin warp sequence). Besides this, many partly very specialized sequences exist, for example, rapid imaging, relaxometric imaging, and motion sensitive imaging (Callaghan, 1991; Blümich, 2000).

Hardware

Schematically, the necessary hardware consists of following components (Figure 2): (1) a cylindrical magnet with a bore, in which the gradient system (2) and the transmitter–receiver coil (3) is placed. Stationary magnets are mostly superconductors, where permanent current flows in a liquid helium cooled coil, which creates a main magnetic field $\boldsymbol{B}_0$ pointing along the axis of the cylinder (*z*-direction). The gradient system consists of three additional coils that create orthogonal magnetic field gradients in the *x*-, *y*-, and *z*-directions. These gradients are operated by the spectrometer (4), which creates and controls the pulse sequences via gradient amplifiers (5). The excitation of the spin system and the monitoring of the transmitted signals are performed by the rf-coil (3), which transmits and receives rf-pulses. This is also controlled by the spectrometer (4) and the rf amplifier (6) In order to be able to turn the magnetization M_0 into the *xy*-plane the direction of the magnetic field $\boldsymbol{B}_1$ of the *rf*-pulses must be orthogonal to $\boldsymbol{B}_0$. This is performed in conventional superconducting scanners by a so-called birdcage-rf coil. For novel low-field scanners, which are composed of Halbach-rings of permanent magnets (Raich and Blümler, 2004), $\boldsymbol{B}_0$ points orthogonal to the main axis, and the rf coil can be a simple solenoid coil.

Applications

The application of MRI for soil systems started in the 1980s. A very early example was the unilateral imaging of water content in a natural soil on the field scale, where an electromagnet was positioned on a sledge and pulled across a field by a tractor (Paetzold et al., 1985). The signal created by a radiofrequency irradiation pulse was detected and water content was derived from the signal intensity. Most recently, the imaging of water on the field scale draws again attraction by the further development of magnetic resonance sounding (NMRS) or surface NMR (Roy and Lubczynski, 2005; Mohnke and Yaramanci, 2008; Yaramanci et al., 2008). Originally, this method has been developed for detection of aquifers in geological formations like karsts. But with the advancing technology, especially with respect to noise compensation, the method might get available for the investigation of soils with much less water content and much faster relaxation times (Hertrich et al., 2007).

In the lab, MRI has also been applied for the investigation of water content and dynamics in repacked natural porous media and natural soil cores (Nestle et al., 2002). The general problem for its application in soils is the inherently rapid T_2 relaxation times (Hall et al., 1997;

Votrubova et al., 2000), down to the sub-millisecond range. Also, one must take into consideration that T_2 for a given porous medium is not a constant but depends also on t_E due to diffusional motion in internal gradients (Barrie, 2000; Dunn et al., 2002). The limiting value of t_E is about 1.5 ms at present, so in the past many imaging studies in natural soils failed. However, the group of M. Cislerova was able to apply the method on infiltration processes in natural soil cores (Cislerova et al., 1997; Votrubova et al., 2003), where the infiltrating water followed preferential flow paths in a network of macropores, which are characterized by comparably long T_2 relaxation times. Figure 3 shows an image of a central vertical slice through a soil core after infiltration from top, which was obtained by a spin-echo sequence using t_E =5 ms. Clearly visible are the preferential flow paths.

Besides ^1H_2O imaging, also other nuclei can be used for monitoring soil processes. This method is quite rare, but promising for the quantification of dual phase fluxes. Simpson et al. monitored water and fluorinated compounds (fluorinated benzene, NaF, trifluralin) in four natural soil cores. Since free water possesses longer relaxation times, and it is still visible when imaged at long t_E, the authors varied t_E in the range between 2.5 and 40 ms in order to differentiate between bound water and free water. Then the displacement of water by hexafluorbenzene during infiltration from top was imaged by ^{19}F MRI. This fluorinated liquid has been chosen as model nonaqueous phase liquid (NAPL), because ^{19}F possesses the same spin like water and a similar gyromagnetic ratio of $\gamma_F = 2.52 \times 10^8\ T^{-1}\ s^{-1}$.

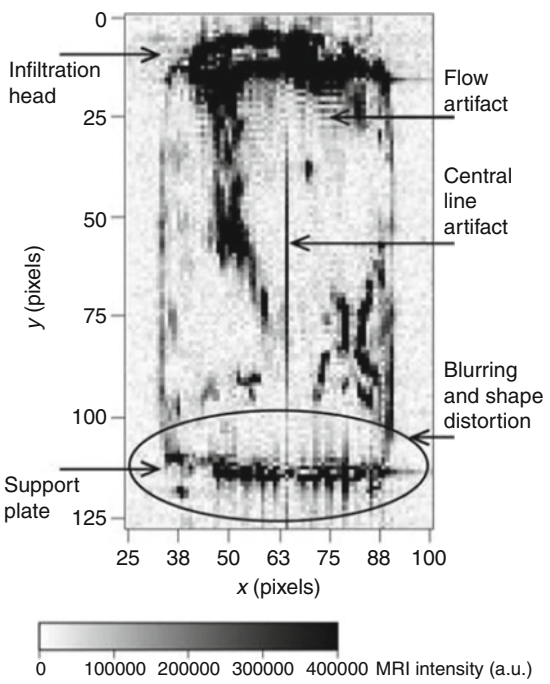

Magnetic Resonance Imaging in Soil Science, Figure 3 MR image of a soil core after infiltratation of water from top. (Modified from Votrubova et al., 2003. Copyright [2003] American Geophysical Union, Reproduced/modified by permission of American Geophysical Union.)

A permanently challenging topic in soil science is the imaging of flow processes. MRI is principally very suitable for such purposes, since it can monitor the motion of water and therefore flow velocities and diffusion coefficients directly (Callaghan et al., 1988; Baumann et al., 2000; Scheenen et al., 2001). This is performed by the introduction of additional motion encoding gradients before the detection of echoes, which prolongates interval between excitation pulse and detection. Therefore, these methods are restricted to the investigation of sediments and model porous media with sufficiently slow transverse relaxation times (Baumann et al., 2000; Herrmann et al., 2002b). For applications in soils, the first difficulty is the short transverse relaxation time, which lets signals vanish after some milliseconds. Secondly, flow processes in soils are mostly slower than the few tenths of mm/s, which is the present limit for flow imaging (Bendel, 2009). So, fluxes should be better visualized indirectly by motion of tracers. Popular tracers are paramagnetic ions like Cu^{2+}, Ni^{2+}, or Mn^{2+} (Greiner et al., 1997; Herrmann et al., 2002a; Oswald et al., 2007), and complexes like $GdDTPA^{2-}$ that are widely used in medicine (Hermann et al., 2008; Haber-Pohlmeier et al., 2009, 2010). The mode of action is predominantly the reduction of the longitudinal relaxation time T_1. If one sets the experimental parameter T_R in Equation 5 to a sufficiently small value, the signal intensity in regions without tracer is low, whereas signal intensities originating from regions with high tracer concentrations remain high. This technique has been successfully applied for quantifying flux processes in natural porous media and very recently for the first time in a natural soil (Haber-Pohlmeier et al., 2009, 2010).

As already mentioned, soils possess short relaxation times, which can reduce the intensities of echoes considerably or prevent the detection of echoes completely. A family of MRI techniques based on *single point imaging* can overcome this restriction by avoiding the creation of echoes and probe directly the free induction decay, which appears after any exciting pulse (Balcom et al., 1996). Their general drawbacks are long measuring times combined with low resolution. However, such methods are used for the investigation of water in porous rocks (Gingras et al., 2002; Chen et al., 2006) and root–soil systems (Pohlmeier et al., 2008).

The final topic to be addressed here is the investigation of root–water–soil relations by MRI. MRI is especially suitable for this, since such interactions are sensitive for classical invasive methods but possess huge importance for the understanding of plant growth and stress tolerance. The earliest investigations range back to the 1980s (Bottomley et al., 1986; Bacic and Ratkovic, 1987; Brown et al., 1990; Chudek et al., 1997). For imaging of root systems, the short transverse relaxation times of soil material helps, since roots possess relative long relaxation times, so

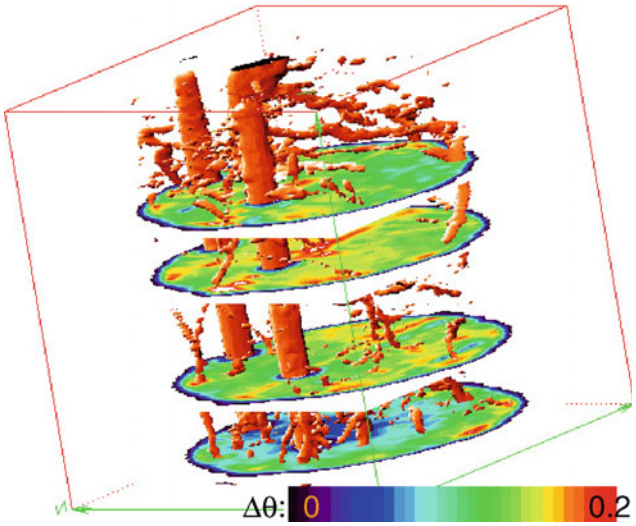

Magnetic Resonance Imaging in Soil Science, Figure 4 *Ricinus* root–soil system. Water content difference maps $\Delta\theta$ between day-6 and day-1, overlaid by the root system. The long cylinders in the left part are reference tubes. (From Pohlmeier et al., 2010.)

by the choice of long echo times (t_E in Equation 5) the signal from the soil is completely faded out, and only the root system appears in the images (MacFall and van As, 1996; Menzel et al., 2007; Pohlmeier et al., 2008). In contrast, if one intends to measure water content in the vicinity of roots one should use very short echo times or even employ single point imaging techniques (Pohlmeier et al., 2007). Figure 4 shows an example of water content changes during a desiccation experiment over 6 days in a ricinus root system grown in fine sand, where the water content was determined by a multi-slice multi-echo pulse sequence with quite short echo time. The resulting echo-trains are fitted by exponential functions and the water content was obtained from the amplitude of these functions and calibration on reference tubes with known water content. The root system architecture was imaged by a fast spin echo method with longer echo time. The stronger depletion in the top layers of the soil is visible, whereas the bottom regions remain wetter.

Using MRI, several authors stated water depletion zones around roots (MacFall et al., 1990; Segal et al., 2008) while under very dry conditions also hints on opposite trend, that is, increased water contents around roots are found (Carminati et al., 2010). This is still a topic of discussion. Further necessary for the interpretation of such effects is the combination of noninvasive 3D images with model calculations based on soil physical principles (Javaux et al., 2008), see also the article Plant Soil Interactions, Modelling of M. Javaux in this encyclopedia.

Summary and outlook

Summarizing, one can state that MRI is very suitable for monitoring processes in model and natural soils like water content changes, root system architecture, flow processes, and tracer motion. One should always take into account that transverse relaxation times decrease with decreasing pore size and water content and increasing content of paramagnetic ions like Fe^{3+} and Mn^{2+}. Thus, MRI is generally more sensitive for water in macropores. Therefore, quantitative water content imaging should employ fast echo times in combination with multi-echo sequences and extrapolation to zero time, or even ultrafast pulse sequences like SPRITE (Single Point Imaging with T_1 Enhancement [Balcom et al., 1996; Pohlmeier et al., 2007]). Such sequences abandon the creation of an echo and sample the FID directly on the expense of enhanced overall measuring time. Flux processes can be visualized directly in macropores or indirectly by the usage of contrast agents (tracers).

Bibliography

Bacic, G., and Ratkovic, S., 1987. NMR Studies of Radial Exchange and Distribution of Water in Maize Roots: The Relevance of Exchange Kinetics. *Journal of Experimental Botany*, **38**, 1284–1297.

Balcom, B. J., MacGregor, R. P., et al., 1996. Single-point ramped imaging with T-1 enhancement (SPRITE). *Journal of Magnetic Resonance Series A*, **123**(1), 131–134.

Barrie, P. J., 2000. Characterization of porous media using NMR methods. *Annual Reports on NMR Spectroscopy*, **41**, 265–316.

Baumann, T., Petsch, R., et al., 2000. Direct 3-d measurement of the flow velocity in porous media using magnetic resonance tomography. *Environmental Science & Technology*, **34**(19), 4242–4248.

Bendel, P., 2009. Quantification of slow flow using FAIR. *Magnetic Resonance Imaging*, **27**(5), 587–593.

Blümich, B., 2000. *NMR imaging of materials*. Oxford: Clarendon.

Bottomley, P. A., Rogers, H. H., et al., 1986. NMR Imaging Shows Water Distribution and Transport in Plant-Root Systems Insitu. *Proceedings of the National Academy of Sciences of the United States of America*, **83**(1), 87–89.

Brown, J. M., Kramer, P. J., et al., 1990. Use of Nuclear Magnetic Resonance Microscopy for Noninvasive Observations of Root-Soil Water Relations. *Theoretical and Applied Climatology*, **42**, 229–236.

Callaghan, P. T., 1991. *Principles of Nuclear Magnetic Resonance Microscopy*. Oxford: Oxford University Press.

Callaghan, P. T., Eccles, C. D., et al., 1988. NMR Microscopy of dynamic displacements – k-space and q-space imaging. *Journal of Physics*, **E21**, 820–822.

Carminati, A., Moradi, A., et al., 2010. Dynamics of soil water content in the rhizosphere. *Plant and Soil*, **332**, 163.

Chen, Q., Rack, F., et al., 2006. Quantitative magnetic resonance imaging methods for core analysis. New techniques in Sediment Cora Analysis. London. *Geological Society London*, **267**, 193–207.

Chudek, J. A., Hunter, G., et al., 1997. An application of NMR microimaging to investigate nitrogen fixing root nodules. *Magnetic Resonance Imaging*, **15**, 361–368.

Cislerova, M., Votrubova, J., et al., 1997. *Magnetic Resonance Imaging and Preferential Flow in Soils. Characterization and Measurement of the Hydraulic Properties of Unsaturated Porous Media.*. Riverside: University of California.

Dunn, K. J., Bergmann, D. J., et al., 2002. *Nuclear Magnetic Resonance, Petrophysical and Logging Applications*. Amsterdam: Pergamon.

Gingras, M. K., MacMillan, B., et al., 2002. Visualizing the internal physical characteristics of carbinate sediments with magnetic

resonance imaging and petrography. *Bulletin of Canadian Petroleum Geology*, **50**(3), 363–369.
Greiner, A., Schreiber, W., et al., 1997. Magnetic resonance imaging of paramagnetic tracers in porous media: quantification of flow and transport parameters. *Water Resources Research*, **33**(6), 1461–1473.
Haber-Pohlmeier, S., Van Dusschoten, D., et al., 2009. Waterflow visualized by tracer transport in root-soil-systems using MRI. *Geophysical Research Abstracts*, **11**, EGU2009–8096.
Haber-Pohlmeier, S., Stapf, S., et al., 2010. Waterflow monitored by tracer transport in natural porous media using MRI. *Vadose Zone Journal*, **9**, 835–845.
Hall, L. D., Amin, M. H. G., et al., 1997. MR properties of water in saturated soils and resulting loss of MRI signal in water content detection at 2 tesla. *Geoderma*, **80**(3–4), 431–448.
Hermann, P., Kotek, J., et al., 2008. Gadolinium (iii)complexes as MRI contrast agents: ligand design and properties of the complexes. *Dalton Transactions*, **June 21**, 3027–3047.
Herrmann, K. H., Pohlmeier, A., et al., 2002a. Three-dimensional imaging of pore water diffusion and motion in porous media by nuclear magnetic resonance imaging. *Journal of Hydrology*, **267**(3–4), 244–257.
Herrmann, K. H., Pohlmeier, A., et al., 2002b. Three-dimensional nickel ion transport through porous media using magnetic resonance Imaging. *Journal of Environmental Quality*, **31**(2), 506–514.
Hertrich, M., Braun, M., et al., 2007. Surface nuclear magnetic resonance tomography. *IEEE Transactions on Geoscience and Remote Sensing*, **45**, 3752–3759.
Javaux, M., Schröder, T., et al., 2008. Use of a Three-Dimensional Detailed Modeling Approach for Predicting Root Water Uptake. *Vadose Zone Journal*, **7**(3), 1079–1088.
MacFall, J. S., and Van As, H., 1996. Magnetic resonance imaging of plants. In Shachar-Hill, Y., and Pfeffer, P. E. (eds.), *Nuclear Magnetic Resonance in Plant Biology*. Rockville: The American Society of Plant Physiologists, pp. 33–76.
MacFall, J. S., Johnson, G. A., et al., 1990. Observation of a water depletion region surrounding loblooly pine roots by magnetic resonance imaging. *Proceedings of the National Academy of Sciences of the United States of America*, **87**, 1203–1207.
Menzel, M. I., Oros-Peusquens, A. M., et al., 2007. 1 H-NMR imaging and relaxation mapping – a tool to distinguish the geographical origin of German white asparagus? *Journal of Plant Nutrition and Soil Science*, **170**, 24–38.
Mohnke, O., and Yaramanci, U., 2008. Pore size distributions and hydraulic conductivities of rocks derived from Magnetic Resonance Sounding relaxation data using multi-exponential decay time inversion. *Journal of Applied Geophysics*, **66**(3–4), 73–81.
Nestle, N., Baumann, T., et al., 2002. Magnetic resonance imaging in environmental science. *Environmental Science & Technology*, **36**(7), 154A–160A.
Oswald, S. E., Spiegel, M. A., et al., 2007. Three-dimensional saltwater-freshwater fingering in porous media: contrast agent MRI as basis for numerical simulations. *Magnetic Resonance Imaging*, **25**, 537–540.
Paetzold, R. F., Matzkanin, G. A., et al., 1985. Surface Soil-Water Content Measurement Using Pulsed Nuclear Magnetic-Resonance Techniques. *Soil Science Society of America Journal*, **49**(3), 537–540.
Pohlmeier, A., Oros-Peusquens, A. M., et al., 2007. Investigation of water content and dynamics of a Ricinus root system in unsaturated sand by means of SPRITE and CISS: correlation of root architecture and water content change. *Magnetic Resonance Imaging*, **25**, 579–580.
Pohlmeier, A., Oros-Peusquens, A. M., et al., 2008. Changes in Soil Water Content Resulting from Ricinus Root Uptake Monitored by Magnetic Resonance Imaging. *Vadose Zone Journal*, **7**, 1010–1017.
Pohlmeier, A., Vergeldt, F., et al., 2010. MRI in Soils: Determination of water content changes due to root water uptake by means of Multi-Slice-Multi-Echo sequence (MSME). *The Open Magnetic Resonance Journal*, **3**, 39–47.
Raich, H., and Blümler, P., 2004. Design and Construction of a Dipolar Halbach Array with an Homogeneous Field from N * 8 Identical Bar-Magnets - NMR-Mandhalas-. *Conc. Magn. Reson. B Magn. Reson. Eng.*, **23B**, 16–25.
Roy, J., and Lubczynski, M. W., 2005. MRS multi exponential decay analysis: aquifer pore size distribution and vadose zone characterization. *Near Surface Geophysics*, **3**(4), 287–298.
Scheenen, T. W. J., Vergeldt, F. J., et al., 2001. Microscopic imaging of slow flow and diffusion: a pulsed field gradient stimulated echo sequence combined with turbo spin echo imaging. *Journal of Magnetic Resonance*, **151**(1), 94–100.
Segal, E., Kushnir, T., et al., 2008. Water uptake and the hydraulics of the root hair rhizosphere. *Vadose Zone Journal*, **7**, 1024–1037.
Votrubova, J., Sanda, M., et al., 2000. The relationships between MR parameters and the content of water in packed samples of two soils. *Geoderma*, **95**(3–4), 267–282.
Votrubova, J., Cislerova, M., et al., 2003. Recurrent ponded infiltration into structured soil: A magnetic resonance imaging study. *Water Resources Research*, **39**(12), 1371.
Yaramanci, U., Legchenko, A., et al., 2008. Magnetic Resonance Sounding Special Issue of Journal of Applied Geophysics, 2008. *Journal of Applied Geophysics*, **66**(3–4), 71–72.

Cross-references

Agrophysical Objects (Soils, Plants, Agricultural Products, and Foods)
Agrophysics: Physics Applied to Agriculture
Image Analysis in Agrophysics
Infiltration in Soils
Magnetic Properties of Soils
Nondestructive Measurements in Soil
Noninvasive Quantification of 3D Pore Space Structures in Soils
Plant Roots and Soil Structure
Plant–Soil Interactions, Modeling
Pore Size Distribution
Proton Nuclear Magnetic Resonance (NMR) Relaxometry in Soil Science
Root Water Uptake: Toward 3-D Functional Approaches
Soil Hydraulic Properties Affecting Root Water Uptake
Soil–Plant–Atmosphere Continuum
Soil Water Flow
Solute Transport in Soils

MAGNETIC TREATMENT OF IRRIGATION WATER, EFFECTS ON CROPS

Basant Maheshwari, Harsharn Grewal
School of Natural Sciences, Hawkesbury Campus, Building H3, University of Western Sydney, Penrith South DC, NSW, Australia

Definition

Water productivity: Crop yield per unit volume of water used. Definitions of water productivity differ based on the context. For example, from the point of view of growing

crops, obtaining more kilograms per unit of transpiration is the main aspect productivity of water. In the case of regional or catchment scale, the focus of water productivity is the value derived from the use of water for purposes such as crops, forests, fisheries, ecosystems, and other uses.

Electromagnetic field: A field of force associated with a moving electric charge equivalent to an electric field and a magnetic field at right angles to each other and to the direction of propagation.

Magnetic treatment: Exposure of material such as water to a magnetic field for a short duration (a few seconds) or longer to possibly change some of its properties for beneficial effects.

Introduction

The total volume of fresh water available is limited but the demand for water is growing at a rapid pace. In this context there has been a growing interest to use water more efficiently and effectively, increase reuse of effluent, develop ways to use lower quality water and improve the overall productivity of water used for irrigation. This means we need to develop ways that will increase the productivity and sustainability of water used for irrigation. One of the ways by which we can reduce the total water used for irrigation is to employ practices that improve crop yield per unit volume of water used (i.e., water productivity). There have been claims made that the magnetic treatment of irrigation water can improve water productivity. If those claims are valid there is scope for magnetic treatment of water to save water and assist in coping with the future water scarcity.

Effects of magnetic field

There is very little study reported, with valid scientific experiments, on the effects of magnetic treatment of water on crop yield and water productivity. However, there have been some closely related studies that report on the effects of magnetic field on seed germination, plant physiology, and overall plant growth and, as such, those studies may indirectly help to understand the role of magnetic treatment of irrigation water and plant growth. For example, Lin and Yotvat (1990) reported an increase in water productivity in both livestock and crop farming with magnetically treated water. Some studies have shown that there is an increase in the number of flowers, earliness and total fruit yield of strawberry and tomatoes by using magnetic fields (Esitken and Turan, 2004; Danilov et al., 1994). An increase in nutrient uptake by magnetic treatment was also observed in tomatoes by Duarte Diaz et al. (1997).

External electric and magnetic fields influence both the activation of ions and polarization of dipoles in living cells (Johnson and Guy, 1972; Moon and Chung, 2000). Electromagnetic fields (EMFs) can alter the plasma membrane structure and function (Paradisi et al., 1993; Blank, 1995). Goodman et al. (1983) reported an alteration of the level of some mRNA after exposure to EMFs. Amaya et al. (1996) and Podleśny et al. (2004) have shown that an optimal external electromagnetic field accelerates the plant growth, especially seed germination percentage and speed of emergence.

Some studies focused on how static magnetic field affect chlorophyll and phytohormone levels in some plants. Turker et al. (2007) observed that chlorophyll and phytohormone levels decreased when static magnetic field, parallel either to gravity force (field-down) or anti-parallel (field-up) was applied to maize plants. However, chlorophyll concentration increased in sunflowers by applying magnetic field in either direction.

Magnetic fields can also influence the root growth of some plant species (Belyavskaya, 2001, 2004; Muraji et al., 1992, 1998; Turker et al., 2007). In the case of maize (*Zea mays*) the exposure of maize seedlings to 5 mT magnetic fields at alternating frequencies of 40–160 Hz improved root growth (Muraji et al., 1992). However, there was a reduction in primary root growth of maize plants grown in a magnetic field alternating at 240–320 Hz. The highest growth rate of maize roots was achieved in a magnetic field of 5 mT at 10 Hz. Turker et al. (2007) reported an inhibitory effect of static magnetic field on root dry weight of maize plants but there was a beneficial effect of magnetic fields on root dry weight of sunflower plants.

Belyavskaya (2004) and Turker et al. (2007) reported that a weak magnetic field has an inhibitory effect on the growth of primary roots during early growth. The proliferative activity and cell reproduction in meristem in plant roots are reduced in weak magnetic fields (Belyavskaya, 2004). The cell reproductive cycle slows down due to the expansion of the G1 phase in many plant species and the G2 phase in flax and lentil roots. There was a decrease in the functional activity of genomes at early pre-replicate period in plant cells exposed to weak magnetic fields. In general, these studies conclude that weak magnetic fields cause intensification of protein synthesis and disintegration in plant roots.

Impact of heat stress at 40°C, 42°C, and 45°C for 40 min in cress seedlings (*Lepidium sativum*) was reduced by exposing plants to extremely low-frequency (ELF) magnetic field (50 Hz, 100 μT) (Ruzic and Jerman, 2002). Magnetic fields act on the same cellular metabolic pathways as temperature stress and as such the study suggests that magnetic fields act as a protective factor against heat stress.

Magnetic treatment and seed germination

Magnetic treatment of seed or water used for germination can influence germination and seedling emergence. Reina et al. (2001) reported an increase in germination percentages of lettuce seeds by treating these with 10 mT stationary magnetic fields. They reported that magnetic fields resulted in an increase in water absorption rate of lettuce seeds and may have contributed to increased germination percentages. Some studies reported that the magnetic exposure of seeds, viz., cereals and beans, prior to sowing can improve germination rate and early growth (Pittman 1963a, b;

Pittman and Anstey, 1967). Similarly, the application of stationary magnetic fields before sowing had a significant increase in germination rates and seedling vigor in groundnut, onion, and rice seeds (Vakharia et al., 1991; Alexander and Doijode, 1995). The exposure of broad bean seeds by Podleśny et al. (2004) to variable magnetic strengths before sowing showed some beneficial effects on seed germination and emergence. In particular, they found that seedling emergence was more regular after the use of the magnetic treatment and occurred 2–3 days earlier in comparison to seedlings in the control treatment. In tomatoes, De Souza et al. (2006) observed that the magnetically treated tomato seeds improved the leaf area, leaf dry weight, and yield of tomato crop under field conditions.

The beneficial effects of magnetically treated irrigation water have also been reported on germination percentages of seeds. For example, an increase in germination of *Pinus tropicalis* seeds from 43% in the control to 81% with magnetically treated water was observed by Morejon et al. (2007). For tomatoes, pepper, cucumber and wheat seeds Hilal and Hilal (2000) reported that germination and seedling emergence was improved when magnetically treated water and seeds were used. In particular, germination of pepper seeds was higher with magnetically treated seeds when compared with magnetically treated irrigation water and cucumber seeds had the highest germination percentage when both irrigation water and seeds were magnetically treated.

How do magnetic fields influence?

The mechanisms that influence plant growth and seed germination through magnetic treatment are not well understood. Some beneficial effects of the treatment could be related to the "gas bubble-water interface" (Vallée et al., 2005). Furthermore, these effects may be related to mechanisms such as intramolecular and intra-ionic interactions, effects of Lorentz forces, dissolution of contaminants and interfacial effects (Baker and Simon, 1996). The changes in hydrogen bonding and increased mobility of Na^+ and Cl^- ions with exposure of irrigation water to magnetic fields may also play some role in the plant growth and seed germination (Chang and Weng, 2008). It is also suggested that the magnetic treatment of water may result in changes in physical and chemical properties of water such as hydrogen bonding, polarity, surface tension, conductivity, pH, refractive index and solubility of salts (Smikhina, 1981; Srebrenik et al., 1993; Amiri and Dadkhah, 2006; Otsuka and Ozeki, 2006; Chang and Weng, 2008).

Magnetic treatment and water productivity

Maheshwari and Grewal (2009) investigated the effects of magnetically treated potable water, recycled water and saline water on crop yields and water productivity under controlled environmental conditions in a glasshouse. The main aim of the study was to examine the impact of magnetic treatment of different water sources on water productivity and yield of snow peas, celery, and peas.

The study has provided some preliminary results on how the magnetic treatment influences the key parameters of (1) water – pH and EC; (2) crop – yield, water productivity, total crop water use and crop nutrient composition; and (3) soil – pH, EC, and available N, P, and K. Statistical analysis of the data indicated that the effects of the magnetic treatment varied with crop type and the source of water. There was no statistically significant effect of magnetic treatment on the total water used by the crop during the growing season in any of the three crops. However, the magnetic treatment of water tends to increase (statistically significant) crop yield (fresh weight) and water productivity (kg of fresh or dry produce per kL of water used) of celery and snow peas. On the other hand, the magnetic treatment had no significant effect on both crop yield and water productivity for peas.

In general, the results obtained during this preliminary study on the use of magnetically treated water on celery and snow peas are interesting but the effect of the magnetic treatment on crop yield and water productivity was variable and occurred under some set of conditions and not in others. Therefore, from the glasshouse experimental data, it is difficult to make any recommendation with certainty as to the effectiveness of the magnetic treatment under field conditions.

Summary

The past studies reveal that the magnetic field or treatment can affect plant growth and other related parameters. Similarly, the past studies have indicated that there are some beneficial effects of magnetic treatment on seed germination and seedling emergence. Nevertheless, we have no clear understanding yet as to the mechanisms behind these effects on plant growth, water productivity, and the changes magnetic treatment brings about in nutritional aspects of seed germination and seedling growth.

To assess the potential of the magnetic treatment for practical applications, we need further testing under field conditions to clearly understand and demonstrate the beneficial effects of the magnetically treated irrigation water for crop production under real-world situations. Further research is also warranted to understand how the magnetic treatment affects crop and soil parameters and therefore soil, crop and water quality conditions under which the treatment will be effective to provide water productivity gains.

Bibliography

Alexander, M. P., and Doijode, S. D., 1995. Electromagnetic field: a novel tool to increase germination and seedling vigour of conserved onion (*Allium cepa* L.) and rice (*Oryza sativa* L.) seeds with low viability. *Plant Genetic Resources Newsletter*, **104**, 1–5.

Amaya, J. M., Carbonell, M. V., Martinez, E., and Raya, A., 1996. Effects of stationary magnetic fields on germination and growth of seeds. *Horticultural Abstracts*, **68**, 1363.

Amiri, M. C., and Dadkhah, A. A., 2006. On reduction in the surface tension of water due to magnetic treatment. *Colloids and Surfaces, A: Physicochemical and Engineering Aspects*, **278**, 252–255.

Baker, J. S., and Simon, J. J., 1996. Magnetic amelioration of scale formation. *Water Research*, **30**, 247–260.
Belyavskaya, N. A., 2001. Ultrastructure and calcium balance in meristem cells of pea roots exposed to extremely low magnetic fields. *Advances in Space Research*, **28**, 645–650.
Belyavskaya, N. A., 2004. Biological effects due to weak magnetic field on plants. *Advances in Space Research*, **34**, 1566–1574.
Blank, M., 1995. Biological effects of environmental electromagnetic fields: molecular mechanisms. *BioSystems*, **35**, 175–178.
Chang, K. T., and Weng, C. I., 2008. An investigation into structure of aqueous NaCl electrolyte solutions under magnetic fields. *Computational Materials Science*, **43**, 1048–1055.
Danilov, V., Bas, T., Eltez, M., and Rizakulyeva, A., 1994. Artificial magnetic field effects on yield and quality of tomatoes. *Acta Horticulturae*, **366**, 279–285.
De Souza, A., Garci, D., Sueiro, L., Gilart, F., Porras, E., and Licea, L., 2006. Pre-sowing magnetic treatments of tomato seeds increase the growth and yield of plants. *Bioelectromagnetics*, **27**, 247–257.
Duarte Diaz, C. E., Riquenes, J. A., Sotolongo, B., Portuondo, M. A., Quintana, E. O., and Perez, R., 1997. Effects of magnetic treatment of irrigation water on the tomato crop. *Horticultural Abstracts*, **69**, 494.
Esitken, A., and Turan, M., 2004. Alternating magnetic field effects on yield and plant nutrient element composition of strawberry (Fragaria x ananassa cv. camarosa). *Acta Agriculturae Scandinavica. Section B: Soil and Plant Science*, **54**, 135–139.
Goodman, R., Basset, C. A., and Henderson, A., 1983. Pulsing electromagnetic fields induce cellular transcription. *Science*, **220**, 1283–1285.
Hilal, M. H., and Hilal, M. M., 2000. Application of magnetic technologies in desert agriculture. 1 – Seed germination and seedling emergence of some crops in a saline calcareous soil. *Egyptian Journal of Soil Science*, **40**, 413–422.
Johnson, C. C., and Guy, A. W., 1972. Non-ionizing electrostatic wave effects in biological materials and systems. *Proceedings of Institute of Electrical and Electronics Engineers*, **60**, 692–718.
Lin, I. J., and Yotvat, J., 1990. Exposure of irrigation and drinking water to a magnetic field with controlled power and direction. *Journal of Magnetism and Magnetic Materials*, **83**, 525–526.
Maheshwari, B. L., and Grewal, H. S., 2009. Magnetic treatment of irrigation water: its effects on vegetable crop yield and water productivity. *Agricultural Water Management*, **96**, 1229–1236.
Moon, J., and Chung, H., 2000. Acceleration of germination of tomato seeds by applying AC electric and magnetic fields. *Journal of Electrostatics*, **48**, 103–114.
Morejon, L. P., Castro Palacio, J. C., Velazquez Abad, L. G., and Govea, A. P., 2007. Simulation of pinus tropicalis M. seeds by magnetically treated water. *International Agrophysics*, **21**, 173–177.
Muraji, M., Nishimura, M., Tatebe, W., and Fujii, T., 1992. Effect of alternating magnetic field on the growth of the primary root of corn. *Institute of Electrical and Electronics Engineers Transaction of Magnetics*, **28**, 1996–2000.
Muraji, M., Asai, T., and Tatebe, W., 1998. Primary root growth rate of Zea mays seedlings grown in an alternating magnetic field of different frequencies. *Biochemistry and Bioenergetics*, **44**, 271–273.
Otsuka, I., and Ozeki, S., 2006. Does magnetic treatment of water change its properties? *The Journal of Physical Chemistry*, **110**, 1509–1512.
Paradisi, S., Donelli, G., Santini, M. T., Straface, E., and Malorni, W., 1993. A 50-Hz magnetic field induces structural and biophysical changes in membranes. *Bioelectromagnetics*, **14**, 247–255.
Pittman, U. J., 1963a. Magnetism and plant growth. 1. Effect on germination and early growth of cereal seeds. *Canadian Journal of Plant Science*, **43**, 512–518.
Pittman, U. J., 1963b. Magnetism and plant growth. III. Effect on germination and early growth of corn and beans. *Canadian Journal of Plant Science*, **45**, 549–555.
Pittman, U. J., and Anstey, T. H., 1967. Magnetic treatment of seed orientation of a single harvest snap bean (Phaseolus vulgaris L). *Proceedings of American Society of Horticultural Science*, **91**, 310–314.
Podleśny, J., Pietruszewski, S., and Podleśna, A., 2004. Efficiency of the magnetic treatment of broad bean seeds cultivated under experimental plot conditions. *International Agrophysics*, **18**, 65–71.
Reina, F. G., Pascual, L. A., and Fundora, I. A., 2001. Influence of a stationary magnetic field on water relations in lettuce seeds. Part II: experimental results. *Bioelectromagnetics*, **22**, 596–602.
Ruzic, R., and Jerman, I., 2002. Weak magnetic field decreases heat stress in cress seedlings. *Electromagnetic Biology and Medicine*, **21**, 69–80.
Smikhina, L. P., 1981. Changes in refractive index of water on magnetic treatment. *Colloid Journal*, **2**, 401–404.
Srebrenik, S., Nadiv, S., and Lin, L. J., 1993. Magnetic treatment of water- a theoretical quantum model. *Magnetic and Electrical Separation*, **5**, 71–91.
Turker, M., Temirci, C., Battal, P., and Erez, M. E., 2007. The effects of an artificial and static magnetic field on plant growth, chlorophyll and phytohormone levels in maize and sunflower plants. *Phyton- Annales Rei Botanicae*, **46**(2), 271–284.
Vakharia, D. N., Davariya, R. L., and Parameswaran, M., 1991. Influence of magnetic treatment on groundnut yield and yield attributes. *Indian Journal of Plant Physiology*, **34**, 131–136.
Vallée, P., Lafait, J., Mentré, P., Monod, M. O., and Thomas, Y., 2005. Effects of pulsed low frequency electromagnetic fields on water using photoluminescence spectroscopy: role of bubble/water interface. *The Journal of Chemical Physics*, **122**, 114513–8.

Cross-references

Irrigation with Treated Wastewater, Effects on Soil Structure
Magnetic Properties of Soils
Physics of Plant Nutrition
Plant Roots and Soil Structure
Plant–Soil Interactions, Modeling
Plant Wellness
Water Use Efficiency in Agriculture: Opportunities for Improvement

MANAGEMENT EFFECTS ON SOIL PROPERTIES AND FUNCTIONS

Rainer Horn
Institute for Plant Nutrition and Soil Science, Christian-Albrechts-University zu Kiel, Kiel, Germany

Definition

The introduction and application of agricultural and forestry machinery often result in severe soil compaction and soil deformation with intense decrease in total pore volume, alterations in the pore-size distribution, and especially in their functions concerning gas, water and heat transfer as well as altered accessibility of chemical adsorption sites of clay minerals, organic substances, and further variable exchange places.

Introduction

Soils as three-phase systems fulfill not only the archive function (historical memory of former properties, climates, management practices, land use, etc.), they are essentially needed for plant growth and yield, as reservoir for microbes and they are also responsible for filtering and buffering of soil water in order to get clean drinking- and groundwater, they contribute to the transformation under in situ conditions and serve as the resource for raw material. In the following, the process of soil deformation will be shortly summarized in order to derive the interactions between soil structure and chemical as well as physical and biological properties, which are affected by soil deformation. Finally, some conclusions for a sustainable land use and soil management will be given.

Soils: their functions in view of the existing soil protection laws or recommendations

Soils as nonrenewable goods have to be protected and should be only used according to their properties. The European Soil Charta 1972 of the European Assembly was the first, which did underline and support this idea and which in 1998 became the nucleus for the German Soil Protection Law. This law was the first and until now the only one in Europe while, e.g., the European Soil Framework Directive (2006) is still under a very controversial debate. However, there is an urgent need to specify more in detail the requests and limitations but also to quantify the limits of an unprevented or unhindered land use. It has to be pointed out that for a sustainable soil land use their physical, chemical, and biological soil functions must be related to the intensity and function values and have to include the dependent recommendations in order to prevent any irreversible soil degradation.

If we consider the properties for arable horticulture, landscape planning, and in forestry soils, they all require primarily a sufficiently rigid pore system, which guarantees the water, gas and heat exchange, nutrient transport and adsorption as well as an optimal rootability, which also includes a sufficient microbial activity and composition in order to also decompose the plant debris. All these requests must be included in a quantitative way in the Protection law but there is still an urgent need to specify these "optimal" properties. However, it is very difficult for the land user to forecast and to relate their own farming management practices to coming weather conditions, e.g., the storage capacity for water and nutrients in the topsoil sufficient to grow a good crop yield during the following season under dry conditions or are the soils permeable enough to drain off the access rain water and to reaerate the root zone quick enough in order to avoid declining redox potential values and the accumulation of anoxic gases in the pores. Thus, the major challenges are interlinked between soil and weather conditions, which request a more intense analysis of the effect of soil structure on the nutrient, gas, and water fluxes in anthropogenically managed soils under various land uses.

Processes of aggregate formation and persistence

Soils containing more than 12% clay (particle size < 2 μm) or even pure sandy soils with some salts tend to form aggregates. Usually the process occurs when soils dry and swell, and it is further enhanced by biological activity. Aggregates may show great variation in size from crumbs (diameter < 2 mm) to polyhedres or subangular blocks of 0.005–0.02 m, or even to prisms or columns of more than 0.1 m. During the first period of shrinkage, mineral particles are pulled together by capillary forces, which increase the number of points of contact and result in a higher bulk density. The initial aggregates always have rectangular-shaped edges because, under these conditions, stress release would occur perpendicular to the initial crack and stress would remain parallel to the crack (strain-induced fracturing). However, due to the increased mechanical strength the particle mobility declines and results in the formation of nonrectangular shear plains as the following crack generation. They are created after repeated swelling and shrinking processes and result in fractures in which the value of the angle of internal friction determines the deviation from 90° (Or and Ghezzehei, 2002). In newly formed aggregates, the number of contact points depends on the range of water potential and on the distribution of particle sizes as well as on their mobility (i.e., state of dispersion, flocculation, and cementation). Soil shrinkage, including crack formation, increases bulk density of aggregates. The increase in bulk density with the initial wetting and drying of the soil permits the aggregates to withstand structural collapse. The increase of the strength of single aggregates is further enhanced by a particle rearrangement, if the soil is nearly saturated with water increasing the mobility of clay particles due to dispersion and greater menisci forces of water (Horn and Dexter, 1989). Subsequent drying causes enhanced adhesion by capillary forces, which lead to greater cohesion as mineral particles are brought into contact following the evaporatory losses of the capillary water. Thus, the strength of the bigger, i.e., initial aggregates is increased due to a particle mobilization and results both in smaller and stronger aggregates with even a smaller aggregate bulk density. The strongest aggregate type under this aspect is the spherical shape, which has reached the stage of the smallest free entropy. Therefore, aggregate strength depends on (1) capillary forces, (2) intensity of shrinkage (normal/residual), (3) number of swelling and shrinkage cycles, i.e., the shrinkage/swelling history, (4) mineral particle mobility (i.e., rearrangement of particles to achieve arrangements of lowest free energy), and (5) bonding energy between particles in/or between aggregates or in the bulk soil. Generally, aggregates persist as long as the soil strength (defined by the failure line of Mohr–Coulomb) is higher than the given load or shrinkage forces soils remain rigid. If however, additional kinetic energy (which even is more efficient in combination with accessible water) is applied, aggregate deterioration and homogenization occur. Thus, a complete

homogenization of the soil structure due to shearing and/or puddling takes place if kneading (expressed as octahedral shear stresses and mean normal stresses) exceeds the aggregate and structure strength. After a mostly complete homogenization normal shrinkage, processes restart again (Horn et al., 1994). Consequently, a weaker soil structure and finally a pasty structure can be defined by very small cohesion and angle of internal friction values (Horn, 1976; Janssen et al., 2006). Thus, the determination of soil and/or aggregate strength has always to be subdivided into (1) mechanically, hydraulically, or chemically prestressed and (2) virgin conditions, which also ultimately affect the predictability of physical properties. These general ideas have been described in greater detail by Horn and Baumgartl (2002), Groenevelt and Grant (2002), Grant et al. (2002), and Peng and Horn (2005).

In conclusion, it has to be stated, that aggregate formations as well as changes in aggregate strength are directly related also to tillage systems. Conventional tillage especially of the A-horizon annually includes plowing, chiseling, and the seedbed preparation apart from multiple wheeling events depending on the crop management requirements, which ends in mostly homogenized structure conditions annually. Thus, a more complete aggregate formation will not take place. Conservational tillage systems on the other hand causes less disturbance and allow a more complete rearrangement of particles and strengthening of the structure system if preserved throughout several years.

Soil structure and soil use: how to sustain the required and natural soil and site-specific functions

During the last 4 decades, not only the mass of the agricultural and forestry machines but also the frequency of wheeling has increased intensely and resulted in a compression and soil deformation status, which can be suboptimal concerning plant growth and crop yield as well as the uncertainty of getting a predictable yield. At present, the maximum mass of machines exceeds by far 60 Mg and therefore also enhance the probability of subsoil compaction and long-term soil degradation. Not only in agriculture but also in forestry, such enlarged machines are used for tree harvesting and clear cutting and results in an intense subsoil degradation due to shear and vibration induced soil deformation especially if the soil water content in the subsoil is high and the internal soil strength very low (Horn et al., 2007).

Soil processes like the formation of a platy structure, deterioration of a continuous pore system are therefore signs of an intense soil degradation, which also coincides with an increased anisotropy of pore functions and may cause an increased lateral soil movement (= soil water erosion). For more details, see Soane and van Ouwerkerk (1994), Pagliai and Jones (2002), Ehlers et al. (2003), Lipiec and Hatano (2003), and Horn et al. (2005, 2006).

Consequences of soil deformation on changes in soil functions

Cation adsorption capacity, intensity, and accessibility

Soil aggregates can be classified by a certain accessibility of the exchange places for cations, which in comparison with that one of the homogenized material may be intensely reduced. We have to differentiate between the capacity and intensity properties. In homogenized soils, capacity (= potential) and intensity (= actual) parameters are identical, which holds true especially for the seedbed where fertilized ions are mostly adsorbed at the exchange places of the soil particles. For soil horizons with a prismatic structure, we can assume a reduction of up to 15% from the potential properties, while soil horizons with blocky or subangular blocky structure will even have a reduction of up to 50–80%.

In this context also soil texture and bulk density of the bulk soil and of the single aggregates further affect these actual conditions. Soils with a crumbly structure have again an improved accessibility due to a macroscopic homogenization of the aggregates themselves by the microbial activity as can be also derived from their particle and organic substance arrangement in the bulk soil. Thus, we can assume a nearly 90% accessibility of the cation exchange capacity values under these conditions. If, however, soils have a platy structure, the intensity (= actual) properties are as small as 30% of the capacity values due to the compressed pores in between singles particles within the plats and because of correspondingly retarded ion mass flow and diffusion within the plats. Thus, plats provide the greatest differences between the capacity and intensity properties and therefore also the most reduced accessibility of the exchange places. These differences can also be derived from the relationship between the exchangeable cations and the actual hydraulic conductivity, which is a measure of the effect of preferential flow processes. Compared to the theoretical CEC of 140 mmol kg^{-1} soil, the actual values were the smaller the higher was the hydraulic conductivity (Figure 1). The drier the soil the smaller the water fluxes and the more retarded are the exchange processes the higher is the actual value but it will not reach the maximum values under the dominating hydraulic site properties (Figure 2).

Thus, neither the fertilized nutrients nor the natural ions within the soil can be fully accounted for a good yield, if the aeration, the accessibility, and nutrient availability are not provided.

Soil water and gas

An increased soil volume coincides with a reduced pore volume with the dominance of finer pores and less coarser ones. Thus, the air capacity is reduced with increasing soil deformation but the changes in the pores, which contain the water available for plants depends on the applied stresses as well as the texture and the bulk density.

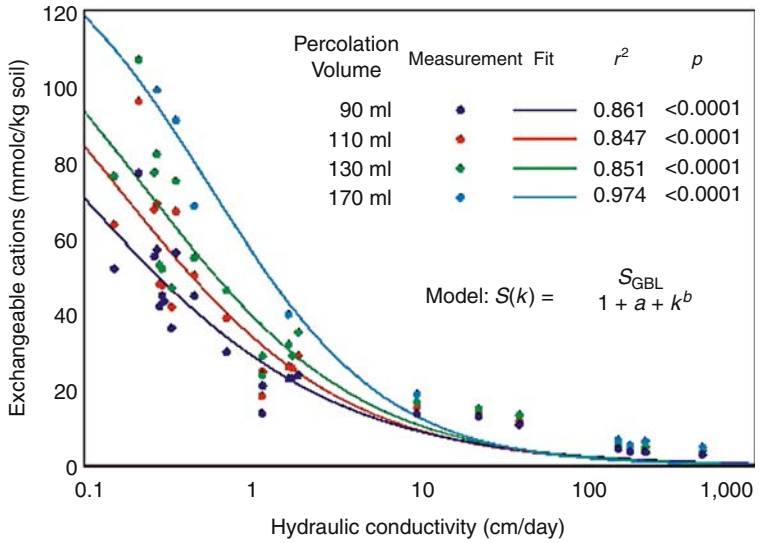

Management Effects on Soil Properties and Functions, Figure 1 Effect of soil structure on chemical exchange processes (taken from Hartmann et al., 1998).

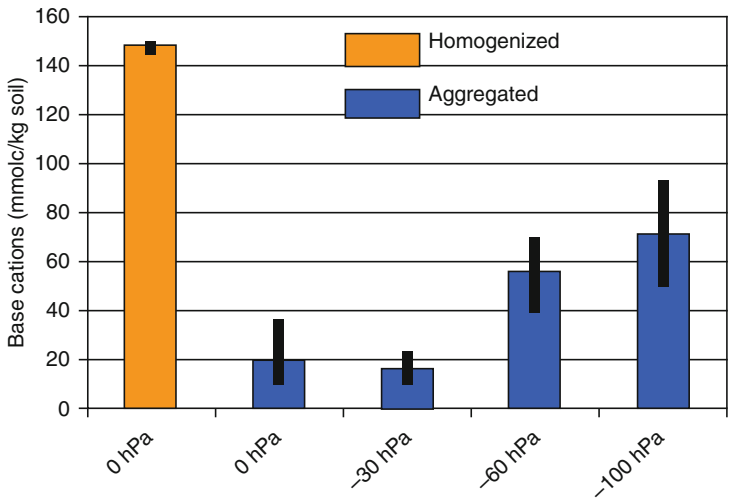

Management Effects on Soil Properties and Functions, Figure 2 Effect of predrying and of aggregation on the base cation adsorption in comparison to the homogenized conditions (Bt-horizon of a Luvisol derived from loess, blocky structure).

The hydraulic conductivity as a water available for plants depends tensorial function in principle decreases with applied stresses by many orders of magnitude while the unsaturated hydraulic conductivity is even increased at a given matric potential value (Figure 3).

Even more important is the increased relevance of the anisotropy of hydraulic functions. Mualem (1984), Tigges (2000), Doerner (2005), and Doerner and Horn (2009) documented the increasing effect of stress-and shear-affected horizontal anisotropy of the hydraulic and gas permeability, which coincides not only with a retarded gas exchange and an increased proportion of, e.g., CO_2 in the pores but which will also result in an enhanced lateral water flow and soil erosion. Figure 4 documents the stress-and strain-induced changes in hydraulic properties and functions.

Effect of soil management on gas composition

Each reduction in conducting coarse pores also result not only in a prevented CO_2 exchange to the atmosphere and a prevented O_2 flux in the soil but will also lead to anoxic conditions in the soil, which will also affect the quality and quantity of the emitted gas (Glinski and Stepniewski, 1985).

Aeration and gas exchange in soils always depend on the microbial composition and activity, which depending on the pH value and water saturation can lead to an enormous alteration of the gas composition, microbial activity and composition, and redox potential values. As an example of possible stress effects on redox potential changes in dependence of the internal soil strength (expressed as precompression stress) Figure 5 informs stress-dependent Eh value changes in an Ah horizon of a Cambisol. It can be seen that stressing with up to 35 kPa followed by a stress release (0 kPa) at both depths always resulted in a complete recovery. If exceeding the internal soil strength of approximately 42 kPa by a further increase to 47 kPa a significant and irreversible decline was detected with no recovery after stress release. Thus, all chemical elements, which undergo a valence change, depending on the actual Eh value at the given pH may be also mobilized and translocated to the more aerated soil volumes. Amongst the Eh-sensitive elements are under more un-aerated soil conditions, e.g., from the completely aerated condition: NO_3^- (to N_2O or at last NH_4^+) or CO_2 (to CH_4 in case of complete anoxic conditions) as well as Fe ($^{3+}$ to $^{2+}$) or Mn ($^{4+}$ to $^{2+}$). Thus, also the chemical compositions of the gas composition in the soil or that of the seepage water are affected.

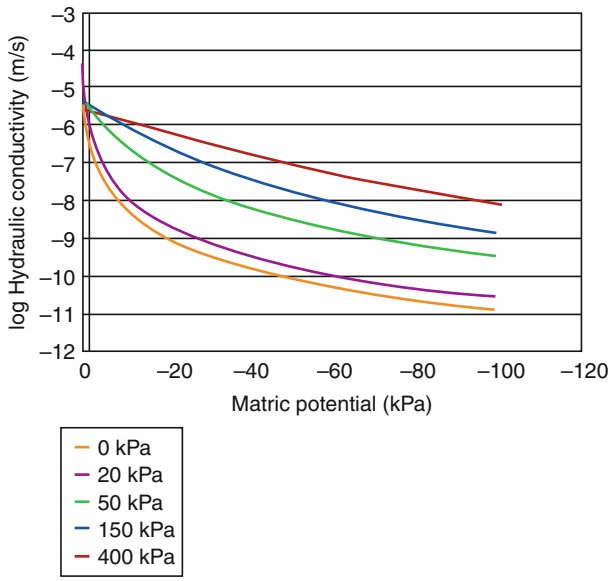

Management Effects on Soil Properties and Functions, Figure 3 Stress-dependent change of hydraulic properties: hydraulic conductivity as a function of matric potential.

Ball et al. (2000), e.g., described the effect of N_2O emission due to wheeling throughout the year and also included N-fertilization. In compacted soils, N_2O emission was significantly increased after fertilization and especially if in addition rainfall had re-saturated the soil. Under zero compaction, no intense changes were to be seen, which can be explained by a higher water infiltration rate and a quicker reaeration of the coarse and gas and water-conducting pores. If we further consider the compaction dependent reduction of CH_4 consumption in soils, which is approximately 50%, we can also calculate the CO_2 equivalents from CH_4 consumption are texture dependent (Teepe et al., 2004): 47 kg ha^{-1} a (silty clay loam), 157 (silt), and 249 (sandy loam). Assuming that

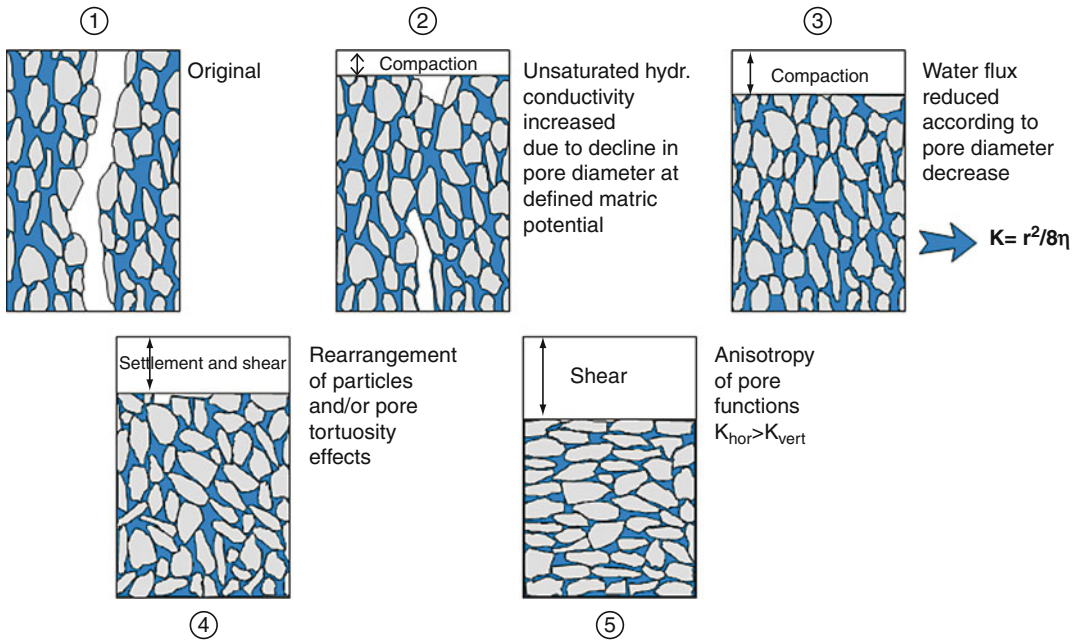

Management Effects on Soil Properties and Functions, Figure 4 Stress and strain effects on hydraulic properties.

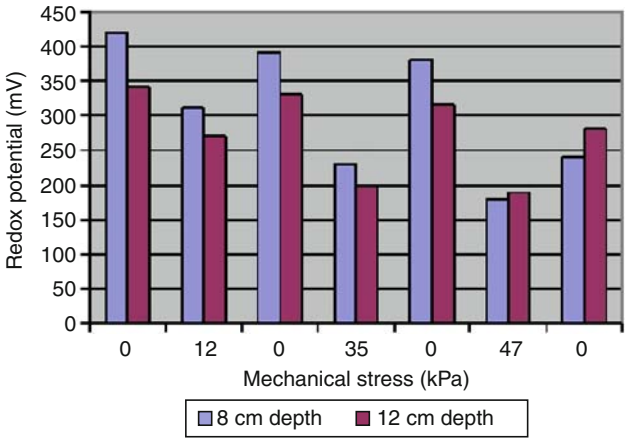

Management Effects on Soil Properties and Functions, Figure 5 Redox potential values as a function of applied cyclic mechanical stress. Cambisol Ah horizon, pH: 5.2, −60 hPa (data taken from Horn, 1985).

only 6% of the area was compacted, the reduction of the CH_4 consumption in terms of CO_2 equivalents resulted in 4, 11, and 13 kg CO_2 ha^{-1} a^{-1}. In forest soils, the spatial pattern of the depth dependent CO_2 concentration reveals a significant increase directly below the wheel track, which fades off to the side and to the depth (Figure 6).

Based on the dataset of Stepniewska et al. (1997), a soil texture-dependent resistivity values for a given redox potential value of 300 mV could be used to quantify the resistance against Eh changes. If 300 mV irrespective of the stress applied at a given texture is still available after 5 days, we could classify the soil as rigid. If, on the other hand, within less than 3 days the critical value is further declined a more severe stress effect has to be considered.

Soil deformation and thermal properties

Denser, less aerated, and more water saturated soils are not only less aerated but they are mostly cold due to the higher specific heat capacity and thermal conductivity.

Additionally, radiation effects are reduced during cold nights but as a negative effect also the often expected freezing effect for structure reamelioration is furthermore reduced.

Under European climatic conditions, such soil amelioration is mostly restricted to the plowed A horizon but does not deeper down. Even if the subsoil gets frozen, the ice lense formation gain would primarily create a horizontal platy structure due to water volume expansion during freezing. Furthermore, we have to evaluate the orientation of newly formed pores, which as soon as they are mostly horizontally oriented would collapse during the following restressing of the topsoil during trafficking.

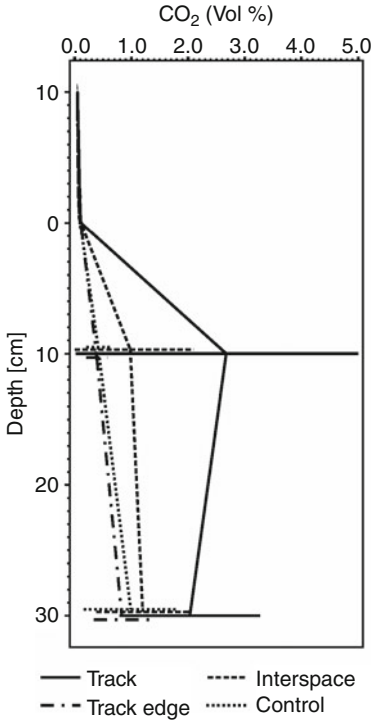

Management Effects on Soil Properties and Functions, Figure 6 CO_2-concentration in the soil air at different depths and distance from the wheel track due to the application of a chain harvester (45 Mg) in the Black Forest. The wheeling was carried out in 2000 (taken with courtesy from J. Schäffer, 2005).

Soil deformation and microbial activity

Soil compaction causes a reduced accessibility for soil microbes, which may be partly not negative because the damages caused by ingestion through collemboles and mollusk are reduced. The activity of earthworms (penetration and formation of new burrows) depends on the internal soil strength. They can apply up to 200 kPa lateral pressure in order to translocate soil particles to the side and even 100 kPa in radial direction. The less intense the tillage treatments the higher are the number of earthworms. Under conservation tillage, more than 100 individuals were counted per meter square, while less than ten were available at the same time under conventional tillage in a luvisol derived from loess. However, even if we consider these 100 individuals/m² their activity results only in the realeviation of 30 Mg/ha *a (for year), which is an enormous amount but less than 1% of the strain-affected soil compaction. McKenzie et al. (2009) documented that earthworms like Lumbricus and Allolobophora species can withstand high external stresses, which is not the fact for mesofauna: acari and collembolae, which will be squeezed under the wheels even within the top 30-cm apart from the fact that soil compaction and deformation result in a retarded aeration and accumulation of CO_2 or even CH_4 in soil pores and hinders the normal population growth.

Consequences of soil deformation on further environmental processes

The effects of soil compaction on plant growth are widespread. They depend not only on the intensity of soil compaction but also on the plant properties themselves.

The closer to the soil surface and the thicker the compacted layer is, the more pronounced negative effect on plant growth and yield. It is essential to analyze whether or not the compacted soil layer is completely impermeable or there are still a few coarse pores, which can help to reach the deeper and less dense soil layers and to overcome such limitations in the topsoil. Oxygen deficiency results in a reduced root growth, increased CO_2 and ethylene concentration and the formation of short-chained fatty acids in the soil. Because the stress propagation with depth in always three-dimensional, we also have to analyze the effects in deeper depth because compacted areas at depth will be mostly surrounded by roots but not penetrated and cause a reduced availability of nutrients and also of oxygen at these depths.

Consequences of soil deformation on soil erosion

It is obvious that stress application always results in the formation of a platy structure and horizontally oriented coarse pores, which increase the horizontal hydraulic conductivity and result in an increased water and solute transport. Among others Fleige (2000) proofed that the soil loss due to water erosion in the slightly sloppy glacial till region of Schleswig Holstein increased ten times compared to non compacted sites and also resulted in a downhill mass transport of more than 35 Mg ha^{-1} a^{-1} and the formation of a colluvisol in the flatter region (onsite damage compared to the even worse offsite effects).

Some remarks on crop yield

From the agricultural point of view, crop yield and the net benefit are the main criterion. Thus, yield decline of up to 35% in the first year after soil compaction are to be considered as more than critical. But even if these reductions are only rarely to be seen the uncertainty of getting sufficient yield continuously increased over the years. At present, more than 32 Mio ha of arable soils are irreversibly degraded even only in Europe due to soil compaction the effect is even continuously increasing in recent years. The yield decline due to soil compaction for sugar beets can be derived from the smaller beet weight per ha also because the destruction of the beets during harvest is increased.

Van den Akker et al. (1999) mentioned that a single wheeling with a 38 Mg sugar beet harvester results in an annual yield loss of 0.5%, which sums up to approximately 100 Mio € a^{-1} loss calculated on the basis of 500,000 ha in Europe.

If the machine mass of the sugar beet harvesters increases with 5 Mg/10 years (as it was the fact in the past), we have to even expect higher yield losses in the future. Concerning the yield losses of corn in the USA we have to consider approximately 6%/year due to soil compaction while corresponding losses of grain in the former USSR results in 7–8% of the total yield; sugar beets showed a decline by 3% while corn yield was lowered by 4% due to soil compaction effects. Finally, in Germany the often predicted wheat yield increase due to the beneficial climate, soil and genetic properties of the seeds under the improved CO_2 concentration in the atmosphere and the higher temperature only resulted in 0.1 Mg $ha^{-1}a^{-1}$ in Schleswig Holstein while in Bavaria the yield remained only constant irrespective of all these improvements because the proportion of the headland increased because of the larger machines, which require more space for turning round in comparison to the total field area.

Effect of soil structure degradation on the landscape hydrology

Deep drainage of rainwater requires permeable soils with a continuous and large pore system. As soon as the arable landscapes remain compacted with a reduced water infiltrability (can be reduced up to three orders of magnitude) and storage capacity. Very pronounced are these effects during and after heavy rainstorm events and can result in an increased surface water runoff also in combination with a pronounced nutrient and heavy metal leaching. If during a rain storm most of the pores become water saturated but only the coarse pores (which due to soil compaction are reduced in diameter and total amount) are still aerated but additional rainwater will completely saturate the soil volume, then the storage capacity is quickly filled and all the additional rainwater will result in surface water runoff.

If we further assume that the natural saturated hydraulic conductivity of uncompacted soils in the loess area with approximately 40% pore volume reaches 2.7 cm day^{-1} on average we can assume a corresponding water infiltration of 2.7 cm day^{-1} at a hydraulic gradient of 1. If due to soil compaction the hydraulic conductivity is reduced to 1 cm day^{-1} but the rainfall is the same as before, 1.7 cm day^{-1} of water contribute to the surface water volume. If we now multiply this amount with the total landscape area, the small value of 17 l m^{-2} result in 17,000 m^3 km^{-2}. Thus, the high floods in riverbeds like the Rhine or Elbe in Germany can be easily also related to the negative effects of subsoil compaction. Soil slaking due to the kinetic energy input of the water droplets, which is the more pronounced, the higher is the initial water saturation in combination with the increased shear forces of the water suspensions result in an even higher soil deterioration and soil loss (for more detailed information see Van der Ploeg and Schweigert, 2001 and Gieska et al., 2003).

Protection measures

The worldwide identical tendency of increased machine masses at an identical contact area pressure, which is far beyond the acceptable values for a sustainable land management prevent a natural reamelioration of the

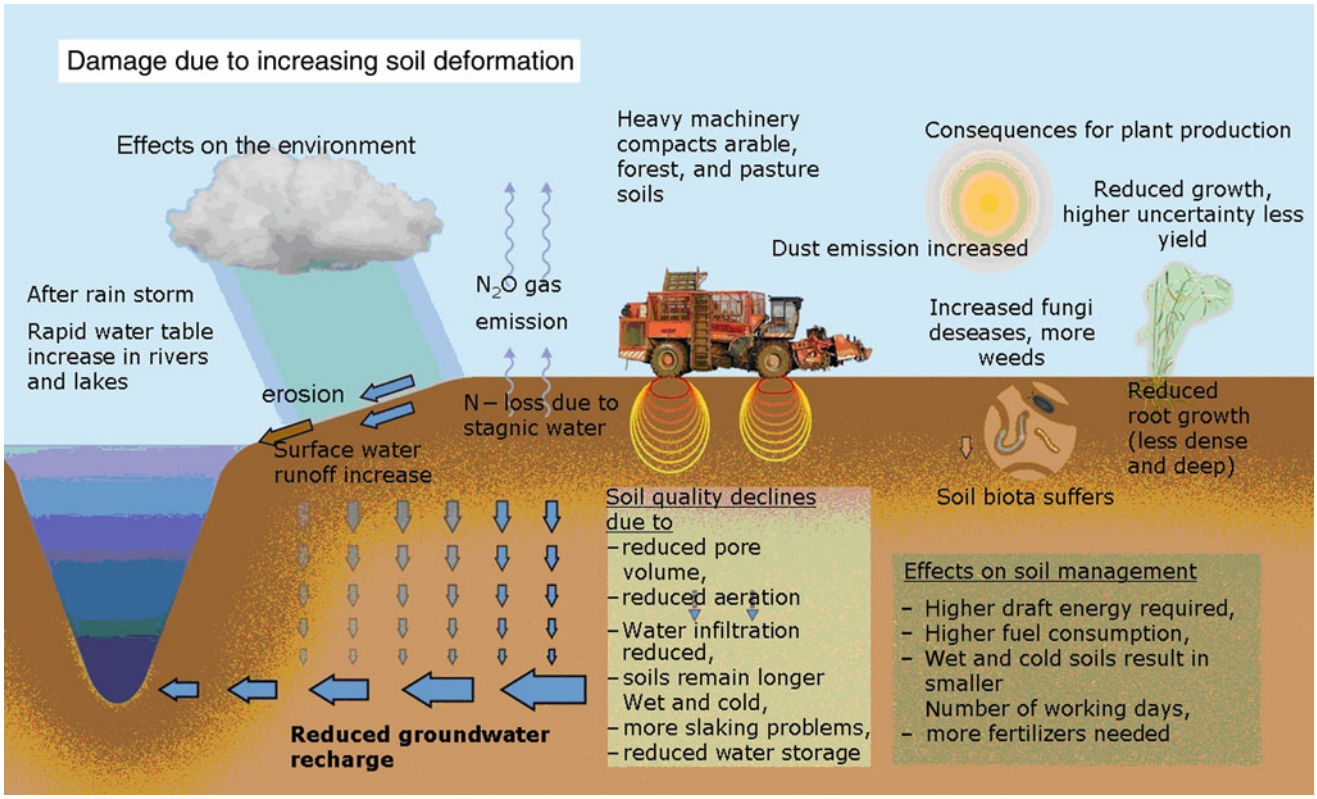

Management Effects on Soil Properties and Functions, Figure 7 Summary of the effects of stress application on soil properties and functions (translated and slightly modified from van der Ploeg et al., 2006).

precompressed (= overcompacted) soils by increasing the pore volume and improved pore continuity. In order to gain better and safer growth conditions, these precompressed (= overcompacted) and deformed soils must be improved by more site-adjusted soil management systems (conservation instead of conventional tillage and a more intense shrinkage due to water uptake by roots followed by a corresponding increased soil shrinkage and stabilization. The consequent application of traffic lanes for all field operations would result in normal compacted seedbeds in between (like in horticulture) with highest yields, the consequent application of machines, which are light and have a contact area pressure smaller than the precompression stress over depth throughout the years/decades will certainly result in a newly arranged and stronger pore system, which guarantees a better aeration and quicker water infiltration linked with a better rootability.

In the past, numerous approaches tried to improve the effectivity of the machines and to reduce the soil deformation risk but all attempts like reduced tire inflation pressure, belts, larger tires were not as successful as expected because the main problem remains the still increasing machine mass and/or the frequency of wheeling throughout the year. The final concluding picture, which underlines the multidisciplinary effects of soil deformation on site properties is shown in Figure 7.

Summary

The rigidity of soils depends primarily on the internal particle arrangement and thus on the rigidity of the soil structure, which guarantee gas, water, heat, and nutrient transport and exchange processes. If, however, the external stresses applied exceed the internal soil strength, not only the pore system collapse and will be diminished in volume and size but also the pore continuity and the accessibility of surfaces (e.g., for cation exchange) are negatively affected. Consequently, not only the plant growth, yield, and the predictability of them become more undefined but also the emission of green house gases increases or flooding events will occur more often.

Bibliography

Ball, B. C., Horgan, G. W., and Parker, J. P., 2000. Short range spatial variation of nitrous oxide fluxes in relation to compaction and straw residue. *European Journal of Soil Science*, **51**, 607–616.

Doerner, J., 2005. *Anisotropie von Bodenstrukturen und Porenfunktionen in Böden und deren Auswirkung auf Transportprozesse im gesättigten und ungesättigten Zustand*. PhD thesis, H. 68, ISBN: 0933-680X.

Doerner, J., and Horn, R., 2009. Direction-dependent behavior of hydraulic and mechanical properties in structured soils under conventional and conservation tillage. *Soil and Tillage Research*, **102**, 225–233.

European Soil Framework Directive (2006) Proposal for a directive of the European parliament and of the council establishing a framework for the protection of soil and amending directive. 2004/35/EC, p. 30.
Ehlers, W., Schmidtke, K., and Rauber, R., 2003. Änderung der Dichte und Gefügefunktion südniedersächsischer Lössböden unter Ackernutzung. *Landnutzung und Landentwicklung*, **44**, 9–18.
Fleige, H., 2000. *Ökonomische und ökologische Bewertung der Bodenerosion am Beispiel einer Jungmoränenlandschaft Ostholsteins*. PhD thesis, Schriftenreihe des Instituts für Pflanzenernährung und Bodenkunde, H. 53, ISBN: 0933-680X.
Gieska, M., van der Ploeg, R. R., Schweigert, P., and Pinter, N., 2003. Physikalische Bodendegradierung in der Hildesheimer Börde und das Bundes-Bodenschutzgesetz. *Berichte über Landwirtschaft*, **81**(4), 485–511.
Glinski, J., and Stepniewski, W., 1985. *Soil Aeration and Its Role for Plants*. Bocca Raton: CRC Press. 287 pp.
Grant, C. D., Groenevelt, P. H., and Bolt, G. H., 2002. On hydrostatics and matristatics of swelling soils. In Raats, P. A. C. et al. (eds.), *Environmental Mechanics: Water, Mass, and Energy Transfer in the Biosphere*. Geophysical Monograph 129, AGU, pp. 95–105.
Groenevelt, P. H., and Grant, C. D., 2002. Curvature of shrinkage lines in relation to the consistency and structure of a Norwegian clay soil. *Geoderma*, **106**, 235–247.
Hartmann, A., Gräsle, W., and Horn, R., 1998. Cation exchange processes in structured soils at hydraulic properties. *Soil and Tillage Research*, **47**, 67–73.
Horn, R., 1976. Festigkeitsänderungen infolge von Aggregierungsprozessen eines mesozoischen Tones. Diss. TU Hannover.
Horn, R., 1985. Die Bedeutung der Trittverdichtung durch Tiere auf physikalische. *Eigenschaften alpiner Böden.Z.f. Kulturtechnik u.Flurbereinigung* **26**, 42–51.
Horn, R., and Dexter, A. R., 1989. Dynamics of soil aggregation in an irrigated desert loess. *Soil and Tillage Research*, **13**, 253–266.
Horn, R., Taubner, H., Wuttke, M., and Baumgartl, T., 1994. Soil physical properties and processes related to soil structure. *Soil and Tillage Research*, **30**(Special Issue), 187–216.
Horn, R., Van Den Akker, J. J. H., and Arvidsson, J. (eds.), 2000. Subsoil compaction: distribution, processes and consequences. *Advances in GeoEcology*, **32**, 480S, Reiskirchen.
Horn, R., and Baumgartl, T., 2002. Dynamic properties of soils. In Warrick, A. W. (ed.), *Soil Physics Companion*. Boca Raton: CRC, pp. 17–48.
Horn, R., Fleige, H., Peth, S., and Peng, X. H. (eds.), 2006. Soil management for sustainability. *Advances in GeoEcology*, **38**, 497 pp. ISBN: 3-923381-52-2.
Horn, R., Fleige, H., Richter, F.-H., Czyz, E. A., Dexter, A., Diaz-Pereira, E., Dumitru, E., Enache, R., Rajkai, K., De La Rosa, D., and Simota, C., 2005. SIDASS project part 5: prediction of mechanical strength of arable soils and its effects on physical properties at various map scales. *Soil and Tillage Research*, **82**, 47–56.
Horn, R., Vossbrink, J., Peth, S., and Becker, S., 2007. Impact of modern forest vehicles on soil physical properties. *Forest Ecology and Management*, **248**, 56–63.
Janssen, I., Peng, X., and Horn, R., 2006, Physical soil properties of paddy fields as a function of cultivation history and texture. *Advances in GeoEcology*, **38**, 446–455, ISBN: 3-923381-52.
Lipiec, J., and Hatano, R., 2003. Quantification of compaction effects on soil physical properties and crop growth. *Geoderma*, **116**, 107–136.
McKenzie, B. M., Kühner, S., MacKenzie, K., Peth, S., and Horn, R., 2009. Soil compaction by uniaxial loading and the survival of the earthworm Aporrectodea caliginosa. *Soil and Tillage Research*, **104**, 320–323.
Mualem, Y., 1984. Anisotropy of unsaturated soils. *Soil Science Society of America Journal*, **48**, 505–509.
Or, D., and Ghezzehei, T. A., 2002. Modeling post-tillage soil structural dynamics: a review. *Soil and Tillage Research*, **64**, 41–59.
Pagliai, M., and Jones, R. (eds.), 2002. Sustainable Land Management – Environmental Protection – A Soil Physical Approach. *Advances in GeoEcology*, **35**, Catena, Reiskirchen. ISBN: 3-923381-48-4.
Peng, X., and Horn, R., 2005. Modelling soil shrinkage curve across a wide range of soil types. *Soil Science Society of America Journal*, **69**, 584–592.
Schäffer, J., 2005. Bodenverformung und Wurzelraum. In Teuffel von, K., Baumgarten, M., Hanewinkel, M., Konold, W., Spiecker, H., Sauter, H.-U., von Wilpert, K. (Hrsg.) (eds.), *Waldumbau für eine zukunftsorientierte Waldwirtschaft*. Springer, Berlin, 422 S, pp. 345–361, ISBN: 3-540-23980-4.
Soane, B., and van Ouwerkerk, C. (eds.), 1994. Soil Compaction. Elsevier Verlag, Amsterdam, ISBN: 0-444-88286-3.
Stepniewska, Z., Stępniewski, W., Gliński, J., and Ostrowski, J., 1997. *Atlas of Redox Properties of Arable Soils of Poland*. Lublin-Falenty: Institute of Agrophysics PAS and Institute of Land Reclamation and Grassland Farming.
Teepe, R., Brumme, R., Beese, F., and Ludwig, B., 2004. Nitrous oxide emission and methane consumption following compaction of forest soils. *Soil Science Society of America Journal*, **68**, 605–611.
Tigges, U., 2000. Untersuchungen zum mehrdimensionalen Wassertransport unter besonderer Berücksichtigung der Anisotropie der hydraulischen Leitfähigkeit. PHD thesis, Schriftenreihe des Instituts für Pflanzenernährung und Bodenkunde, H. 56, ISBN: 0933-680X.
Van der Ploeg, R. R., and Schweigert, P., 2001. Reduzierte Bodenbearbeitung im Ackerbau – eine Chance für Wasserwirtschaft, Umwelt und Landwirtschaft. *Wasserwirtschaft*, **91**, 9.
van der Ploeg, R. R., Ehlers, W., and Horn, R., 2006. Schwerlast auf dem Acker. *Spektrum der Wissenschaft*. August 2006, 80–88.
van den Akker, J. J. H., Arvidsson, J., and Horn, R., (eds.), 1999. Experiences with the impact and prevention in the European Community. Report 168, ISSN: 0927–4499.

Cross-references

Agrophysical Objects (Soils, Plants, Agricultural Products, and Foods)
Crop Responses to Soil Physical Conditions
Earthworms as Ecosystem Engineers
Physical Degradation of Soils, Risks and Threats

MAPPING OF SOIL PHYSICAL PROPERTIES

Jan Gliński[1], Janusz Ostrowski[2]
[1]Institute of Agrophysics, Polish Academy of Sciences, Lublin, Poland
[2]Institute of Technology and Life Sciences, Raszyn, Poland

Definition

A map is a visual reflection of an area drawn to different scales. To illustrate special purposes thematic maps are designed.

Introduction

Soil physical properties show great variability as well in vertical as horizontal scale. Their significance for

agricultural and environmental purposes requires maps (Várallyay, 1989; Várallyay, 1994; Stępniewska et al., 1997; Ostrowski et al., 1998; Wösten, 2000; Walczak et al., 2002a; Duffera et al., 2007; Iqbal et al., 2005; Leenhardt et al., 2006; Santra et al., 2008).

One can distinguish two groups of soil physical properties which are mapped:

- Current such as: water content, soil temperature
- Not significantly dependent on time such as soil mineral composition, texture, specific surface area

Maps can reflect:

- Physical short-lasting properties such as soil moisture, soil temperature.
- Physical long-lasting processes such as soil erosion and soil desertification. These maps are continuously repeated.
- Soil physical properties based on their spatial variability.

A variety of different techniques are used for construction of maps of soil physical properties. They are based on: delineation of soil units, which represent areas of determined classes of soil physical property units, remote sensing, digital format, and spatial interpretation of point-based measurements of soil physical properties. The conversion of point data into continuous raster maps allows the survey data to be incorporated into computer and more easily used for decisionmakers (Taylor and Minasny, 2006). Maps can be prepared on the basis of existing data or on data coming from analyses of field soil samples derived from representative places (areas) appointed in advance. Most maps of soil physical properties concern top soil layers, but for modeling of environmental processes mapping of deeper soil layers is also made (Stępniewska et al., 1997; Stawiński et al., 2000; Walczak et al., 2002a; Walczak et al., 2002b). Within soil taxonomic unit areas of some soil maps, the extent and distribution of physical properties such as texture and hydrology are distinguished (Białousz et al., 2005). Now, the general procedure applied in the preparation soil maps is based on the estimation semivariogram parameters of soil properties using geostatistical tools and further applying them to drawing maps using ordinary kriging (Usowicz et al., 1996; Santra et al., 2008).

Computer maps of physical properties of soils

Wösten (2000) elaborated the map of total available water for plants on a European scale. In his work he based on the database of HYdraulic PRoperties of European Soils (HYPRES) which contained information on about 4,500 soil horizons representing 95 different soil types of 12 European countries. Computerized manipulation of this database and its derived pedotransfer functions in combination with the 1:1,000,000 scale Soil Map allowed for the generation of the spatial distribution of soil water availability within Europe.

On the smaller, regional (country) scale application, the construction of maps of field water capacity, water conductivity, specific surface area, redox properties, and also potential denitrification in soils is presented on the example of Poland. These maps were prepared in cooperation between two institutes: the Institute of Agrophysics of the Polish Academy of Sciences in Lublin and the Institute of Grassland Farming and Land Reclamation in Falenty.

Construction of maps

Polish soils (mostly mineral arable soils) are very much differentiated in terms of their origin, connected with different parent rocks (mostly sands, loams and silts of glacial and post-glacial formations), location in the landscape (lowlands, uplands, mountains), and influences of climate which has a transition character between the maritime and continental. On the surface of the land, they form a mosaic of various soil taxonomic units which are cartographically presented on maps of different scales. According to the FAO classification they are Rendzinas, Phaeozems, Cambisols, Luvisols, Podzols, Fluvisols, Gleysols, and Histosols (Białousz et al., 2005). The preparation of maps of physical properties variability and differentiation of Polish arable soils was based on data derived from the existing Bank of Soil Samples (Gliński et al., 1992) stored in the Institute of Agrophysics in Lublin. The samples represent 29 soil units of similar properties concerning homogeneous areas (Table 1), distinguished on the basis of works of the Institute of Soil Science and Plant Cultivation in Puławy (Witek, 1974).

The area of soil units ranges from 380 to 40,980 km^2 in terms of their appearance in Poland. Each of the unit is represented by a number of soil profiles in proportions appropriate to its area. Soil samples with disturbed and undisturbed structures were taken from topsoils (0–20 cm), upper subsoils (20–40 cm), with predominance of the mineralization processes of the organic matter contained in it, and lower subsoils (below 40 cm) with natural features of the mineral soil substrate. This way a collection was created of soil samples coming from 1,000 soil profiles localized throughout the country, representative of the variability and differentiation of the soil cover. Soil samples collected in the Bank served for the acquisition of point data from measurements and standardized studies on physical properties of soils which were stored in the Soil–Cartographic Database (Ostrowski et al., 1998) and then computer processed to generate color maps of: field water capacity, water hydraulic conductivity, specific surface area, redox properties, and potential denitrification in soils. The maps were obtained through statistical analysis of a set of soil units and of individual measurements of random soil samples. They were plotted using computer technology by combining the results of measurements with the content of the arable land map on a scale of 1:1,000,000 and digitally recorded in the Soil–Cartographic Database. The base consists of a set of files containing the contents of the soil map and the software necessary for the storing and

Mapping of Soil Physical Properties, Table 1 Soil units, their area in Poland, and number of profiles representing particular units

No. of soil unit	Soil unit	Area (km^2)	No. of soil profiles
1	Rendzic Leptosols – pure	1,900	8
2	Rendzic Leptosols – mixed	450	8
3	Haplic Phaeozems	2,360	10
4	Haplic Luvisols and Dystric Cambisols – loose sands	40,980	169
5	Haplic Luvisols and Dystric Cambisols – light loamy sands	1,630	18
6	Haplic Luvisols and Eutric Cambisols – loamy sands	6,050	10
7	Eutric Cambisols – loamy sands over loams		26
7a	Haplic Podsols – loamy sands	18,580 (7 + 7a)	47
8	Eutric Cambisols – light loams		34
8a	Haplic Podzols – light loams	18,970 (8 + 8a)	43
9	Eutric Cambisols – medium loams		27
9a	Haplic Podzols – medium loams	9,370 (9 + 9a)	13
10	Eutric Cambisols and Haplic Luvisols – heavy loams	1,210	9
11	Eutric Cambisols and Haplic Luvisols – loams	5,700	11
12	Haplic Luvisols and Distric Cambisols – gravels	880	23
13	Eutric Cambisols – hydrogenic silts		8
13a	Haplic Podzols – hydrogenic silts	7,980 (13 + 13a)	13
14	Haplic Luvisols and Eutric Cambisols – loess	10,560	23
15	Haplic Luvisols and Eutric Cambisols – clays	500	9
16	Haplic Luvisols and Eutric Cambisols – loams and skeleton loams	1,680	10
17	Haplic Luvisols and Eutric Cambisols – loams	1,920	34
18	Haplic Luvisols and Eutric Cambisols – clays	380	7
19	Haplic Luvisols and Eutric Cambisols – silt	2,010	13
20	Eutric Fluvisols – loams and silts	5,050	10
21	Distric Fluvisols – sands	2,110	13
22	Eutric Fluvisols – light silty loam	700	7
23	Mollic Gleysols – dev. from loams and silts	6,600	31
24	Mollic Gleysols – dev. from sands	3,940	27
25	Terric Histosols	11,400	11
	Total	162,320	672

creating of various sorts of derivative maps relating to the soil cover (Walczak et al., 2002a). The basic file contains a map of soil units distribution. The main function of the processing system is grouping the soils into appropriate classes and then applying an identical color to the contours of all soils belonging to this class. As a result, a color topical map showing class distribution is created. In the mathematical approach, the solution consists in a topological connection of soil contours into one topical contour according to the assumed function of subordination. When working out the topical maps, a preliminary assumption is that a soil map will be introduced to the computer for the automatic generation of topical data by the input of transformation tables of soil units into topical units (expressed for given physical soil property values). The basis for the generation of a computer map image is a procedure based on an algorithm:

$$< J_{g1} \in_{-} O_n, J_{g2} \in O_n \ldots\ldots, J_{gm} \in O_n >\in TJ_n,$$

where TJ_n – the nth topical unit, O_n _ the nth soil evaluation, J_{g1},....., J_{gm} _ soil units belonging to the n evaluation.

Due to the character of the generalization of results, it was established that maps would be generated on the scale of 1:2,500,000, so that they can be sized to an A-3 format, ensuring appropriate clarity and legibility of the spatial structure of soil feature carted. It was assumed that soil contours with a determined property would be signaled with a coloring into which other forms of land use would be incorporated, i.e., grassland, larger housing areas (towns), forests, and inland water reservoirs. Since the distribution of the above elements, supplementing the content of the map gives sufficient information on the spatial location on the country scale, no topographic content was introduced into the maps of physical soil properties such as roads, river nets, names of towns, so as not to disrupt legibility and clarity of their content or diminish their informative value. The contours shown in the color maps group mean physical properties values within the classes of the property determined preserving also individual deviations resulting from detailed studies.

Maps of hydro-physical properties of soils

The hydro-physical properties of soils play a significant role both in agriculture, through biomass production, and in natural environment through water quality. Their knowledge is necessary for the interpretation and forecasting of nearly all physical, chemical, and biological processes which occur in soil environment. Two main hydro-physical properties of soils were mapped, e.g., those concerning field water capacity (Walczak et al., 2002b) and water conductivity (Walczak et al., 2002a). Using the standard method (pressure chamber),the relation between

soil water potential and water content within the range from 0.1 kJ m^{-3} (pF 0) to 1,500 kJ m^{-3} (pF4.2) was determined in soil samples representing the plough layers, subsoils, and deeper layers. The results obtained were subordinated to ten 5% intervals from <5 to 45–50% water capacity (cm cm^{-3}) and used to construct color maps for topsoils, upper subsoils, and lower subsoils. An example of one of such maps is shown in Figure 1.

Water conductivity coefficient k was determined in standard 100-cm^3 cylinders filled with undisturbed soil in which holes were drilled at heights of 1, 2.5, and 4 cm from the bottom and TDR humidity measuring probes together with micro-tensiometers measuring soil water potential were installed in the holes. The soil samples were saturated with water till full water capacity was reached and then left under cover for 24 h in order to reach a state of thermodynamic equilibrium. Afterward, the samples were uncovered and their humidity level and soil water potentials (at 0.1, 16, and 100 kJ m^{-3}) were monitored during evaporation. The TDR gauges were linked to a PC which made automatic measurements possible, and the values of humidity and water potential taken were recorded on the computer. These measurements were used to calculate the coefficient of water conductivity k. Its values were divided into three intervals:

- For 0.1 kJ m^{-3}– above 0.5 cm day^{-1}
- For 16 kJ m^{-3} – from 0.01 to 0.5 cm day^{-1}
- For 100 kJ m^{-3} – below 0.01 cm day^{-1}

and were then related to generalized soil units on color maps for topsoils, upper subsoils, and lower subsoils.

Maps of soil specific surface area

Knowledge of the specific surface area of soils permits joint interpretation of clay and humus content and composition in soil phenomena and processes affecting productive properties of soils and natural environment. This knowledge and cartography of this feature also makes possible better creation of spatial hydro-physical and fertility prognostic models of soil processes. Four color maps of total and external soil surface area expressed in m^2 g^{-1} of soil were elaborated for the topsoils and upper subsoils (Stawiński et al., 2000). Soils for mapping were grouped in categories, e.g., eight categories of total specific surface area for topsoils: <12, 12–16, 16–20, 20–30, 30–50, 50–70, 70–90, and >90 m^2 g^{-1}.

Maps of soil redox properties

Redox status of soils is a base for understanding many soil properties such as composition of soil solution, soil reaction, availability of water and nutrients for plants, gases emission to the atmosphere, stability of metal-organic compounds, electrokinetic soil properties, biological activity, and others. Redox potential (Eh) is a measure of soil aeration status. When analyzing soil properties under oxygen deficit due to an excessive soil moisture, a new term – *redox resistance of soil* was found purposeful to introduce (Gliński and Stępniewska, 1986). Its measure is a time (in days) after which, in a fixed conditions of moisture (full saturation with water) and temperature, soil Eh drops below 300 or 400 mV. These values, named t_{300} and t_{400} indicators, correspond with the reduction of iron and manganese in soil at 300 mV and nitrate decomposition at 400 mV. For surface layers of Polish soils, at a temperature of +20°C, values of t_{300} range from 0.2 to 4.4 days and t_{400} from 0 to 1.7 days. For deeper layers they are higher. The color maps, in the amount of 33, were gathered in the Atlas of the Redox Properties of Arable Soils in Poland (Stępniewska et al., 1997).

These maps show:

- Soil redox resistance indicators t_{300} and t_{400} of plough layers, subsoils and deeper layers at the temperatures of 4°C, 10°C, 15°C, and 20°C for t_{300}, and 4°C, 7°C, and 20°C for t_{400}
- Standardized redox potential (Eh at pH 7) at two temperatures 4°C and 20°C

The maps may be used for:

- Evaluation of hazards and agricultural damage (e.g., crop yield losses) connected with temporal water saturation of soil.
- Estimation of ecological damage connected with nitrogen losses due to denitrification and the emission of nitrous oxide (strong greenhouse gas) to the atmosphere.
- Prediction of negative ecological and agricultural effects of climate change.
- Using t_{300} and t_{400} values for land reclamation design and as an environmental parameter for hydrological calculations (admission time of soil waterlogging).

Map of potential denitrification in soils

Denitrification of nitrates (V) is the main mechanism responsible for N_2O production in ecosystems under hypoxic conditions. To show its importance the term *potential denitrification* (*PD*) was proposed as an important feature in agriculture (efficiency of nitrate fertilization) and natural environment (greenhouse gas emission). The formula used for the calculation of *PD* (kg ha^{-1} day^{-1} $N–N_2O$) is based on the knowledge of soil redox resistance indicators t_{300} and t_{400}, nitrogen content C_{NO_3-N} (mg (kg $soil^{-1}$)), soil layer thickness H (m), and soil bulk density d (Mg m^{-3}):

$$PD = 10HdC_{NO_3-N}/t_{300} - t_{400}.$$

The analyses carried out on about 700 samples representing topsoils gathered in the Bank of Soil Samples allowed to calculate *PD* for soil units of the entire territory of Poland. On the basis of homogenous values of potential denitrification six groups of *PD* were distinguished (<7.5, 7.5–15, 15–30, 30–50, 50–80, and >80) and presented in the form of a map (Gliński et al., 2000).

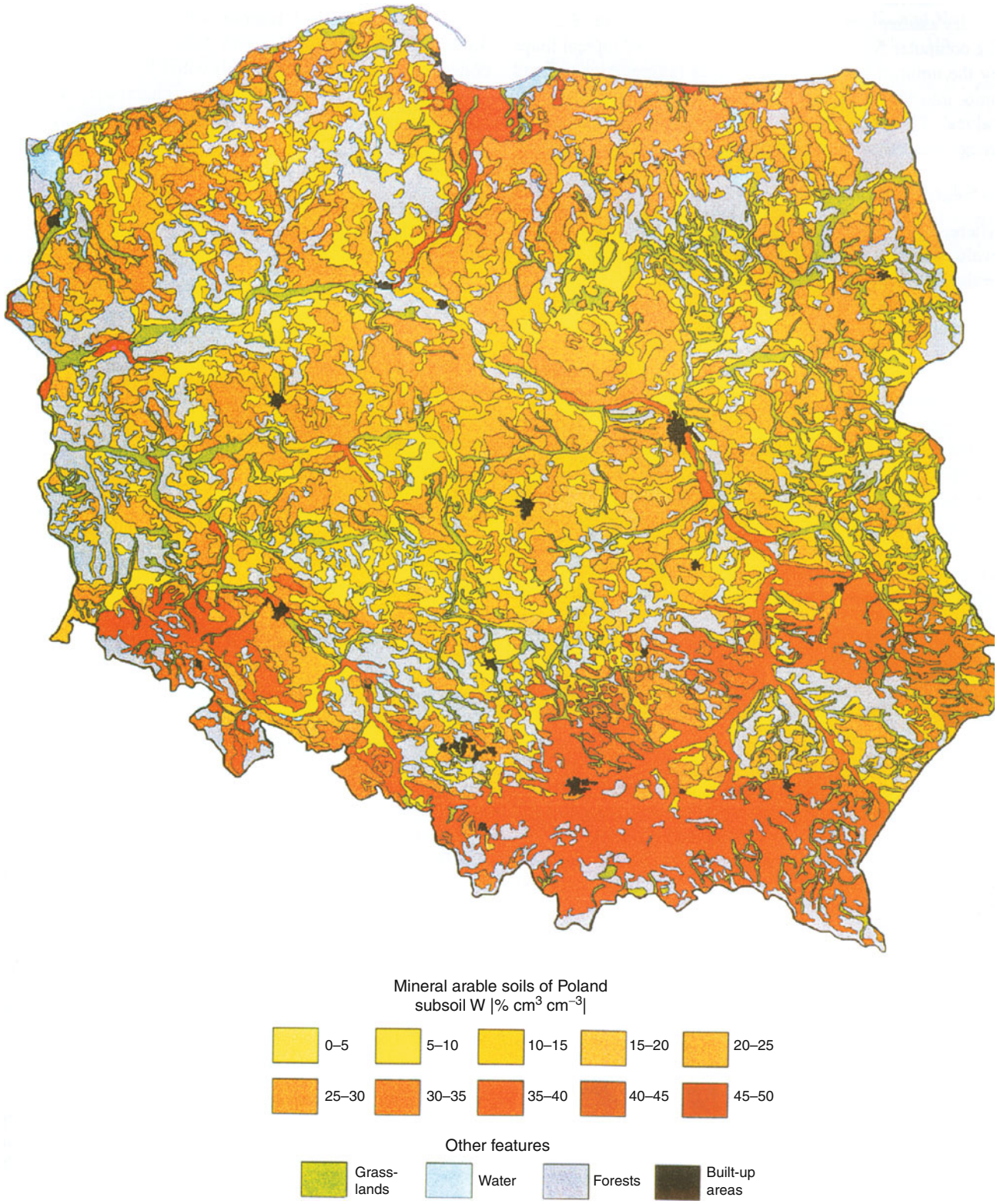

Mapping of Soil Physical Properties, Figure 1 Map of water retention at field water capacity (pF 2.2) of Polish soils. (From Walczak et al., 2002b.)

Conclusions

Maps constructed on local (plot, field) and regional scale showing distribution of soil physical properties have a definite area of interest, e.g., for irrigation planning, soil water management, land reclamation, precision agriculture (precision farming, precision tillage), drought mitigation, and efficient use of fertilizers. They are also essential for modeling various current and predicted soil physical properties (processes) and are helpful for decisions on application of these management practices to defined soil areas.

Bibliography

Białousz, S., Marcinek, J., Stuczyński, T., and Turski, R., 2005. *Soil survey, soil monitoring and soil databases in Poland*. European Soil Bureau – Research Report No. 9 ESB-RR9, pp. 263–273.

Duffera, M., White, J., and Weisz, R., 2007. Spatial variability of Southeastern U.S. Coastal Plain soil physical properties: implications for site-specific management. *Geoderma*, **137**, 327–339.

Gliński, J., and Stępniewska, Z., 1986. An evaluation of soil resistance to reduction processes. *Polish Journal of Soil Science*, **19**, 15–19.

Gliński, J., Ostrowski, J., Stępniewska, Z., and Stępniewski, W., 1992. Soil samples bank representing mineral soils of Poland (in Polish). *Problemy Agrofizyki (Series Monographs)*, **66**, 4–57.

Gliński, J., Stępniewska, Z., Stępniewski, W., Ostrowski, J., and Szmagara, A., 2000. A contribution to the assessment of potential denitrification in arable mineral soils of Poland. *Journal of Water and Land Development*, **4**, 175–183.

Iqbal, J., Thomasson, J. A., Jenkins, J. N., Owens, P. R., and Whisler, F. D., 2005. Spatial variability analysis of soil physical properties of alluvial soils. *Soil Science Society of America Journal*, **69**, 1338–1350.

Leenhardt, D., Voltz, M., Bornand, M., and Webster, R., 2006. Evaluating soil maps for prediction of soil water properties. *European Journal of Soil Science*, **45**, 293–301.

Ostrowski, J., Stępniewska, Z., Stępniewski, W., and Gliński, J., 1998. Computer maps of the redox properties of arable soils in Poland. *Journal of Water and Land Development*, **2**, 19–29.

Santra, P., Chopra, U. K., and Chakraborty, D., 2008. Spatial variability of soil properties and its application in predicting surface map of hydraulic parameters in an agricultural farm. *Current Science*, **95**, 937–945.

Stawiński, J., Gliński, J., Ostrowski, J., Stępniewska, Z., Sokołowska, Z., Bowanko, G., Józefaciuk, G., Księżopolska, A., and Matyka-Sarzyńska, D., 2000. Spatial characterization of specific surface area of Arable soils in Poland (in Polish). *Acta Agrophysica (Series Monographs)*, **33**, 1–52.

Stępniewska, Z., Stępniewski, W., Gliński, J., and Ostrowski, J., 1997. *Atlas of the Redox Properties of Arable Soils of Poland*. Lublin: IA PAN Lublin – IMUZ Falenty.

Taylor, J. A., and Minasny, B., 2006. A protocol for converting qualitative point soil pit survey data into continuous soil property maps. *Australian Journal of Soil Research*, **44**(5), 543–550.

Usowicz, B., Kossowski, J., and Baranowski, P., 1996. Spatial variability of soil thermal properties in cultivated fields. *Soil Tillage Research*, **39**, 85–100.

Várallyay, Gy., 1989. Mapping of hydrophysical properties and moisture regime of soils. *Agrokémia és Talajtan*, **38**, 800–817.

Várallyay, Gy., 1994. Soil databases, soil mapping, soil information and soil monitoring systems in Hungary. FAO/ECE International Workshop on Harmonization of Soil Conservation Monitoring Systems (Budapest, 14–17 September 1993). Budapest: RISSAC, pp. 107–124.

Walczak, R., Ostrowski, J., Witkowska-Walczak, B., and Sławiński, C., 2002a. Spatial characteristics of water conductivity in the surface level of Polish arable soils. *International Agrophysics*, **16**, 239–247.

Walczak, R., Ostrowski, J., Witkowska-Walczak, B., and Sławiński, C., 2002b. Spatial characteristic of hydro-physical properties in arable mineral soils in Poland as illustrated by the field water capacity (FWC). *International Agrophysics*, **16**, 151–159.

Walczak, R., Ostrowski, J., Witkowska-Walczak, B., and Sławiński, C., 2002c. Hydrophysical Characteristics of Mineral Arable Soils of Poland (in Polish with English summary). *Acta Agrophysica (Series Monographs)*, **79**, 5–98.

Witek, T., 1974. *An agricultural productive space in numbers* (in Polish). Puławy: Institute of Soil Science and Plant Cultivation.

Wösten, J. H. M., 2000. The HYPRES database of hydraulic properties of European soils. *Advances in GeoEcology*, **32**, 135–143.

Cross-references

Remote Sensing of Soils and Plants Imagery
Spatial Variability of Soil Physical Properties

MATRIC POTENTIAL

See *Physical Dimensions and Units Use in Agriculture*; *Water Use Efficiency in Agriculture: Opportunities for Improvement*

MATRIX OF THE SOIL

The assemblage and arrangement of the solid phase (mineral and organic components) constituting the body of the soil, and the interstices (pores) contained within it.

Bibliography

Introduction to Environmental Soil Physics (First Edition) 2003 Elsevier Inc. Daniel Hillel (ed.) http://www.sciencedirect.com/science/book/9780123486554

MEASUREMENTS NON-DESTRUCTIVE

See *Nondestructive Measurements in Fruits*; *Nondestructive Measurements in Soil*

MECHANICAL IMPACTS AT HARVEST AND AFTER HARVEST TECHNOLOGIES

Zbigniew Ślipek, Jarosław Frączek
Department of Mechanical Engineering and Agrophysics, University of Agriculture, Kraków, Poland

Definition

Mechanical impact. A complex of physical phenomena that takes place at impact of two or more bodies.

Harvest technology. A sequence of activities and operations occurring one after the other, performed by machine or carried out manually in order to gather the ripened crop from the field.

After harvest technology. Operations regarding the handling of harvested crop, including transportation, sorting, cleaning, drying or cooling, storing, and packaging.

Introduction

Each technological system of harvest and post-harvest handling requires the use of machines whose operating elements bring about plant material load, thus permitting the end product to be satisfactory both in terms of quantity and quality (Figure 1). On the one hand mechanical impact is required in order to permit the machine to function according to its purpose, but on the other hand this often causes undesired effects (loss). The desire to increase machine output is connected with the ever more aggressive impact of machines on material, which usually leads to greater damage being caused to crops.

There are two ways in which the rational use of machines for harvest and post-harvest handling may take place:

- By appropriate selection and by steering the operating parameters
- By selecting the best time for performing the technological process

Theory

Machine–plant interaction that takes place during the post-harvest collection and handling process is primarily of an impact nature. Concerning the physical description of interaction that occurs in such situations, it is necessary to take into account the mechanics of impact and its implication to plant materials (Mohsenin, 1986).

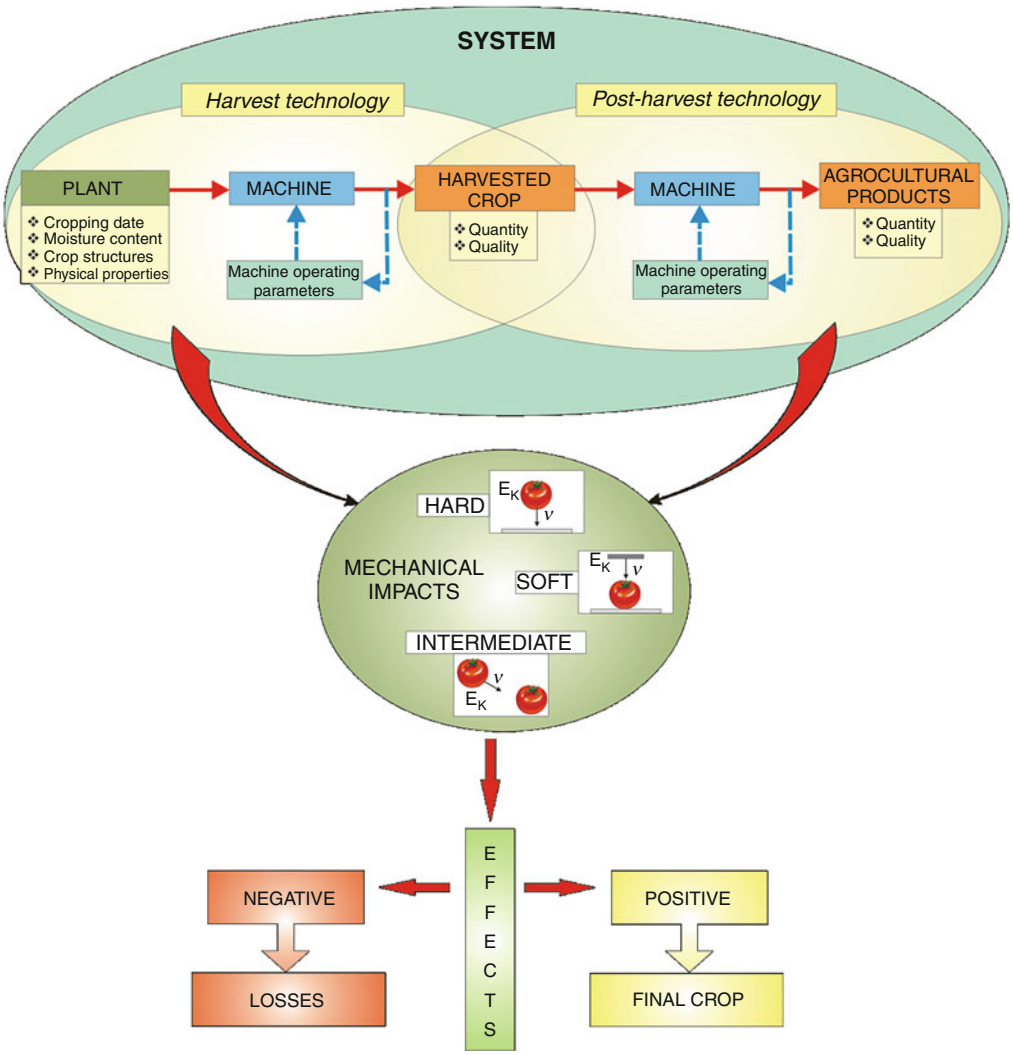

Mechanical Impacts at Harvest and After Harvest Technologies, Figure 1 Machine–plant material system relations.

In order to indicate the presence of forces during impact it is necessary to consider the mechanical properties of both the impacting object and the object being impacted. A typical characteristic of impact is the occurrence of so-called instantaneous forces, which act very briefly ($\Delta t \rightarrow 0$) and attain high values in comparison to other forces that occur. The measure for instantaneous forces is the impact pulse:

$$S = \int_{t_0}^{t_0+\Delta t} P(t)\mathrm{d}t \tag{1}$$

where S – impact pulse t_0 – moment of occurrence of the instantaneous force Δt – time of operation of the instantaneous force $P(t)$ – instantaneous force.

The course of impact may be divided into two phases: compression and restitution (Gilardi and Sharf, 2002). The first phase, which involves a sudden increase in force, starts as soon as the bodies encounter each other at t_0 point and end at t_m point when distortion attains maximum value (Figure 2a). The relative velocity of both bodies is then equal to zero. In the second phase instantaneous force decreases. The shape of the $P(t)$ curve depends on:

- The elastic–plastic properties and dimensions of the impacting bodies
- Body surface shape (particularly at the point of contact)
- The direction of the velocity vector
- Impact energy value
- Freedom of distortion

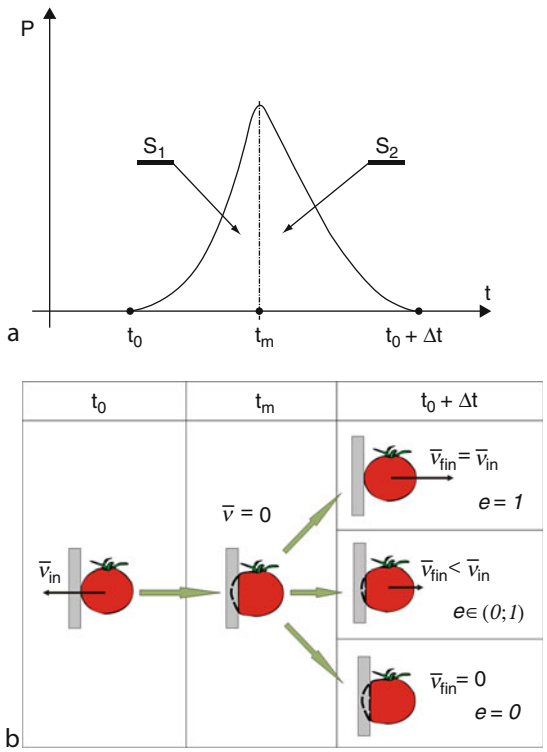

Mechanical Impacts at Harvest and After Harvest Technologies, Figure 2 Body impact against a motionless obstacle (**a**) change of instantaneous force; (**b**) types of impacts.

For plant materials this curve is determined empirically. S_1 and S_2, impact pulse values, respectively in phases one and two of impact, serve the purpose of determining the restitution coefficient:

$$e = \frac{S_1}{S_2} \tag{2}$$

It defines the proportion between elastic and plastic distortion. If $e = 1$ we have to do with ideally elastic impact; however for $e = 0$ impact is ideally plastic. For true plant materials "e" belongs to the (0; 1) range and to a very large degree depends on the moisture content of the material (the lower the moisture content the greater the restitution coefficient). It is determined when a body impacts a motionless obstacle (Figure 2b). In such cases normal velocity is defined: initial v_{in} and final v_{fin}, while the restitution coefficient is calculated as the ratio of both velocities.

Total distortion ε that takes place during impact is the sum of elastic distortion ε_s and plastic distortion ε_p. The magnitude of these distortions depends on anatomical and morphological structure and the physical properties of plant material. The anisotropicity of these types of materials hinders any clear definition of mechanical and endurance parameters, which are very strongly correlated with moisture, which has a decisive influence on elastic and plastic properties (and therefore on the type of distortion). Plant materials with large water content are dominated by plastic traits, while dry material contains elastic or brittle characteristics. This is reflected in the effects of impact. Concerning materials with large water content, the energy of elastic distortions constitutes only a small part of overall distortion energy. During harvest and post-harvest handling one may distinguish the following types of load (Figure 1):

- Hard – these are manifest when the initial value of E_{in} impact kinetic energy is dissipated by the impacting body (e.g., the fall of an apple, tomato, or melon onto the hard surface of a crate leads only to the distortion of the impacting fruit).
- Soft – this is the kind of impact in which distortion of the impacted body is considerably greater than distortion of the impacting body (e.g., the impact of a beater against threshed material leads only to the distortion of the impacted plant mass).
- Intermediate – this is the simultaneous distortion of the impacting body and of the impacted body (e.g., the fall of a single piece of fruit onto a pile of fruit kept in a container leads to all of the impacted bodies being distorted).

In terms of agrophysics the negative effect of impact is plastic distortion, which leads to a permanent deterioration

in the quality of the biological material. The following should be distinguished:

- Local distortion – these cover a relatively small area that focuses immediately on the point of impact and leads to different types of micro-damage (abrasion, skin puncture, etc.). These distortions are the result of instantaneous force and depend on local plant material susceptibility and the shape of the surface at the point of contact.
- Global distortion – these appear in the form of disturbance waves (distortions, stress) covering the entire volume of the impacted body. Under such circumstances permanent distortions appear on a macro scale (grain fragmentation, tomato cracking, apple crushing etc.).

It must be noted that surface and internal stress caused during impact are far greater at the point of contact than beyond that point.

Harvest and after harvest processes – agrophysical aspects

Grain crops

Most frequently the harvesting of these plants takes place in the form of a single phase. The technological process involves the cutting of plants, transport, threshing, separation and cleaning, and the gathering of grain (seed) in a container. In combine-harvesters, the most intensive effect on plant material takes place in the threshing unit which, depending on the construction, threshes by striking, wiping, and vibrating the threshed material. Threshing drum operations considerably distort plant mass (e.g., cereals) by soft impacts, which, depending on instantaneous contact conditions (moisture content in grain, grain orientation in terms of the working element, collision velocity, and friction) could lead to total grain fragmentation or to a variety of damage to the grain. Low intensity threshing which is favorable in terms of mechanical damage (low drum revolutions, large operating slot between the drum and the threshing floor) may, however, cause grain loss through incomplete grain threshing.

Threshing output and effectiveness depends on:

- The properties of the threshed material (type and variety, material threshing capacity, moisture content, the elastic properties of stalks or culms, the ration of grain to straw, and others)
- Technical conditions (the type of threshing unit, regulating parameters, and others)
- Threshing unit feed (the volume of feed, evenness, the arranging of plants in the threshing layer, and others)

The operating parameters of modern combine-harvesters may be steered electronically, on the basis of information on the exit and entry points of harvested material, supplied online. The implementation of information used for steering purposes is the subject of research. The gauging of the mechanical properties of plant material, including susceptibility to mechanical impact, is carried out at laboratory workstations, which permit the application of precise loads under determined and controlled conditions (Kang et al., 1995).

Transport, cleaning, and drying take place after the harvesting of grain. During these processes the material is subject to a variety of additional mechanical impacts. The danger of damaging the grain during these processes is, admittedly, far smaller; however, mechanical load may overlap and the damage previously caused to grain may become worse (Frączek and Ślipek, 1999). This leads to a reduction in raw material quality during storage (infestation by microorganisms, the settling of pests, increased respiration intensity) and processing. Mechanical damage to grains to be used as seeds (in particular damage to the germ) may reduce their ability to germinate and emerge.

Fruits and vegetables

The market of today requires that fruits and vegetables, in particular those items intended to be eaten directly, be of high quality – this includes the right shape, color and, above all, the absence of any damage. The collection of these products with the use of machines, therefore, requires that extreme care be exerted as a result of load impact. The technological collection of fruit is based on the mechanical effects of vibrating or rotating parts.

Mechanical collection from trees usually takes place by means of vibration (e.g., Mateev and Kostadinov, 2004). The fruit falls on special screens which are spread out beneath the crowns of trees or (when using simplified technologies) directly onto the ground from where it is gathered and loaded onto containers. These types of technologies are primarily used when fruit is collected for processing.

Fruits such as raspberries, currants, gooseberries, and strawberries are collected with the use of harvesters only for processing purposes. Collection for consumption purposes still takes place by hand. That does not mean that with this technology the fruit does not come in direct contact with mechanical elements. During collection various types of devices are used in order to facilitate manual collection and increase output (conveyors, elevators). In recent times, the use of autonomous robots for collecting fruit considerably decreases load impact, which is the reason why fruit gets damaged. Further development of these robots will undoubtedly help reduce the damage caused to fruit, particularly if collected for direct consumption purposes.

During the mechanical collection of fruit it is also important to make sure that machines operate under conditions not permitting any considerable damage to occur to the parent plant because of the need for yielding in the next vegetation season.

The main purpose of post-harvest technologies is to increase the added value of the product. Various technological lines perform the selection, cleaning, washing, sanitation, classification, weighing, and packing of products. While these technologies are in operation, mechanical influence, admittedly, takes place at low mechanical speed, but still the fruits and vegetables are exposed to the danger of damage and bruising (e.g., Ragni and Berardinelli, 2001). When products are subject to gravitational transport or change the direction in which they move they are particularly prone to damage.

The technologies for collecting vegetables usually involve separating the usable part growing above the ground (e.g., cabbage, cucumber, tomato), extracting the root (e.g., carrot, parsley) or tubers (potatoes), separation, gathering the yield, and transporting it. Most frequently machines damage the skin and bruise the harvestable products. During post-harvest handling the products are calibrated, washed, weighed, and packed. Multiple impact events and associated damage result later in greater respiration intensity and loss of storage life.

Conclusion

Originally, research in agrophysics concentrated on assessing various mechanical traits of agricultural plants and was based primarily on destructive methods. In recent years a range of nondestructive methods of assessing the physical condition of plant material has been elaborated (e.g., Ortiz et al., 2001). These methods include image analysis (size, shape, weight, surface morphology, skin color), electrical and optical properties, vibration and acoustic tests and nuclear magnetic resonance techniques. Destructive methods that offer direct information about the mechanical properties of fruits and vegetables (mechanical impact tests) are used less and less frequently when assessing the suitability of plants for collection. These tests, however, are used for verifying the methods of direct assessment, outlining the mechanical characteristics of materials for the purpose of designing machines or for modelling work processes.

Post-harvest collection and handling machines whose designs are based on comprehensive scientific know-how, should meet the requirements on high quality and safety of agricultural products. The implementation of mechatronic systems permits, to an increasingly large degree, the subtle control and steering of technological processes. Comprehensive operations aimed at improving the quality of agricultural products require thorough knowledge of machine and plant systems. It is particularly important to be aware of the physical parameters of plant material, which are quickly and easily gauged in the dynamic technological processes.

Bibliography

Frączek, J., and Ślipek, Z., 1999. Fatigue strength of wheat grains. The analysis of grain deformation at multiple loads. Part 1. *International Agrophysics*, **13**, 93–97.
Gilardi, G., and Sharf, I., 2002. Literature survey of contact dynamics modelling. *Mechanism and Machine Theory*, **37**, 1213–1239.
Kang, Y. S., Spillman, C. K., Steele, J. L., and Chung, D. S., 1995. Mechanical properties of wheat. *Transactions of the American Society of Agricultural Engineers*, **38**, 573–578.
Mateev, L. M., and Kostadinov, G. D., 2004. Probabilistic model of fruit removal during vibratory morello harvesting. *Biosystems Engineering*, **87**, 425–435.
Mohsenin, N. N., 1986. *Physical Properties of Plant and Animal Materials*, 2nd edn. New York: Gordon and Breach Science.
Ortiz, C., Barreiro, P., Correa, E. F., Riquelme, F., and Ruiz-Altisent, M., 2001. Non-destructive identification of woolly peaches using impact response and near-infrared spectroscopy. *Journal of Agricultural Engineering Research*, **78**, 281–289.
Ragni, L., and Berardinelli, A., 2001. Mechanical behaviour of apples, and damage during sorting and packaging. *Journal of Agricultural Engineering Research*, **78**, 273–279.

Cross-references

Agrophysical Properties and Processes
Crop Yield Losses Reduction at Harvest, from Research to Adoption
Nondestructive Measurements in Fruits

MECHANICAL RESILIENCE OF DEGRADED SOILS

Heiner Fleige
Institute for Plant Nutrition and Soil Science, Christian-Albrechts-University zu Kiel, Kiel, Germany

Mechanical resilience of soils can be defined by the value of the precompression stress (Pc), which depends especially on soil texture, soil structure, and water content. Pc is derived from confined compression tests on undisturbed, aggregated, and unsaturated soils. It is assumed that at stresses lower than the Pc, an elastic stress path exists, resulting in no extra soil deformation and thus, no change in the pore system and its function. Stresses beyond the Pc induce changes of pore functions and pore continuity because of plastic soil deformation (= degraded soil). Consequently, not only water infiltration will be reduced but it also causes reduced gas, and water fluxes, as well as water logging, interflow, runoff, and soil erosion. The prediction of the Pc and its effects on physical properties by pedotransfer functions as well as Pc-maps on different scales (e.g., Europe, Germany, farm scale) are demonstrated in Horn et al. (2005) and Horn and Fleige (2009).

Bibliography

Horn, R., Fleige, H., Richter, F.-H., Czyż, E. A., Dexter, A., Diaz-Pereira, E., Dumitru, E., Enarche, R., Mayol, F., Rajkai, K., De la Rosa, D., and Simota, C., 2005. Prediction of mechanical strength of arable soils and its effects on physical properties at various map scales. *Soil and Tillage Research*, **82**, 47–56.
Horn, R., and Fleige, H., 2009. Risk assessment of subsoil compaction for arable soils in Northwest Germany at farm scale. *Soil and Tillage Research*, **102**, 201–208.

MEMBRANES, ROLE IN WATER TRANSPORT IN THE SOIL–ROOT–XYLEM SYSTEM

Marian Kargol
Independent Department of Environment Protection and Modelling, The Jan Kochanowski University of Humanities and Sciences, Kielce, Poland

Introduction

This article discusses agrobiophysical aspects of soil water intake by a plant root and water transport along its radial route. In other words, this article presents certain interpretative ideas explaining the mechanisms of water transport in the soil–root–xylem system. In this context, a certain amount of basic information on membranes (cell membranes in particular) and permeability of various substances across them shall be presented first. Next, major membrane theories on the processes of water intake from the soil and its two-way transport across the root (from the soil to the xylem of the vascular cylinder, and in the opposite direction) shall be discussed. The issue of root pressure generation shall also be investigated (Fiscus, 1975, 1986; Ginsburg, 1971; Kargol, 1994, 1995, 2007; Pitman, 1982; Steudle et al., 1987; Taura et al., 1987).

Membranes and mathematical formalisms of their substance transport

Porous membranes

In general, membranes can be divided into *artificial* and *biological*. The former include, for example, cellophane, nephrophan, or collodion membranes. The latter include cell and cellular organelle membranes, as well as tissue membranes.

In research practice, we mostly deal with porous membranes. This also pertains to cell membranes. Porous membranes can be divided into two groups, that is, *homogeneous* and *heterogeneous*. A membrane is homogeneous if its pores do not differ from one another in cross-section radius dimensions. If a membrane's pores do differ from one another in their cross-section radius dimensions, it is to be treated as heterogeneous. Processes of permeability across a variety of membranes have been investigated mainly with the use of the Kedem & Katchalsky (KK) formalism equations (Katchalsky and Curran, 1965). In recent years, equations of the mechanistic formalism (MF) have been developed (Kargol, 2002, 2006, 2007; Kargol and Kargol, 2003, 2006).

Equations of the KK formalism

Transport equations of the KK formalism have been derived on the grounds of linear thermodynamics of irreversible processes, basing on a model of a membrane treated as a "black box." A practical version of these equations may be thus written:

$$J_v = L_p \Delta P - L_p \sigma \Delta \Pi, \tag{1}$$

$$j_s = \omega \Delta \Pi + (1 - \sigma)\bar{c}_s J_v, \tag{2}$$

where J_v and j_s are density of the solution volume flow (v) and density of the solute flow (s); $\Delta P = P_2 - P_1$ is the mechanical pressure difference between P_2 and P_1; $\Delta \Pi = RT(C_2 - C_1)$ is osmotic pressure difference; L_p, σ and ω are coefficients (of filtration, reflection, and permeability); $\bar{c}_s = 0.5\ (C_1 + C_2)$ is the mean concentration of concentrations C_1 and C_2; R is the gas constant; T is temperature.

Transport parameters occurring therein are given by the formulas

$$L_p = \left(\frac{J_V}{\Delta P}\right)_{\Delta \Pi = 0}, \tag{3}$$

$$\sigma = \left(\frac{\Delta P}{\Delta \Pi}\right)_{J_v = 0}, \tag{4}$$

$$\omega = \left(\frac{j_S}{\Delta \Pi}\right)_{J_v = 0}. \tag{5}$$

The above notation of Equations 1 is adequate to the membrane system as schematically depicted in Figure 1. In this system, the membrane M separates the compartments A and B, filled with solutions, which satisfy the inequality $C_1 < C_2$. They are under mechanical pressures, which satisfy the relation $P_1 < P_2$. Generally speaking, the KK equations are rather difficult in terms of interpretation. This pertains particularly to the parameter ω, which appears in Equation 2. This results from the fact that this parameter, as defined by the Formula 5, is determined at $J_v = 0$, that is, at simultaneous existence on the membrane of two stimuli that satisfy the relation: $|\Delta P| = |-\sigma \Delta \Pi|$.

This means that, in the case of membranes for which σ is found in the interval $0 < \sigma < 1$, the transport of a given solute across the membrane is generated by two stimuli. Hence it follows that ω is not only the coefficient of diffusive solute permeability. The terms $\omega \Delta \Pi$ and $(1-\sigma)\bar{c}_s J_v$ also pose problems for interpretation. According to this

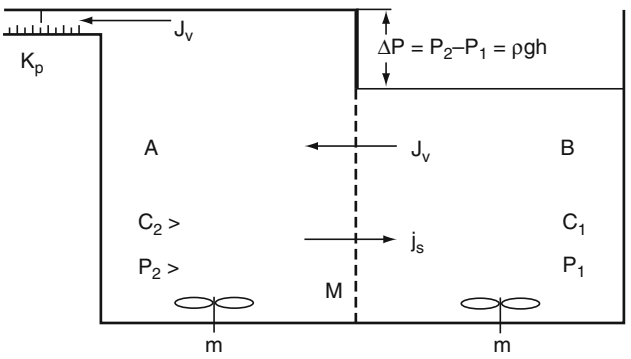

Membranes, Role in Water Transport in the Soil–Root–Xylem System, Figure 1 Model membrane system with stirrers m,m (description in text).

formalism, membranes can be divided into *semipermeable* (at $\sigma = 1$), *selective* (when $0 < \sigma < 1$), and nonselective (if $\sigma = 0$).

Equations of the mechanistic formalism (MF)

In research work, we mainly deal with porous membranes. This also pertains, as we now know, to cell membranes. Consequently, in recent years, we have developed the so-called mechanistic formalism for membrane substance transport (Kargol, 2002, 2006, 2007; Kargol and Kargol, 2003, 2006). The equations of this formalism take the following forms:

$$J_{vm} = L_p \Delta P - L_p \sigma \Delta \Pi, \tag{6}$$

$$j_{sm} = \omega_d \Delta \Pi + (1 - \sigma)\bar{c}_s L_p \Delta P, \tag{7}$$

where (analogous to the KK equations), J_{vM} is the solution volume flow and j_{sM} is the solute flow. These flows are functions of the pressure difference ΔP and the pressure difference $\Delta \Pi$.

Individual terms of these equations signify filtration, osmosis, diffusion, and convection. The equations have been derived on the basis of a model of the membrane system as shown in Figure 2. In this system, the heterogeneous porous membrane M contains the statistical number of cylindrical pores permeable to water. The membrane separates the compartments A and B, which contain solutions of the concentrations C_1 and C_2 under mechanical pressures P_1 and P_2.

In a real membrane, pores are arranged randomly. In order to facilitate the present considerations, it has been assumed that pores of that membrane are arranged according to their dimensions in one direction, from the pores with the smallest radiuses (r_1^{min}), to the largest ones (r_N^{max}). With reference to this membrane, it is possible to find such a solute (s) with such a molecule radius r_s that the following relation will be fulfilled:

$$r_1^{min} = r_w < r_2 \ldots < r_s < \ldots < r_N^{max},$$

where r_w is the radius of the solvent (water) molecules. Under the circumstances, the membrane M may be divided into Part (a), which contains a certain number n_a of semipermeable pores (with the reflection coefficient $\sigma_a = 1$ and filtration coefficient L_{pa}), and Part (b), which contains $n_b = N - n_a$ of permeable pores. This part of the membrane has the filtration coefficient L_{pb} and reflection coefficient $\sigma_b = 0$. From the above, it follows that a single pore of the membrane may take values of the reflection coefficient σ_p amounting to either 0 or 1 (Kargol, 2002, 2006; Kargol and Kargol, 2003a, b, 2006).

Having analyzed the membrane system as shown in Figure 2, it is easy to understand that $J_{va} = J_{vwa}$ is the solvent (water, w) volume flow, while J_{vb} is the solution volume flow, which permeates across Part (b) of the membrane. The flow J_{vb} has two components, that is, J_{vwb} (water volume flux) and J_{vsb} (solute volume flux). These flows, in turn, also have two components each, that is, $J_{vwb}^{\Delta P}$ and $J_{vwb}^{\Delta \Pi}$, and J_{vsd} and J_{vsk} (which are solvent (w) and solute (s) volume flows respectively). All these flows are generated by the stimuli ΔP and $\Delta \Pi$ respectively. It must be noted that in the light of this membrane model, the transport situation appears to be absolutely clear in terms of interpretation. On this basis, it also makes sense to say that the mechanistic formalism for membrane transport (MF) offers a more thorough investigation tool than the KK formalism.

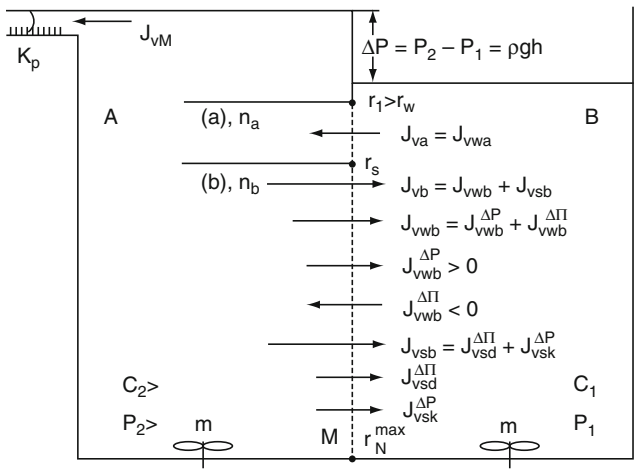

Membranes, Role in Water Transport in the Soil–Root–Xylem System, Figure 2 Membrane system (M, membrane; A and B, compartments; m, m, stirrers).

On the equivalence of the equations of the KK formalism and the MF formalism

Transport equations of the mechanistic formalism (MF) may in general be treated as alternative to the equations of the KK formalism. This view results mainly from the fact that the equations for the solute flow of these formalisms, that is, Equations 2 and 7, display certain differences. Yet thanks to our introduction of the so-called transport parameter correlations between L_p, σ and ω (KK), and L_p, σ and ω_d (MF), it is easy to observe that these (KK and MF) equations are mutually equivalent (Kargol, 2007; Kargol and Kargol, 2006). The relations are given by the formulas

$$\omega = (1 - \sigma^2)\bar{c}_s L_p, \tag{8}$$

$$\omega_d = (1 - \sigma)\bar{c}_s L_p. \tag{9}$$

On the basis of the above, the following relation is obtained: $\omega = \omega_d (1 + \sigma)$.

Thanks to these relations, it becomes possible to use – for further and more thorough investigations – the enormous experimental potential (related to substance permeation across cell membranes), which has so far been obtained on the basis of the transport equations of the KK formalism.

Cell membranes as porous structures

In general, it may be stated that in research practice we mainly deal with porous membranes. As is becoming increasingly well known, cell membranes are porous, too. Suffice it to say that cell membranes have various pores (channels), through which in a controlled manner various substances, including water can penetrate (Kargol, 2007; Stryer, 2000). Speaking about these pores, we also mean water channels, formed by certain transport proteins (called aquaporins). The porous structure of the cell membrane is also formed by ion channels through which (when open) not only ions but also water can pass. These channels have hydrophilic internal walls and are filled with water. Pores formed by some antibiotics, located in the lipid bilayer of the cell membrane, may also be permeable to water. Moreover, certain pores can occur directly in the lipid bilayer of cell membranes. All these pores vary from one to another in terms of their cross-section radius dimensions. They fulfill various specialized transport functions pertaining to permeability of water and various solutes through them.

Membrane ideas for explanation of water transport processes across the root

We shall now consider some basic issues related to agrobiophysical aspects of water intake from the soil by plants, and water transport across the root (Fiscus, 1975, 1986; Ginsburg, 1971; Kargol, 1994, 1995, 2007; Pitman, 1982; Steudle et al., 1987; Taura et al., 1987). The discussion of these issues will be preceded by an outline of the root structure.

Anatomical structure of the root

In the soil, the root must have particular contact with the water found therein. It is also important for the contact to occur mainly in the trichome zone of the root. This zone is the most capable of water intake. With a view to facilitating our discussion of the mechanisms of root water intake (as well as water movement to the xylem of the vascular cylinder), let us look at its main structural features. They have been shown schematically in Figure 3. The protoplasts of primary bark cells are, as we know, joined with one another by means of cytoplasmic bridges (plasmodesmata). With the help of these bridges, they are also linked – on the outside – with epidermis cell protoplasts, and on the inside – with endodermis cell protoplasts. The protoplasts of the parenchyma cells of the vascular cylinder are similarly joined to the endodermis. Thus, the root symplast spreads from the epidermis to the xylem, forming a cytoplasmatic continuum. This continuum provides a symplastic water route. It is illustrated by Line (S_y).

Cell walls and intra-cell voids form the so-called apoplastic water route. This route is shown by the broken line (A_p) in Figure 3. Even though it stretches from the epidermis to the xylem, it still has in the endodermis layer a significant barrier (in connection with the existence of the Casparian band therein). In general, in the root radial water route, three barriers can be distinguished. They have been marked with Figures 1, 2, and 3.

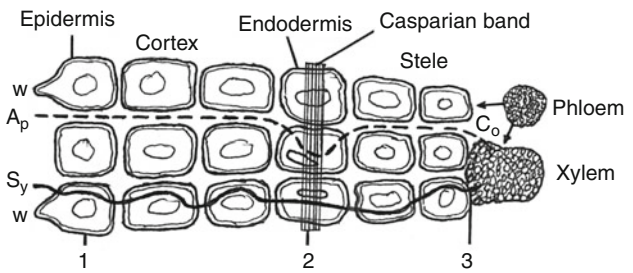

Membranes, Role in Water Transport in the Soil–Root–Xylem System, Figure 3 Fragment of root cross section, trichome zone (S_y, symplastic route; A_p, apoplastic route; w,w, trichomes; 1, 2 and 3, barriers).

The Fiscus single-membrane theory of water transport across the root

Ascribing to barriers 1, 2, and 3 (cf. Figure 3) the status of membranes, several membrane models have been developed to emulate the root radial water route. The simplest of these is the single-membrane model, as proposed by Fiscus (Fiscus, 1975, 1986). In this model, shown in Figure 4, all the three above mentioned barriers have been replaced with one membrane M with the filtration coefficient L_{pr}, the reflection coefficient σ_r and the permeability coefficient ω_r. The membrane separates two solutions of the concentrations C_{so} and C_{sx}, that is, the soil solution and the exudate (the xylem solution). These remain under mechanical pressures P_o and P_x respectively. Basing on that model, it has been possible (on the basis of the KK equations) to determine experimentally the values of all

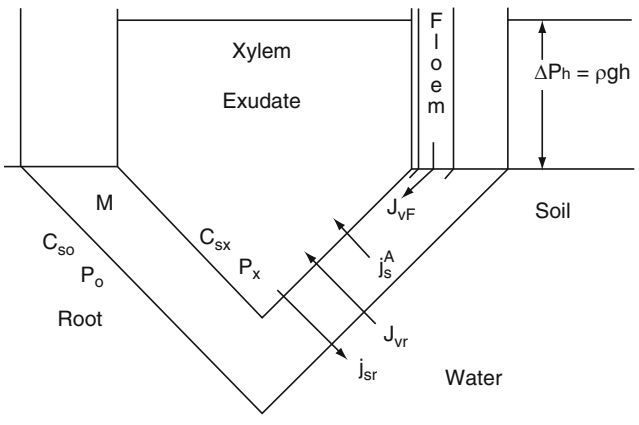

Membranes, Role in Water Transport in the Soil–Root–Xylem System, Figure 4 Single-membrane model of root radial route (M is the membrane; C_{sx}, C_{so} are concentrations; P_x, P_o and ΔP_h are mechanical pressures; J_{vr} and j_{sr} are passive flows; j_s^A is the active solute flow; J_{vf} is the phloem volume flow; ρ is density; g is gravitational acceleration; h is height).

the three transport parameters (L_{pr}, σ_r, and ω_r), for roots of various crop plants and for various solutes. Due to the determination of these parameters, it has been possible to describe transport properties (of the model root) by means of the KK equations thus written

$$J_{vr} = L_{pr}\Delta P - L_{pr}\sigma_r\Delta\Pi = L_{pr}(P_x - P_o) - L_{pr}\sigma_r RT(C_x - C_o), \quad (10)$$

$$J_{sr} = \omega_r\Delta\Pi + (1-\sigma_r)\bar{c}_s J_{vr} = \omega_r RT(C_{sx} - C_o) + (1-\sigma_r)\bar{c}_s J_{vr}, \quad (11)$$

where J_v is the volume flow; j_s is the solute flow; $\Delta\Pi$ and ΔP are (mechanical and osmotic) pressure differences; $\bar{c}_s = 0{,}5(C_x + C_o)$ is the mean concentration (of the concentrations C_{sx} and C_{so}); P_x and P_o are mechanical pressures in the xylem and the soil; R and T are the gas constant and temperature.

According to the model described with Equations 13 and 14, the flows J_{vr} and j_{sr} are determined (in their value and direction (sense)) by the values of pressure differences $\Delta\Pi$ and ΔP. This model appears to be rather far removed from the biological reality. Nonetheless, it has played a particularly important role in experimental and theoretical investigations pertaining to determination of transport properties of the root radial transport route in a variety of crop plants (Fiscus, 1975, 1986; Steudle et al., 1987; Kargol, 1994, 2007). Moreover, it explains to a large extent the agrobiophysical water transport mechanisms across the root as well as generation of the so-called root pressure. This pressure is expressed by the formula $\Delta P_\eta = \rho g h$, where ρ is density, g is gravitational acceleration; h is the height to which the root can pump water under that pressure.

According to this model, root pressure is osmosis driven, as the experimentally determined coefficient σ_r pertaining to the membrane M, which emulates the root radial water route takes the value of $\sigma_r > 0$. On the basis of this model (Fiscus, 1975, 1986) as well as Steudle and others (Steudle et al., 1987), experimentally determined the parameters L_{pr}, σ_r, and ω_r for many crop plant roots.

The Ginsburg double-membrane model, which explains radial water transport in the root

Another model, which emulates the radial water route is Ginsburg's double-membrane model shown in Figure 5 (Ginsburg, 1971). While constructing it, Ginsburg assumed that, in the radial segment of the root symplastic route, water encountered two barriers (1 and 2: cf. Figure 3). He gave these barriers the status of membranes M_o and M_i, and ascribed filtration coefficients (L_{po} and L_{pi}), as well as reflection coefficients (σ_o and σ_{and}) to them respectively. In this model, the membrane M_o separates solutions of the concentrations C_{so}, and C_s, while the membrane M_i – solutions of the concentrations C_s and C_{si}, where C_{so}, C_s and C_{si} are the concentrations of the solution in the soil, between the membranes and in

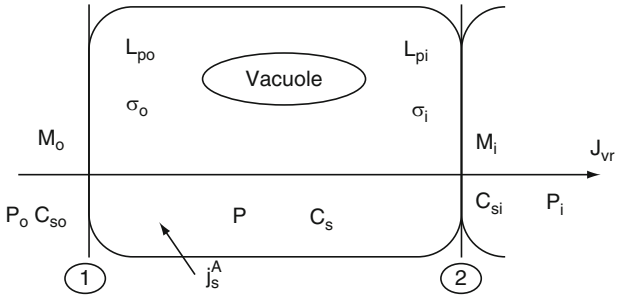

Membranes, Role in Water Transport in the Soil–Root–Xylem System, Figure 5 Two-membrane Ginsburg model (description in text).

the apoplast of the vascular cylinder. With the use of the Kedem–Katchalsky equation for the flow J_v (i.e., Equation 1), Ginsburg demonstrated that transport properties of his model are thus formulated:

$$J_{vr} = -LRT(\sigma_i - \sigma_o)C_s + LRT(\sigma_{si}C_i - \sigma_i C_{so}) - L(P_i - P_o), \quad (12)$$

where J_{vr} is the volume flow; P_i and P_o are mechanical pressures in the soil and in the apoplast of the vascular cylinder; and $L = L_{po}L_{pi}(L_{po} + L_{pi})^{-1}$.

From an analysis of this equation, it follows that – depending on the value of the concentration C_s (which may be regulated with the active flow j_s^A of the solute (s)) – the flow J_{vr} may occur in accordance with the concentration gradient (at $C_{s0} < C_{si}$), under iso-osmotic conditions (at $C_{s0} = C_{si}$), as well as against the concentration gradient (at $C_{s0} > C_{si}$). These conclusions, if referred to water transport across the root, are the main research achievement resulting from the Ginsburg model.

It must be added here that many membrane models have been developed to emulate the root radial water route, including multi-membrane models (Pitman, 1982; Taura et al., 1987; Kargol, 1995, 2007).

Single-membrane theory of two-way water transport along the root radial route

We shall presently consider the single-membrane model of the root radial water route, which we have developed (Kargol, 2007) on the basis of the MF formalism. Schematically, it has been presented in Figure 6. In this model, the assumption is that the membrane M is a heterogeneous porous structure, which emulates (in a manner analogous to the Fiscus model) the entire radial water route in the root. It contains the statistical number of N pores, which are permeable to water. Individual pores vary in areas (A) of their cross sections and are arranged randomly (arbitrarily). To facilitate our considerations, the pores have been arranged in one direction, from the smallest A_1, to the largest A_N^{max}. With reference to this membrane, it is possible to select such a solute (s), with the molecule

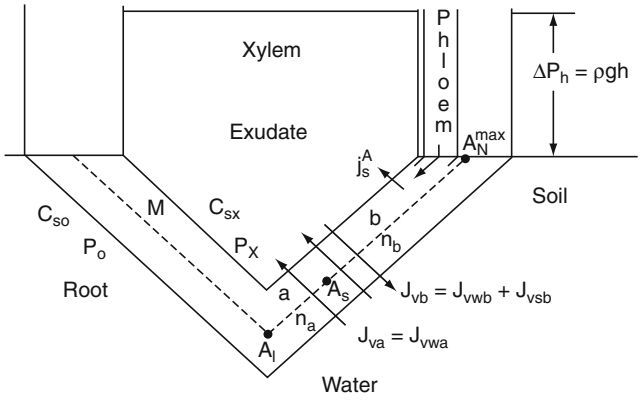

Membranes, Role in Water Transport in the Soil–Root–Xylem System, Figure 6 Single-membrane root model in which the membrane M is a heterogeneous porous structure (C_{si}, C_{so} are concentrations; P_i, P_o are mechanical pressures; J_{va}, J_{vb} are volume flows; n_a and n_b are numbers of semipermeable and permeable pores; j_s^A is the active flow of the substance (s)).

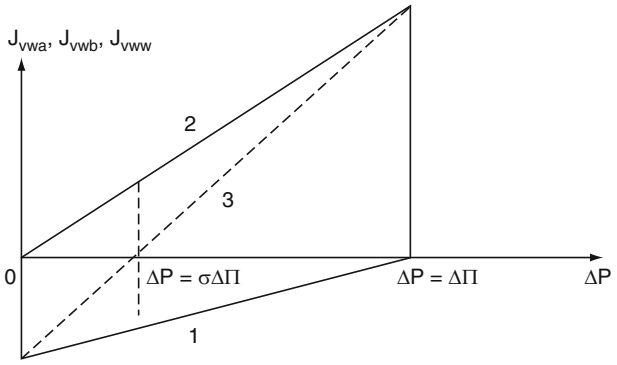

Membranes, Role in Water Transport in the Soil–Root–Xylem System, Figure 7 Plots of relations of flows $J_{vwa} = f(\Delta P)$ and $J_{vwb}^{\Delta P} = f(\Delta P)$, obtained on the basis of Equation 13 – Plot 1, and Equation 16 – Plot 2. Plot 3 depicts the relation $J_{vw} = J_{vwa} + J_{vwb}^{\Delta P} = f(\Delta P)$.

cross-section area A_s, that the following relation will be satisfied: $A_1 < A_2 < \ldots < A_s < \ldots < A_N^{max}$.

Under the circumstances, it is justified to divide the membrane M into Part (a) that contains n_a semipermeable pores and Part (b) that contains n_b permeable pores. These parts are to be ascribed the reflection coefficients $\sigma_a = 1$ and $\sigma_b = 0$ respectively. This membrane (according to Figure 6) separates the soil water with the solute (s) concentration C_{so} and the xylem solution (the exudate) with the solute concentration C_{sx}. Due to the occurrence of active transport j_s^A of the solute (s) in the root, it may be assumed that on the membrane M there occurs the pressure difference $\Delta C = C_{sx} - C_{so}$. Thus, there also occurs the osmotic pressure difference $\Delta\Pi = RT\Delta C = RT(C_{sx} - C_{so})$. As a consequence, within the pores n_a, the osmotic volume flow will be generated $J_{va} = J_{vwa}$ (which is in fact a water flow). This means, in turn, that the model root under consideration is able to generate root pressure $\Delta P_\eta = \rho gh$. In connection with the existence of this pressure, on the membrane at issue there also occurs, apart from the pressure difference $\Delta\Pi$, the mechanical pressure difference $\Delta P = P_x - P_o = \Delta P_h$. In the presented situation (according to the MF formalism), it may be written that [7]

$$\begin{aligned} J_{vwa} &= L_{pa}\Delta P - L_{pa}\Delta\Pi \\ &= L_{pa}(P_x - P_o) - L_{pa}RT(C_{sx} - C_{so}), \end{aligned} \tag{13}$$

where L_{pa} is the filtration coefficient of semipermeable pores n_a. Because $L_{pa} = L_{pr}\sigma_r$, the above equation, which describes the osmotic transport of water takes the following form:

$$J_{vwa} = L_{pr}\sigma_r(\Delta P - \Delta\Pi), \tag{14}$$

where L_{pr} is the filtration coefficient for the entire membrane (all N pores), and σ_r is the reflection coefficient of the membrane M.

In connection with the occurrence on the membrane M of the pressure difference ΔP, within its pores n_b the volume flow J_{vb} will be generated and given by the formula

$$J_{vb} = L_{pb}\Delta P = (1 - \sigma_r)L_{pr}\Delta P, \tag{15}$$

where $L_{pb} = (1 - \sigma)L_{pr}$ is the filtration coefficient of the pores n_b. While analyzing Figure 5, it is easy to see that

$$J_{vb} = J_{vwb} + J_{vsb} = J_{vwb}^{\Delta P} + J_{vwb}^{\Delta\Pi} + J_{vsb}^{\Delta P} + J_{vsb}^{\Delta\Pi},$$

where J_{vwb} and J_{vsb} are the volume flows of water (w) and the solute (s); and $J_{vwb}^{\Delta P}$ and $J_{vsb}^{\Delta P}$ are volume flows of water and the solute, driven by the pressure difference ΔP; while $J_{vwb}^{\Delta\Pi}$ and $J_{vsb}^{\Delta\Pi}$ are volume flows of water and the solute, driven by the pressure difference $\Delta\Pi$. The flow $J_{vwb}^{\Delta\Pi}$ may be expressed by the following formula (Kargol, 2007):

$$\begin{aligned} J_{vwb}^{\Delta P} &= (1 - \sigma_r)(1 - \bar{c}_s\bar{V}_s)L_{pr}\Delta P \\ &\approx (1 - \sigma_r)L_{pr}\Delta P, \end{aligned} \tag{16}$$

where $\bar{c}_s$ is the mean concentration of the concentrations C_{sx} and C_{so}; and $\bar{V}_s$ is the molar volume of the substance (s). Equation 14 and the Formula 16 are the sought expressions that pertain to water transport along the root radial route. This transport is realized simultaneously in two opposite directions. Equation 14 formulates osmotic transport of water from the soil to the xylem of the vascular cylinder, and Equation 16 depicts water transport in the opposite direction. In order to clarify this, Plots 1 and 2 of these equations have been provided. They have been presented and explained in Figure 7. Plot 3, in turn, illustrates the relation of the net flow J_{vw}, given by the formula:

$$J_{vw} = J_{vwa} + J_{vwb}^{\Delta P} = L_{pr}\Delta P - L_{pr}\sigma_r\Delta\Pi. \tag{17}$$

From the discussion of the latter relation (Equation 17), two main conclusions follow. If $\Delta P = 0$,

then $J_{vwa}+J^{\Delta P}_{vwb} = -L_{pr}\sigma_r\Delta\Pi$. If $\Delta P=|-\sigma\Delta\Pi|$, then $J_{vwa}+J^{\Delta P}_{vwb} = 0$, which means that the amounts of water absorbed or removed by the root are the same.

Conclusions

- The above discussion of water transport across the plant root has demonstrated that the root is capable of generating root pressure. Under the influence of this pressure, water may be pumped through the stem xylem up to a certain height.
- The discussion has also demonstrated that the proposed single-membrane model of the root radial route (containing a heterogeneous porous membrane) displays the properties of simultaneous water transport in opposite directions (to the xylem of the vascular cylinder and out of the root – to the soil). This original investigation result is particularly important from the agrophysical viewpoint, particularly in terms of plants maintaining homeostasis.
- Due to this two-way water transport, the plant can also obtain necessary nutrients from the soil as well as simultaneously removing into the soil both water and superfluous (and frequently harmful) products of metabolism occurring in root cells. These unneeded products are food for many bacteria, which subsist in the direct vicinity of the root. Their superfluous metabolism products, in turn, may provide the plant with necessary nutrients.

Bibliography

Fiscus, E. L., 1975. The interaction between osmotic- and pressure-induced water flow in plant roots. *Plant Physiology*, **55**, 917–922.

Fiscus, E. L., 1986. Diurnal changes in volume and solute transport coefficient of Phaseolus roots. *Plant Physiology*, **80**, 752–759.

Ginsburg, H., 1971. Model for iso-osmotic water flow in plant root. *Journal of Theoretical Biology*, **32**, 917–922.

Kargol, M., 1994. Energetic aspect of radial water transport across the bean root. *Acta Physiologiae Plantarum*, **16**, 45–52.

Kargol, M., 1995. *Introduction to Biophysics*. Ed. WSP. pp.189–215.

Kargol, M., 2002. Mechanistic approach to membrane mass transport processes. *Cellular & Molecular Biology Letters*, **7**, 983–993.

Kargol, M., 2006. *Physical Foundations of Membrane Transport of Non-electrolytes*. Poland: Copyright and printed by PPU "Ekspres Druk" Kielce, pp. 25–31.

Kargol, M., 2007. *Mass Transport Processes in Membranes and Their Biophysical Implications*. Poland: WSTKT Kielce, pp. 19–144.

Kargol, M., and Kargol, A., 2003a. Mechanistic formalism for membrane transport generated by Osmotic and mechanical pressure. *General Physiology and Biophysics*, **22**, 51–68.

Kargol, M., and Kargol, A., 2003b. Mechanistic equations for membrane substance transport and their identity with Kedem-Katchalsky equations. *Biophysical Chemistry*, **103**, 117–127.

Kargol, M., and Kargol, A., 2006. Investigation of reverse osmosis on the basis of the Kedem- Katchalsky equations and mechanistic transport equations. *Desalination*, **190**, 267–276.

Katchalsky, A., and Curran, P. F., 1965. *Nonequilibrium Thermodynamics in Biophysics*. Cambridge, MA: Harvard University Press, pp. 113–132.

Pitman, G. M., 1982. Transport across plant roots. *Quarterly Review of Biophysics*, **15**, 481–553.

Steudle, E., Oren, R., and Schulze, E. D., 1987. Water transport in maize roots. *Plant Physiology*, **84**, 1220–1232.

Stryer, L., 2000. *Biochemistry*. Poland: PWN Warszawa, pp. 280–384.

Taura, T., Furumoto, M., and Katou, K., 1987. A model for water transport in stele of plants roots. *Protoplasma*, **140**, 123–132.

Cross-references

Coupled Heat and Water Transfer in Soil
Plant Roots and Soil Structure
Root Water Uptake: Toward 3-D Functional Approaches
Soil Hydraulic Properties Affecting Root Water Uptake
Soil–Plant–Atmosphere Continuum
Stomatal Conductance, Photosynthesis, and Transpiration, Modeling
Water Budget in Soil
Water Effects on Physical Properties of Raw Materials and Foods
Water Reservoirs, Effects on Soil and Groundwater
Water Uptake and Transports in Plants Over Long Distances

MICROBES AND SOIL STRUCTURE

Vadakattu Gupta
Entomology, CSIRO, Glen Osmond, SA, Australia

Definition

Microbes – Single and multicelled microorganisms that are microscopic in size (<100 μm in body width) including bacteria, fungi, algae, and protozoa.
Soil structure – The arrangement of primary soil particles and the pore spaces between them.

Soil particles are arranged together to form aggregates which are held together by organic matter and microbial agents (Tisdall and Oades, 1978). Aggregates that are stable to wetting are a key component of good soil structure as they help to maintain soil porosity and aeration at optimal levels for soil biota and plants.

Soil microorganisms play an important role in the formation and stabilization of aggregates. Bacteria and fungi produce a variety of mucilaginous polysaccharides, by utilizing the more easily available C substrates from fresh residues and roots, which act like glue and help them attach to clays, sands, and organic materials, resulting in the formation of new aggregates. Fungal hyphal networks facilitate the formation of macroaggregates (250–2,000 μm) through enmeshment of soil particles with organic debris (Gupta and Germida, 1988), whereas, decomposing plant residues and microbial debris encrusted with soil particles, by mucilages, form the core of microaggregates (20–250 μm) (Six et al., 2004). Both mycorrhizal and saprophytic fungi contribute to aggregate formation and stabilization. The influence of mucigels through their binding capacity is mostly seen at a scale <50 μm within the aggregates. As the decomposition of organic material progresses, microbial metabolites further permeate the surrounding mineral crust, increasing the interparticle cohesion and promoting the stability of aggregates. The production of hydrophobic

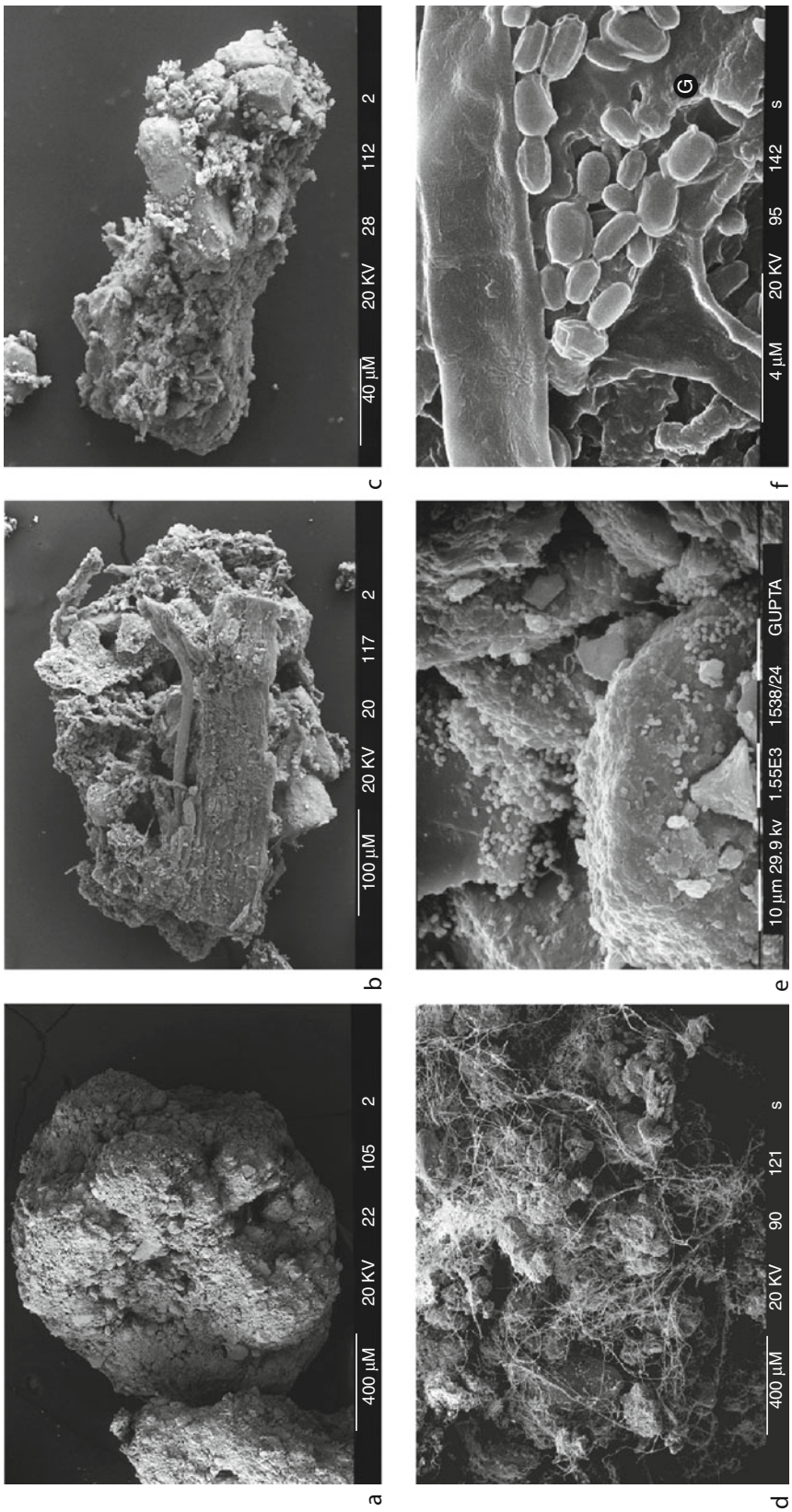

Microbes and Soil Structure, Figure 1 Scanning electron micrographs of soil aggregates, the backbone of soil structure: aggregates offer a diverse array of microsites for microbial colonization over short distances. Stable macroaggregates (**a**, **b**) are composed of decomposing crop residues (particulate organic matter), individual primary particles, microaggregates (**c**), pores of varying sizes, and biota remnants. Fungal hyphal networks (thread-like structures) hold soil particles and micro aggregates onto the surface of crop residues as part of the formation of macroaggregates (**d**). (**e**) Bacteria and fungi colonize the surfaces and small pores of macroaggregates (**e**). Organic compounds (glues, G) produced by bacteria (**f**) and fungi help bind the primary particles and plant debris to form stable aggregates.

substances by microorganisms increases the repellency of aggregates, which decreases the rate of soil wetting and influences aggregate stability. The relative importance of fungi vs. bacteria for aggregation is dependent on soil texture through its influence on porosity characteristics and nutrient availability (Figure 1).

Good soil structure provides an array of niches, i.e., in terms of redox potential and substrate availability, which can house diverse microbial communities. The distribution of bacterial and fungal communities and their function varies between different aggregate size classes (Gupta and Germida, 1988). Macroaggregates generally contain more labile organic matter with rapid turnover times and a greater proportion of fungal biomass. Mycelial networks of fungi help them exploit the heterogeneous soil matrix where carbon and nutrient resources are spatially separated (1) over extended distances at microbial scale and (2) in unconnected pore networks.

The coexistence of diverse bacterial communities within 1-cm^3 area reflects the high degree of spatial heterogeneity in soil microniches. Bacteria often reside in pores and inner surfaces of aggregates as microcolonies of 2–16 bacteria each, and extensive colonization is restricted to microsites with higher C availability, e.g., rhizosphere and outer surfaces of freshly formed macroaggregates (Foster, 1988). Location of different phenotypic and functional groups of bacteria varies in different parts of aggregates, e.g., denitrifying bacteria and diazotrophs are generally located within inner parts of aggregates (Hattori, 1988; Mummy et al., 2006). However, location of aggregates in relation to roots, organic residues, and macropores is more important for determining the microbial community composition and their activity. Bacteria present within inner portions of larger aggregates, microaggregates, and micropores are protected from desiccation and grazing by protozoan predators. The turnover of these organisms is generally low compared to those located in macropores. Disturbance affects aggregation, aeration, and accessibility of substrates, thereby influencing diversity and activity of microbes in soil.

Bibliography

Foster, R. C., 1988. Microenvironments of soil microorganisms. *Biology and Fertility of Soils*, **6**, 189–203.

Gupta, V. V. S. R., and Germida, J. J., 1988. Distribution of microbial biomass and its activity in different soil aggregate size classes as affected by cultivation. *Soil Biology and Biochemistry*, **20**, 777–787.

Hattori, T., 1988. Soil aggregates as microhabitats for microorganisms. *Report of the Institute of Agricultural Research*, Tohoku University, Vol. 37, pp. 23–36.

Mummy, D., Holben, W., Six, J., and Stahl, P., 2006. Spatial stratification of soil bacterial populations in aggregates of diverse soils. *Microbial Ecology*, **51**, 404–411.

Six, J., Bossuyt, H., Degryze, S., and Denef, K., 2004. A history of research on the link between microaggregates, soil biota, and soil organic matter dynamics. *Soil and Tillage Research*, **79**, 7–31.

Tisdall, J. M., and Oades, J. M., 1978. Organic matter and waterstable aggregates in soils. *Journal of Soil Science*, **33**, 141–163.

Cross-references

Earthworms as Ecosystem Engineers
Microbes, Habitat Space, and Transport in Soil
Mineral–Organic–Microbial Interactions
Plant Roots and Soil Structure
Soil Aggregates, Structure, and Stability
Soil Biota, Impact on Physical Properties
Tillage, Impacts on Soil and Environment

MICROBES, HABITAT SPACE, AND TRANSPORT IN SOIL

Karl Ritz
Natural Resources Department, National Soil Resources Institute, School of Applied Sciences, Cranfield University, Cranfield, UK

Definition

Microbes. Life forms that are nominally microscopic (not discernable with the unaided human eye) and typically comprised of one cell (unicellular).

Habitat space. Ecological or environmental volume, encompassing the physical, chemical, and biological environment that is inhabited by particular organisms, populations and communities.

Transport. Movement of entities (e.g., gases, liquids, solutes, particulates, organisms) from one region of a defined space to another.

Microbial life in soil

The living fraction of soils collectively known as the biomass, typically constitutes only a small percent of the total organic matter, but it is of great significance with regard to soil functioning (Paul, 2007). The biota play fundamental roles in delivering the majority of the ecosystem goods and services that soils provide, ranging from soil formation, carbon and nutrient cycling, modulating structural dynamics, regulating biotic populations, and providing biodiversity and genetic resources (Bardgett, 2005; Kibblewhite et al., 2008). Whilst the body size range of soil organisms spans several orders-of-magnitude from centimeters to micrometers (μm, 10^{-6} m), the majority of the soil biomass is always microbial, represented predominantly by bacteria, archaea, and fungi, plus to a lesser extent, protozoa. (Algal biomass in soils is generally present but relatively insignificant, except in some wetland rice systems in the tropics, and is then predominantly confined to the surface, since there is no light beyond a few millimeter depth in most soils, hence phototrophic organisms do not prevail beyond this zone. However, a small biomass does not necessarily mean algae are *functionally* unimportant in soil systems.) Multicellular organisms such as nematodes and the other soil fauna are not deemed microbial and hence are outside the scope of this entry. The soil microbial biomass typically ranges between different ecosystems from tens to thousands of

μg C g^{-1} soil, depending upon the system and a wide variety of factors. However, there is generally a positive relationship between the concentration of organic matter in soil and microbial biomass, since carbonaceous material represents the primary energy source for the majority of the soil biota. Soil biodiversity is generally greater than in any other ecological compartment, particularly within microbial groups.

The soil habitat

The solid phases of soil are comprised of a diverse mixture of inorganic ("mineral" materials derived from the parent geology or glacial deposition) and organic (containing carbon) materials, made up of living matter (biota) or nonliving matter) components (Brady and Weil, 2002). Soils are produced by gradual processes of biogeochemical transformation, including "weathering," a range of erosive chemical, physical, and biological mechanisms that produce a population of mineral particles of varying sizes. The small (nanometer), medium and large (millimeter) components are classified as the clay, silt, and sand fractions respectively. These mineral constituents eventually combine with organic components, predominantly originating from green plants, to form relatively thin "topsoils." The inorganic and organic constituents of soil are arranged in space to form the so-called soil pore network. The origins of soil pore networks are that the fundamental sand-silt-clay components, mediated by organic materials, aggregate to form larger units (Tisdall and Oades, 1983). Generally, the forces binding such aggregates together are greater at smaller-size scales, and hence there tends to be a greater stability of soil structure at these smaller scales. These small units then aggregate further to create larger structures, with an associated hierarchy of scale and structural stability. Since the units are nonuniform, their packing creates a porous matrix, and since the constituents carry such a wide size range, the porous network is heterogeneous across a concomitantly wide range of scales. It is the pore network that comprises the physical, and primary, habitat for all soil organisms, representing a form of "inner space" in which the entirety of belowground life inhabits (Figure 1). The nature of the pore network imparts a structural organization to soil communities and strongly influences the way they function and interact (Young and Ritz, 2005).

How soil structure affects microbial function

The exceptional heterogeneity of the soil pore network imparts some significant properties to the soil system from the perspective of the microbiota. First, it provides a huge surface area for potential colonization. Many soil bacteria are adapted to adhere to surfaces and occur as colonies on the surface of pore walls. Filamentous fungi are also well adapted to grow though soil pore networks by the process of hyphal elongation and branching, but also require some direct contact with substrates in order to absorb water and nutrients released by the action of the extracellular enzymes they produce. It is hypothesized that the extreme structural heterogeneity of soils is one basis for the exceptional diversity found in the soil microbiota, since it provides an extreme range of spatially isolated microhabitats which can lead to adaptive radiation (Zhou et al., 2002). Second, it governs the distribution and availability of nutrient resources to the biota. Unlike in aquatic systems, where most constituents are relatively well mixed by virtue of existing in a fluid matrix, the physical structure of soils essentially discretizes nutrient resources into spatially distinct patches, many of which will then be physically protected from being accessed by organisms. This can occur as a result of coating with soil minerals, or by being located in soil pores smaller than the physical size of potential consumer organisms. Such physical protection mechanisms can equally apply to dead organic matter, or potential prey in the case of active predators such as protozoa.

The connectivity and tortuosity of the pore network governs the movement of gases, liquids, and associated solutes, as well as particulates and organisms, through the matrix. Sessile organisms such as attached bacterial colonies rely upon the delivery of substrates to the colony, usually in water phases, as well as oxygen for aerobic respiration, via such pathways. The foraging distances taken by motile organisms when searching for substrate or prey – and hence the amount of energy consumed – will also be affected by path lengths for movement, which are related to these properties. There is a strong interaction between the pore network, water, and microbial activity, fundamentally linked to the relationships between the matric potential of a soil and the associated distribution of water between differently sized pores. Bacteria and protozoa require water films to move in, and their passage will be curtailed where there is no continuity in such features. Fungi are less constrained since hyphae can grow extended distances through air-filled pores.

As oxygen diffuses about 10,000 times more slowly in water than in air, water-filled pores – or narrow necks to larger pores – effectively act as valves, preventing the passage of oxygen and hence its availability to organisms for aerobic respiration. In these circumstances, many so-called facultative microbes can switch their metabolism to alternative biochemical pathways involving anaerobic processes.

How microbes affect soil structure

Whilst soil structure strongly affects the distribution and functioning of microbes and microbial communities, the microbiota also play important roles in soil structural dynamics (Brussaard and Kooistra, 1993). Microbes create soil structure by a number of direct and indirect processes, including (1) moving and aligning primary particles along cell or hyphal surfaces; (2) adhering particles together by the action of adhesives involved in colony cohesion, and other exudates, such as extracellular polysaccharides (EPS); (3) enmeshment and binding of

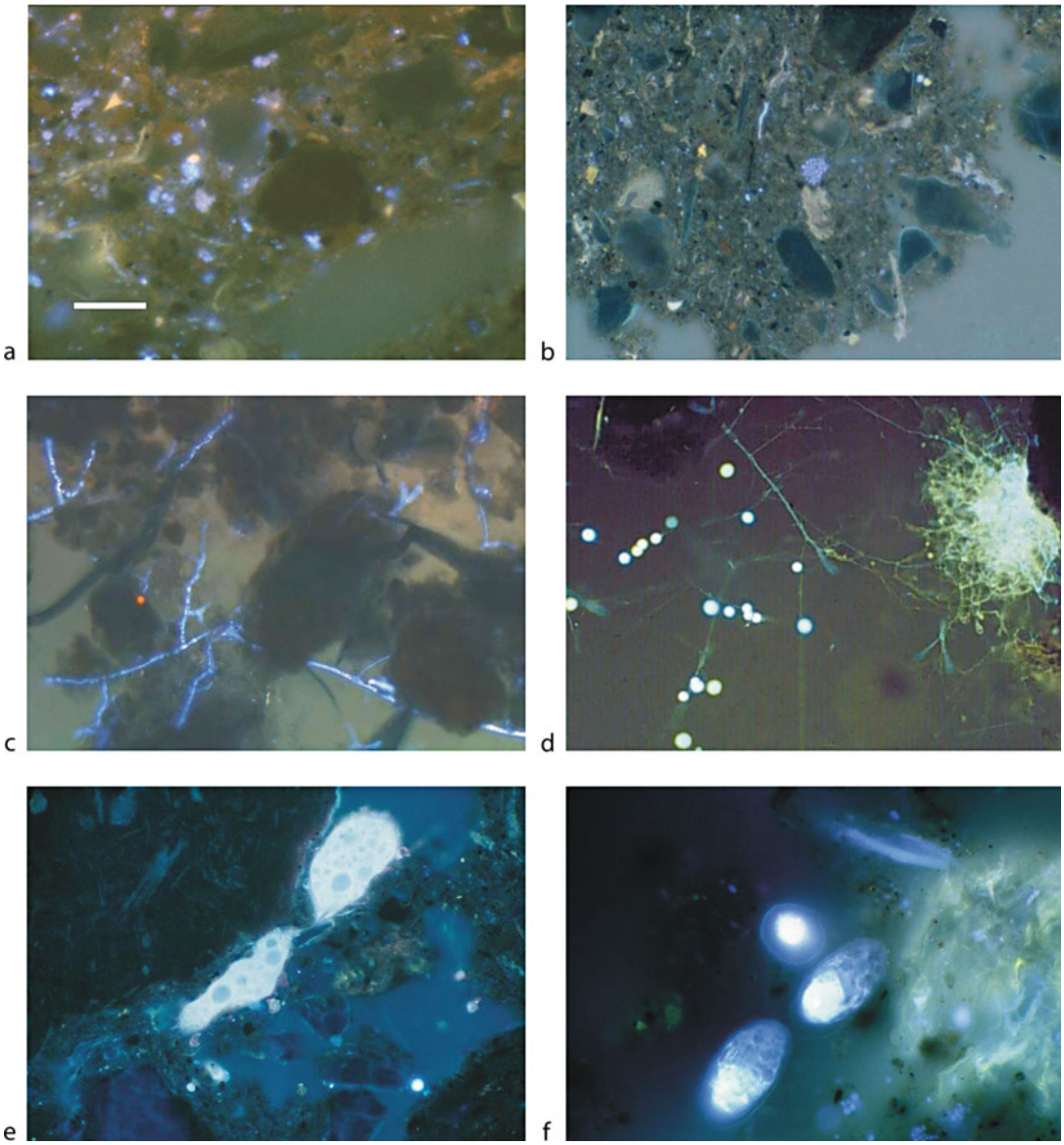

Microbes, Habitat Space, and Transport in Soil, Figure 1 Soil microbes in the soil habitat, visualized in thin sections of undisturbed soil, prepared appropriately to preserve biological tissue (cf. Nunan et al., 2001). (**a**) Bacterial cells in worm cast. (**b**) Bacterial colony embedded in soil matrix. (**c**) Mycelia of *Rhizoctonia solani* in sterilized soil. Note preferential growth in larger pores and apparent lack of penetration of denser masses of soil. (**d**) Unidentified mycelium in field soil, with abundant sporangia in main region of pore. (**e**) Naked amoeba passing through narrow pore in arable soil. (**f**) Testate amoebae accumulating near pore wall of arable soil. Scale bar ca. 25 μm.

aggregates by fungal hyphae and actinomycete filaments, and associated mycelia; and (4) coating pore walls with hydrophobic compounds, particularly by fungi which produce such polymers to insulate their mycelia, which have a relatively large surface area:volume ratio.

Soil structure is also destroyed by the action of microbes, since much of the organic material which serves to bind soil particles together is also potentially energy-containing substrate which microbes will decompose if they can gain access to it. This is the reason why frequent soil disturbance, such as where repeated tillage is applied to soils, typically leads to a degradation of soil structure and a loss of soil C. Undisturbed soils have a high proportion of physically protected organic matter in them. When these are disturbed, such stabilizing material becomes available to microbial assimilation, is decomposed, and a proportion of the C is lost as respired CO_2.

Microbes and transport phenomena

Transport processes in soils are fundamentally affected by (1) the nature of the material being transported – gas, liquid, solute, colloid, particle, or organism; (2) the porosity, connectivity, and tortuosity of the pore network; (3) the exchange properties of the soil, and particularly their distribution in pore surfaces; (4) the distribution of water within the pore network; (5) interactions with the soil biota.

Microbial effects upon transport processes are generally indirect. Via their involvement with a plethora of elemental cycles, microbes transform the constitution and nature of compounds such that their propensity to be transported can be markedly altered, for example, by mineralizing elements from organic forms, or by altering the redox states of compounds, which can have profound effects upon transportability. Soil structure is affected by microbial actions as summarized above – and this in turn affects the moisture release curve, and hence distribution of water.

In relation to direct effects, bacterial movement through the soil matrix will result in a concomitant transport of elements bound in the bacterial cells, but given that the majority of bacteria in soils are sessile, this is not considered to be of great significance. Whilst motile, and hence prone to movement through the soil matrix, protozoan biomass is generally insufficient to likely influence nutrient transport phenomena directly. Protozoa can carry viable bacteria in their cells, including pathogenic forms, and hence may play a role in dispersal of such cells within soils. Fungi, however, have a much greater direct influence upon transport processes (Ritz, 2006). This arises as a result of the mycelium which is essentially a connected and integrated network, which is spatially isolated from the soil matrix. Materials can be translocated within mycelia by both active and passive processes, and are to some extent under the control of the fungal organism. Some primary nutrient elements which appear particularly prone to transport by filamentous fungi are C, N, P, K, S. Other elements, including some heavy metals and radionuclides, have been reported to be directly translocated by fungi. Of particular significance is the transport of P by mycorrhizal fungi to their host plants (Smith and Read, 2008).

Conclusions

Microbial activity creates soil structure which in turn affects the actual and potential function of such organisms. One way of conceptualizing the complex interplay between soil microbes – indeed, the entire soil biota – is that of "soil architecture," which encompasses the notion of communities living in an appropriately physically structured environment, which allows, but modulates, a wide range of direct and indirect interactions which deliver the range of functions that lead to an integrated and sustainable system. An inappropriately structured soil (typically, one which has a low porosity) will be detrimental to the biota since there will be a compromised habitat, manifest as inadequate space and a constrained potential for the dynamics of gases, liquids, solutes, and organisms. Without such dynamics, soil functioning will then inevitably also be impaired.

Bibliography

Bardgett, R. D., 2005. *The Biology of Soil: A Community and Ecosystem Approach*. New York: Oxford University Press.

Brady, N. C., and Weil, R. R., 2002. *The Nature and Properties of Soils*. Upper Saddle River: Prentice-Hall.

Brussaard, L., and Kooistra, M. J., 1993. *Soil Structure/Soil Biota Interrelationships*. Amsterdam: Elsevier.

Kibblewhite, M. G., Ritz, K., and Swift, M. J., 2008. Soil health in agricultural systems. *Philosophical Transactions of the Royal Society London B*, **363**, 685–701.

Nunan, N., Ritz, K., Crabb, D., Harris, K., Wu, K., Crawford, J. W., and Young, I. M., 2001. Quantification of the *in situ* distribution of soil bacteria by large-scale imaging of thin-sections of undisturbed soil. *FEMS Microbiology Ecology*, **37**, 67–77.

Paul, E. A., 2007. *Soil Microbiology, Ecology and Biochemistry*. Oxford: Academic.

Ritz, K., 2006. Fungal roles in transport processes in soils. In Gadd, G. M. (ed.), *Fungi in Biogeochemical Cycles*. Cambridge: Cambridge University Press, pp. 51–73.

Smith, S. E., and Read, D. J., 2008. *Mycorrhizal Symbiosis*. Third edition. London: Academic.

Tisdall, J. M., and Oades, J. M., 1983. Organic matter and water-stable aggregates in soils. *Journal of Soil Science*, **33**, 141–163.

Young, I. M., and Ritz, K., 2005. The habitat of soil microbes. In Bardgett, R. D., Usher, M. B., and Hopkins, D. W. (eds.), *Biological Diversity and Function in Soils*. Cambridge: Cambridge University Press, pp. 31–43.

Zhou, J. Z., Xia, B. C., Treves, D. S., Wu, L. Y., Marsh, T. L., O'Neill, R. V., Palumbo, A. V., and Tiedje, J. M., 2002. Spatial and resource factors influencing high microbial diversity in soil. *Applied and Environmental Microbiology*, **68**, 326–334.

Cross-references

Biofilms in Soil
Earthworms as Ecosystem Engineers
Microbes and Soil Structure
Soil Biota, Impact on Physical Properties

MICROCOSM

A little world; a world in miniature (opposed to macrocosm). Term often used in soil experiments.

Bibliography

Kurt-Karakus, P., and Kevin C. Jones. 2006. Microcosm studies on the air–soil exchange of hexachlorobenzene and polychlorinated biphenyls. *Journal of Environmental Monitoring*, **8**:1227–1234.

MICRO-IRRIGATION

A water management irrigation technique using a micro-sprinkler or drip irrigation system to minimize water runoff.

Cross-references

Water Use Efficiency in Agriculture: Opportunities for Improvement

MICROSTRUCTURE OF PLANT TISSUE

Krystyna Konstankiewicz
Institute of Agrophysics, Polish Academy of Sciences, Lublin, Poland

Synonyms

Microstructure; Structure

Definition

The microstructure of plant tissue is the geometric arrangement of cells as the fundamental elements of that structure. The packing of cells is not tight – between cells, surrounded by stiff call walls, there are intercellular spaces. The system of plant microstructure is a three-phase one – the interior of the cells and of the intercellular spaces is filled with liquid and gas, while the cell walls are the solid phase. The shape and size of cells are determined by the cell walls which, due to their physical properties, play the role of "skeleton" of the whole object and affect its properties.

The microstructure of plant tissue is its fundamental material feature and determines its other properties – chemical, physical, and biological.

Introduction

The latest trends in research of plant tissues relate to the identification and description of the basic features of the material – on the microscale, and then to the search for their relations with the properties of whole objects, including their quality features (Mebatsion et al., 2008). One of the fundamental physical properties that characterize the material under study is its structure, which determines all of its other properties, for example, physical, chemical, and biological (Aguilera and Stanley, 1990). Material studies have a long tradition, supported by practical experience resulting from the production of a variety of materials (Kunzek et al., 1999). Based on the quantitative description of the structure of a material studied one can make comparisons between objects or record changes taking place within a single object as a result of, for example, a technological process, storage, or from nonhomogeneity of the material (Wilkinson et al., 2000). Knowledge on the effect of structure on the properties of a material, in turn, can be utilized for controlling the technological processes so as to obtain materials with desired properties as well as for designing totally new materials (Bourne, 2002).

The fundamental structural element of plant tissue is the cell and that is the element to whose size relations of other properties of the material studied are sought (Konstankiewicz and Zdunek, 2005) (Figure 1).

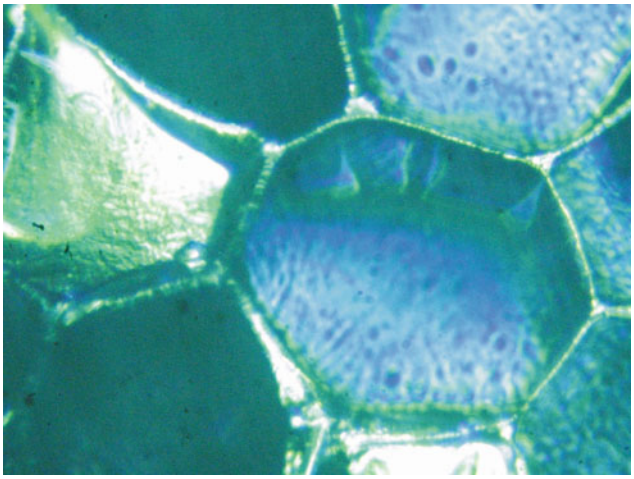

Microstructure of Plant Tissue, Figure 1 Microstructure of potato parenchyma – preparation of sample: 1 mm sliced with a razor blade and washed with tap water. Image obtained with the Tandem Scanning Reflected Light Microscope (TSRLM), 0.47 mm × 0.65 mm.

Many years of research in this field, including also my own, indicate that the cellular structure is a characteristic feature of plant tissues, and every conclusion may only be based on current results of quantitative analysis of structural parameters, especially those relating to cell size (Konstankiewicz et al., 2002; Zdunek and Umeda, 2005).

Microscope observations of cellular structures of plants

Microscope observations are the source of information on cellular structures. Commonly available and continually improved microscope methods permit the observation of cell structures at various rates of magnification, and digital techniques of recording the images obtained permit analysis of the information they contain. The broad array of microscopes of various types – optical, confocal, electron (scanning, transmission), acoustic, X-ray, atom force, Raman – with a variety of additional accessories and software, used for routine observations with very good results for various materials, provides a set of excellent research tools also with relation to plant tissues (Sargent, 1988; Pawley, 1989; Hemminga, 1992; Blonk and van Aalst, 1993; Kaláb et al., 1995; Davies and Harris, 2003; Konstankiewicz and Zdunek, 2005; Figure 2).

A separate group is constituted by methods of imaging of large sample areas – macroscopes, thanks to which it is possible to assess the spatial organization of structural elements, arrangement of cells, and to study identified directions and large zones of structural changes resulting from processes under study (Zdunek et al., 2007; Devaux et al., 2008; Figure 3).

The choice of suitable equipment is not easy, yet it frequently determines the successful solution of problems

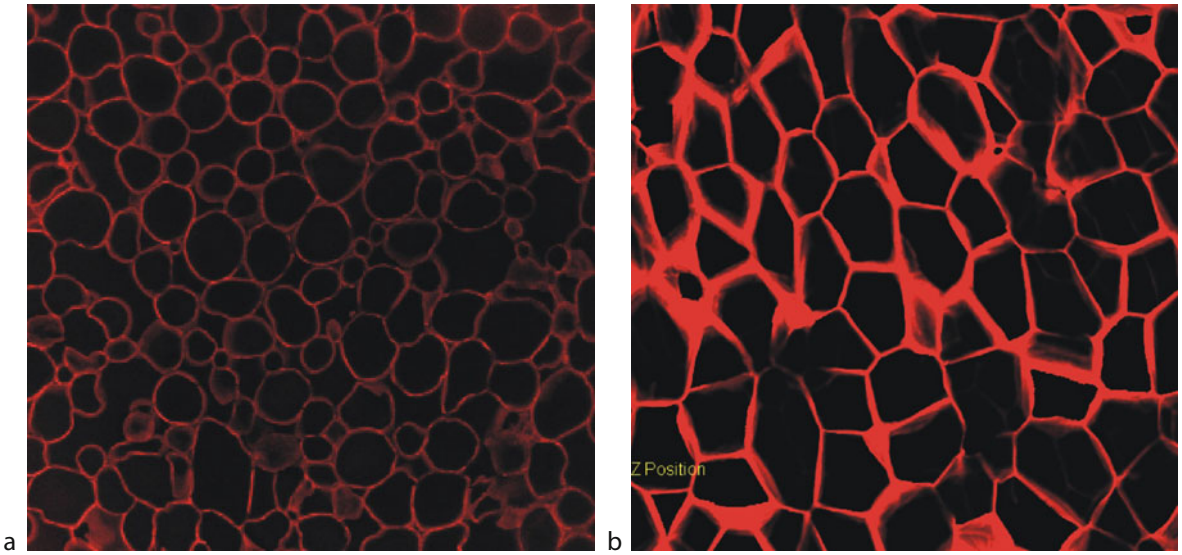

Microstructure of Plant Tissue, Figure 2 Images of microstructure obtained with the Confocal Scanning Laser Microscope (CSLM), each one 1.4 × 1.4 mm (**a**) apple and (**b**) potato parenchyma, sample after preparation procedure.

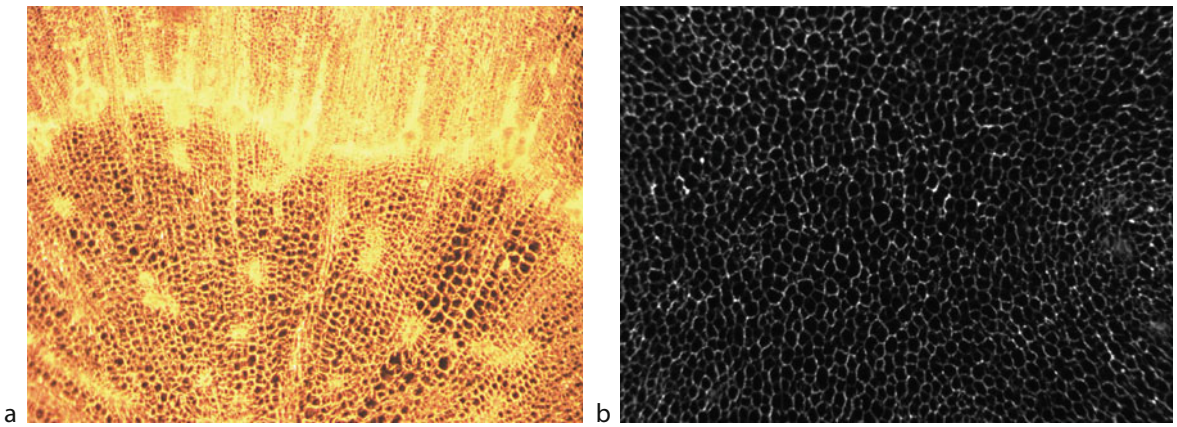

Microstructure of Plant Tissue, Figure 3 Microstructure of carrot (**a**) and potato parenchyma (**b**) sample in natural state. Image obtained with the macroscope, 6 mm × 4.5 mm.

posed, and may also save time and cost. The objective of the research, that is, focusing on the significant elements of the structure and elimination of useless details while ensuring methodological correctness, is of fundamental importance. The location of specimen taking and the choice of the plane of observation are other significant elements. Whereas, the application of preliminary preparation of specimens, from simple slicing to the fixing of structure, may introduce disturbances in the structures under observation that have to be taken into account in subsequent examinations and in the formulation of conclusions (Sun and Li, 2003; Delgado and Rubiolo, 2005; Spector and Goldman, 2006; Otero et al., 2009).

In the studies on the physical properties of plant tissues, methods are sought for the obtainment of such images of the structure that will provide distinct representation of cell walls that determine the overall dimensions of the cells, permit the measurement of those dimensions and then their correlation with other features of the tissue under study (De Smedt et al., 1998; Fornal et al., 1999; Konstankiewicz and Zdunek, 2001; Hepworth and Bruce, 2004).

For an image of a structure to be suitable for computer analysis, it must be of high quality, that is, primarily with a very good level of contrast. The structural elements of interest should be clearly defined, countable, and measurable. This is a difficult task in the case of plant tissues that have a low level of coloring, sometimes are even transparent, and additionally, due to their high content of water, tend to dry quickly and get deformed in the course of observation.

The quantitative description of a cellular structure requires the development of research methodology suitable for a given object. Even with well-developed procedures, the experience and knowledge of the observer are indispensable for correct interpretation of information contained in the images analyzed (Zdunek et al., 2004; Gancarz et al., 2007).

Image analysis of plant tissue microstructure

Good-quality microscope images of the structure of plant tissue can be subjected to detailed analysis leading to quantitative characterization of the object studied. Computer image analysis used for the purpose has been known since the beginning of the 1960s, and has undergone a violent development in the period of common availability of digital cameras and of various types (Serra, 1982; Serra, 1988; Kaláb et al., 1995; Abbott, 1999; Wojnar et al., 2002). Computers, cameras, and software are necessary equipment of every microscope set. The use of software for image analysis may appear to be a simple task, especially when there is easy access to professional offers and an abundance of promising results concerning other materials. It turns out, however, that the task is a complex one and requires good experience as well as knowledge not only about the object of study itself but also about the methods of image taking, acquisition, processing, and analysis. In spite of the continual advances of specialist knowledge in the field of image analysis, and the resultant occasional problems with its understanding, its possession at a basic level is a requirement for every user in order to avoid errors that may bring irreversible effects at the final stage of formulation of conclusions.

Computer image analysis is the most helpful when we need to make multiple computations or measurements, or when comparing images with one another. Such problems are encountered not only in research, but also in diagnostics or in quality control. These tasks require numerous replications and, most importantly, objectivity of the results obtained. For images with sufficiently good quality, it is possible to perform automatic analysis with the help of professional software (Bourne, 1981; Devaux et al., 2005; Cybulska et al., 2008). In practice, however, application of automated image analysis is not always possible even with good quality of the images, and very often image evaluation and manual corrections by an experienced observer are a necessity.

In a flat (2D) image, the size of a cell is defined by measured parameters: surface area, perimeter, diameters, and chords. However, the expected size of a cell as a spatial (3D) object should be its volume and shape and the dimensions of such a solid. Identification of a spatial structural element permits the modeling of the structure of the whole object.

The latest solutions propose highly specialized techniques of computer tomography for mathematic modeling of 3-D cell structures of plant tissues. Such models open up new possibilities in the range of simulation studies on the transport of liquids and gases through the system of cell walls and intercellular spaces and on the processes of deformation under mechanical effects (Lee and Ghosh, 1999; Maire et al., 2003; Tijskens et al., 2003; Kuroki et al., 2004; Mebatsion et al., 2006; Mebatsion et al., 2009).

Stereological methods in studies on microstructure of plant tissue

The need for practical application of structural studies was at the root of the appearance of quantitative methods for structure description – the stereological methods (Underwood, 1970). The notable advance of theoretical stereology in recent years is related, among other things, with the development of microstructure observation techniques and precision sampling methods (Kurzydłowski and Ralph, 1995). It is the method of selection of objects to be studied that largely determines the systematic error of measurement. One of the fundamental errors is to conduct estimations of structure on the basis of a single cross section of a sample or a single selected area of the specimen. That is the erroneous assumption of homogeneity and isotropy of a medium (Ryś, 1995). Plant tissues have a nonhomogeneous and unstable cellular structure, with frequent discontinuities of notable dimensions (Haman and Konstankiewicz, 2000; Konstankiewicz et al., 2002). The morphology of their structure is a resultant of many factors – cultivar, object size and shape, type of tissue, method of cultivation, time of harvest, postharvest processing, and many others. Information on the heterogeneity of structure is obtained on the basis of microscope observation of natural or fixed specimens (Figure 4).

This permits the selection of characteristic areas in the section of the object – heterogeneity of position, as well as finding whether there occurs spatial orientation of elements of the structure – anisotropic heterogeneity (Gao and Pitt, 1991). Such a preliminary assessment determines the choice of the place and direction of taking specimens, as well as of their number, and in consequence determines the correctness of the final result. It is also important whether the results are to describe a specific area of the object studied or the object as a whole. Large areas of uniform structure permit the taking of specimens with sizes sufficient not only for microscope observation but also for other determinations, for example, of mechanical properties (Zdunek et al., 2004). This is important in the study of relations between the geometric parameters of the structure and other properties of plant tissue. In case of doubt as to the homogeneity of studied areas within the object, for example, the type of tissue or anisotropy features, specimens should be taken from various zones – close to the surface, from the center, and also from intermediate areas, varying the directions of specimen taking.

Based on the analysis of large sets of microscope images, it is possible to determine the minimum number of cells representative for the whole population

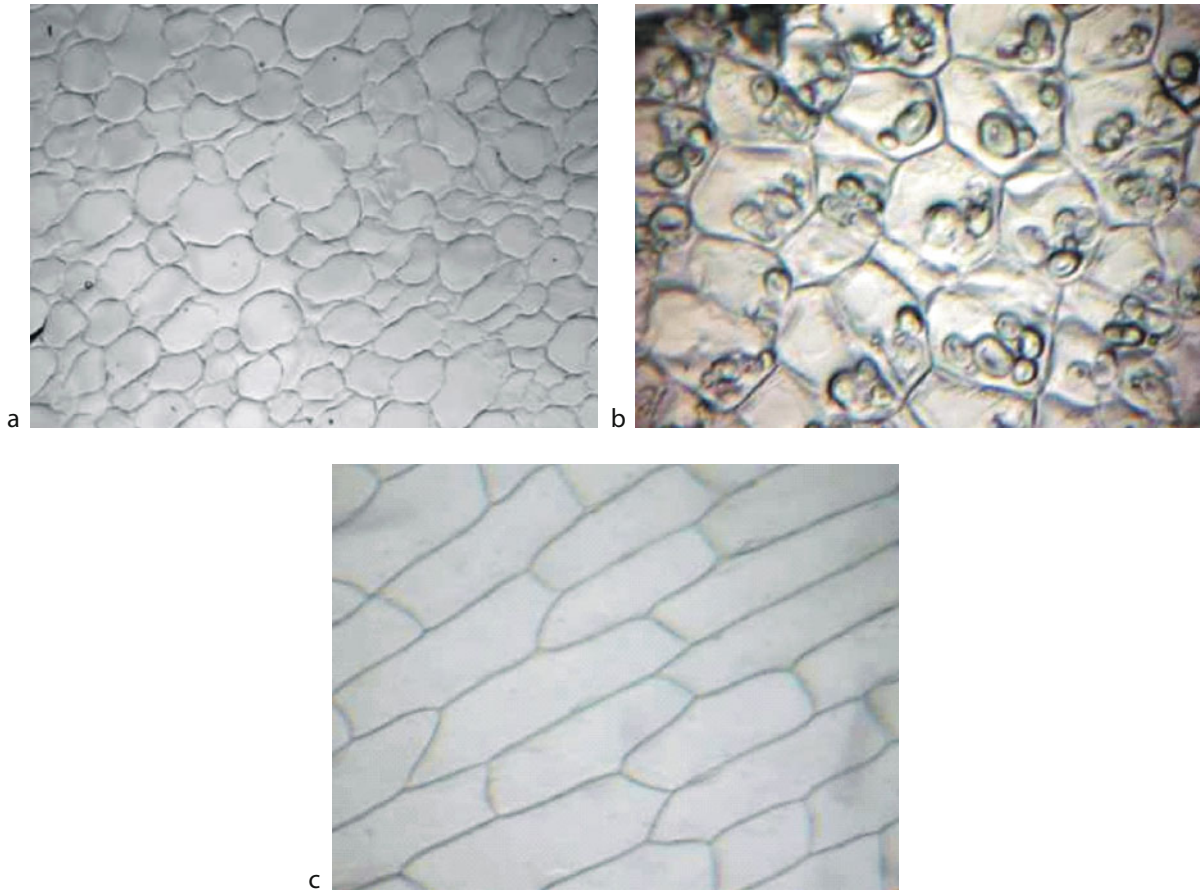

Microstructure of Plant Tissue, Figure 4 Cellular structure of apple (**a**) potato – cells with starch (**b**) and onion (**c**), respectively. Images obtained with optical microscope, samples after preparation, each one 1 mm × 0.8 mm.

(Maliński et al., 2000). As an example, for the parenchyma tissue of potato tuber the minimum number o cells cannot be less than 300, with high repeatability of results for several independent observers. Properly chosen number of cells under analysis permits the determination of not only the mean values of the geometric parameters of the cell but also their distributions within the object studied (Maliński et al., 1991; Figure 5).

Determination of parameters describing a cellular structure requires the development of suitable research methodology for a given object.

Due to the extensive range of variability of plant cell sizes, a microscope image may contain an insufficient number of whole objects. In such situations, it may be necessary to merge images so that the side of the resultant image be severalfold larger than the mean cell diameter.

The procedures relating to the choice of object, specimen, and area in the specimen for microstructure observation, have a significant effect on the final result and determine the weight of the relationships obtained.

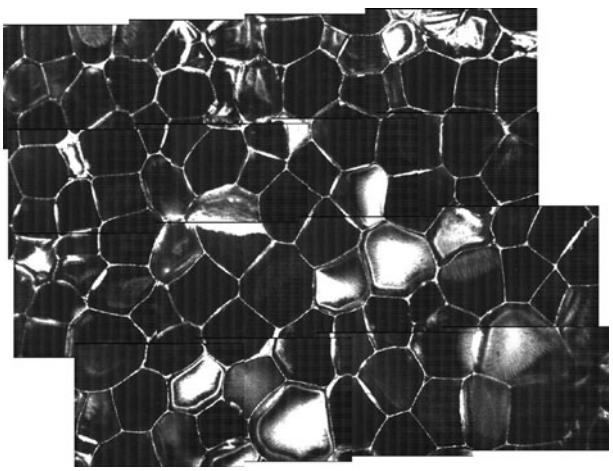

Microstructure of Plant Tissue, Figure 5 Microstructure of potato parenchyma. Example for an image obtained by composing 16 images – TSRLM, 1.5 × 1.2 mm.

Summary

Structure is an important material feature of plant tissue. Investigation of the microstructure of plant tissue is difficult due to the large biological diversity of the material and to the necessity of simultaneous consideration of the effect of a large number of factors resulting from the complex conditions of cultivation and storage and from the increasingly demanding technological processes. Such complex materials, with the rapid development of measurement techniques – microscopes, image analysis – require particularly precise selection of proper measurement methods, preceded with fundamental studies. In most cases, there is no possibility of adaptation of measurement systems commonly used in studies on other materials, and the new research methods being developed require constant improvement due to the rapid development of measurement techniques and to the changing cultivar requirements related with the destined application of agricultural raw materials and products, and with the increasing expectations of the consumers. The utilization of knowledge on plant tissue structure in the process of plant production is the best method of obtaining, in a reproducible manner, materials with expected properties, and of rapid estimation of the quality of plant materials and products.

All the methods for the investigation of the structure, together with other properties, of plant tissues have potential for development, both due to the originality of methodological solutions and to the considerable potential of future practical applications.

Bibliography

Abbott, J. A., 1999. Quality measurements of fruits and vegetables. *Postharvest Biology and Technology*, **15**, 201–225.

Aguilera, J. M., and Stanley, D. W., 1990. *Microstructural Principles of Food Processing and Engineering*. London: Elsevier Applied Science.

Blonk, J. C. G., and van Aalst, H., 1993. Confocal scanning light microscopy in food research. *Food Research International*, **26**, 297–311.

Bourne, M., 1981. Physical properties and structure of horticultural crops. In Peleg, M., and Bagley, E. G. (eds.), *Physical Properties of Foods*. Westport: AVI, pp. 207–228.

Bourne, M. C., 2002. *Food Texture and Viscosity: Concept and Measurement*. London: Academic.

Cybulska, J., Zdunek, A., Konskyy, R., and Konstankiewicz, K., 2008. Image analysis of apple tissue cells after mechanical deformation. *Acta Agrophysica*, **11**(1), 57–69.

Davies, L. M., and Harris, P. J., 2003. Atomic force microscopy of microfibrils in primary cell walls. *Planta*, **217**, 283–289.

De Smedt, V., Pauwels, E., De Baerdemaeker, J., and Nicolaï, B. M., 1998. Microscopic observation of mealiness in apples: a quantitative approach. *Postharvest Biology and Technology*, **14**, 151–158.

Delgado, A. E., and Rubiolo, A. C., 2005. Microstructural changes in strawberry after freezing and thawing processes. *Lebensmittel – Wissenschaft und Technologie*, **38**, 135–142.

Devaux, M.-F., Barakat, A., Robert, P., Bouchet, B., Guillon, F., Navez, B., and Lahaye, M., 2005. Mechanical breakdown and cell wall structure of mealy tomato pericarp tissue. *Postharvest Biology and Technology*, **37**(3), 209–221.

Devaux, M.-F., Bouchet, B., Legland, D., Guillon, F., and Lahaye, M., 2008. Macro-vision and grey level granulometry for quantification of tomato pericarp structure. *Postharvest Biology and Technology*, **47**, 199–206.

Fornal, J., Jeliński, T., Sadowska, J., and Quattrucci, E., 1999. Comparison of endosperm microstructure of wheat and durum whest using digital image analysis. *International Agrophysiscs*, **13**, 215–220.

Gancarz, M., Konstankiewicz, K., Pawlak, K., and Zdunek, A., 2007. Analysis of plant tissue images obtained by confocal tandem scanning reflected light microscope. *International Agrophysics*, **21**(1), 49–53.

Gao, Q., and Pitt, R. E., 1991. Mechanics of parenchyma tissue based on cell orientation and microstructure. *Transactions of the American Society of Agricultural Engineers*, **34**, 232–238.

Haman, J., and Konstankiewicz, K., 2000. Destruction processes in the cellular medium of a plant – theoretical approach. *International Agrophysics*, **14**, 37–42.

Hemminga, M. A., 1992. Introduction to NMR. *Trends in Food Science and Technology*, **3**, 179–186.

Hepworth, D. G., and Bruce, D. M., 2004. Relationships between primary plant cell wall architecture and mechanical properties for onion bulb scale epidermal cells. *Journal of Texture Studies*, **35**(6), 586–602.

Kaláb, M., Allan-Wojtas, P., and Miller, S. S., 1995. Microscopy and other imaging techniques in food structure analysis. *Trends in Food Science and Technology*, **6**, 177–186.

Konstankiewicz, K., Czachor, H., Gancarz, M., Król, A., Pawlak, K., and Zdunek, A., 2002. Cell structural parameters of potato tuber tissue. *International Agrophysics*, **16**(2), 119–127.

Konstankiewicz, K., and Zdunek, A., 2001. Influence of turgor and cell size on the cracking of potato tissue. *International Agrophysics*, **15**(1), 27–30.

Konstankiewicz, K., and Zdunek, A., 2005. *Micro-structure Analysis of Plant Tissues*. Lublin: Centre of Excellence for Applied Physics in Sustainable Agriculture Agrophysics.

Kunzek, H., Kabbert, R., and Gloyna, D., 1999. Aspects of material science in food processing: changes in plant cell walls of fruits and vegetables. *Zeitschrift Lebensmittel Undersuchung Forschung, A*, **208**, 233–250.

Kuroki, S., Oshita, S., Sotome, I., Kawagoe, Y., and Seo, Y., 2004. Visualisation of 3-D network of gas-filled intercellular spaces in cucumber fruit after harvest. *Postharvest Biology and Technology*, **33**, 255–262.

Kurzydłowski, K. J., and Ralph, B., 1995. *The Quantitative Description of the Microstructure of Materials*. London: CRC Press.

Lee, K., and Ghosh, S., 1999. A microstructure based numerical method for constitutive modelling of composite and porous materials. *Material Science and Engineering, A*, **272**, 120–133.

Maire, E., Fazekas, A., Salvo, L., Dendievel, R., Youssef, S., Cloetens, P., and Letang, J. M., 2003. X-ray tomography applied to the characterization of cellular materials. Related finite element medeling problems. *Composites Science and Technology*, **63**, 2431–2443.

Maliński, M., Cwajna, J., and Chrapoński, J., 1991. Grain size distribution. *Acta Stereologica*, **10**, 73–83.

Maliński, M., Cwajna, J., and Mokry, W., 2000. Procedure for determination minimal number of measurements and for testing results repeatability in quantitative evaluation of materials microstructure. *In Proceedings of Sixth International Conference*, Stereology and Image Analysis in Material Science, STERMAT 2000, September 20–23, Cracow, pp. 259–264.

Mebatsion, H. G., Verboven, P., Ho, Q. T., Mendoza, F., Verlinden, B. E., Nguyen, T. A., and Nicolaï, B. M., 2006. Modelling fruit microstructure using novel ellipse tessellation algorithm. *CMES – Computer Modelling in Engineering and Sciences*, **14**(1), 1–14.
Mebatsion, H. G., Verboven, P., Ho, Q. T., Verlinden, B. E., and Nicolaï, B. M., 2008. Modeling fruit (micro)structure, why and how? *Trends in Food Science and Technology*, **19**, 59–66.
Mebatsion, H. G., Verboven, P., Melese, E. A., Billen, J., Ho, Q. T., and Nicolaï, B. M., 2009. A novel method for 3-D microstructure modeling of pome fruit tissue using synchrotron radiation tomography images. *Journal of Food Engineering*, **93**, 141–148.
Otero, L., Martino, M., Zaritzky, N., Solas, M., and Sanz, P. D., 2009. Preservation of microstructure in peach and mango during high-pressure-shift frizing. *Journal of Food Science*, **65**, 466–470.
Pawley, J., 1989. *The Handbook of Biological Confocal Microscopy*. Madison: Electron Microscopy Society of America.
Ryś, J., 1995. *Stereology of Materials*. Cracow: Fotobit-Design (in Polish).
Sargent, J. A., 1988. The application of cold stage scanning electron microscopy to food research. *Food Microstructure*, **7**, 123–135.
Serra, J., 1982. *Image Analysis and Mathematical Morphology*. London: Academic.
Serra, J., 1988. Image analysis and mathematical morphology, Vol. 2: *Theoretical Advances*. London: Academic.
Spector, D. L., and Goldman, R. D., 2006. *Basic Methods in Microscopy. Protocols and Concepts from Cells. A Laboratory Manual*. New York: Cold Spring Harbor Laboratory Press.
Sun, D. W., and Li, B., 2003. Microstructiral change of potato tissues frozen by ultrasound-assisted immersion freezing. *Journal of Food Engineering*, **57**, 337–342.
Tijskens, E., Ramon, H., and De Baerdemaeker, J., 2003. Discrete element modelling for process simulation in agriculture. *Journal of Sound and Vibration*, **266**, 493–514.
Underwood, E. E., 1970. *Quantitative Stereology*. Massachusetts: Addison Wesley.
Wilkinson, C., Dijksterhuis, G. B., and Minekus, M., 2000. From food structure to texture. *Trends in Food Science and Technology*, **11**, 442–450.
Wojnar, L., Kurzydłowski, K. J., and Szala, J., 2002. *Practice of Image Analysis*. Polish Society of Stereology: Cracov (in Polish).
Zdunek, A., Konskyy, R., Cybulska, J., Konstankiewicz, K., and Umeda, M., 2007. Visual textureanalysis for cell size measurements from confocal images. *Acta Agrophysica*, **21**(4), 409–415.
Zdunek, A., and Umeda, M., 2005. Influence of cell size and cell wall volume friction on failure properties of potato and carrot tissue. *Journal of Texture Studies*, **36**, 25–43.
Zdunek, A., Umeda, M., and Konstankiewicz, K., 2004. Method of parenchyma cells parametrisation using fluorescence images obtained by confocal scanning laser microscope. Electronic Journal of Polish Agricultural Universities, Agriculture Engineering, http://www.ejpau.media.pl. 7, 1.

Cross-references

Agrophysics: Physics Applied to Agriculture
Physical Phenomena and Properties Important for Storage of Agricultural Products
Plant Biomechanics
Quality of Agricultural Products in Relation to Physical Conditions
Rheology in Agricultural Products and Foods
Shrinkage and Swelling Phenomena in Agricultural Products

MINERAL FERTILIZERS

See *Fertilizers (Mineral, Organic), Effect on Soil Physical Properties*

MINERALISATION

Conversion to a mineral substance. In soil science the conversion by microbes of organic matter into simple inorganic compounds.

Cross-references

Mineral–Organic–Microbial Interactions

MINERAL–ORGANIC–MICROBIAL INTERACTIONS

Małgorzata Dąbek-Szreniawska[1], Eugene Balashov[2]
[1]Institute of Agrophysics PAN, Polish Academy of Sciences, Lublin, Poland
[2]Agrophysical Research Institute RAAS, Russian Academy of Agricultural Sciences, St. Petersburg, Russia

Introduction

Soil minerals, organic matter, and microorganisms are interacting with each other. These interactions play an important role in creating soil structure, controlling biogeochemical processes, and turnover of organic and inorganic substances in soil.

A great role of clay minerals in the formation of complexes with soil microorganisms and organic substances of microbial origin and new quantitative approaches and hypothesis to the studies of interactions between mineral soil solid phase and microorganisms are pointed out.

Minerals, organic matter, and microorganisms have significant higher-order interactions in terrestrial ecosystem. These reactions exert strong control over soil physical, chemical, and biological processes. Soil mineral surfaces play a vital role in catalysis of abiotic formation of humic substances. Soil minerals, especially noncrystalline minerals, have the ability to chemically stabilize soil organic matter. Organic substances also act as binding agents to promote and stabilize aggregation. There are distinct interactive mechanisms between soil minerals, organic matter, and microbes, which should have a direct influence on the stability and cycling of C, N, P, and S (Huang et al., 2005).

Emerson (1959) presented a physical aspect of the microstructure of a soil aggregate. Assuming that a soil aggregate is composed mainly of clay and quartz, these particles may be linked directly by organic matter or through two or more domains which are themselves linked by organic matter.

A mineral soil solid phase more or less easily adsorbs bacteria on the surface. Negatively charged adsorbents repel rather than attract bacteria of negative charge. An attention of scientists has been drawn to the fact that the type of microorganisms is more significant than the type of adsorbents. For instance, gram-positive, immobile microorganisms are characterized by the highest absorbing affinity to soil particles.

A particle-size fractionation of soils is commonly used to quantify the content of soil organic matter and microbial biomass in different particle-size fractions.

A great role of clay minerals is known in the formation of complexes with soil microorganisms and organic substances of microbial origin (Chenu, 1993; Golchin et al., 1995; Schnitzer et al., 1988). The formation of complexes between extracellular polysaccharides and montmorillonite decreases the rate of microbial decomposition of these polysaccharides and other labile organic matter. Therefore, clay soils have a greater capacity for the protection of biomass of microorganisms within the soil matrix than sand soils (Hassink et al., 1993).

The role of interactions of soil minerals with soil microorganisms and their metabolites in the formation of soil aggregates was being studied for a long-term period (Harris et al., 1966; Bossuyt et al., 2001; Six et al., 2004). An ability of fungi and bacteria to participate in aggregate formation is dependent on soil texture, its composition, and availability of C and N. Compared to bacteria, fungi play a dominant role especially in water-stable macroaggregation of light-textured soils with a poor fertility (Guggenberger et al., 1999).

Hattori and Hattori (1976) observed the physical environment in soil microbiology and undertook an attempt to extend the principles of microbiology to soil microorganisms. A formation of complexes was studied between *Escherichia coli* cells and loam soil particles of different mineralogical origin. Pyrophyllite and kaolinite complexes being combined with *E. coli* cells, showed an adhesion to loam particles and formed microaggregates. The "cell–loam particle" complexes treated with sodium ions were stable in acidic medium and unstable in alkaline medium. The loam particles treated with Cu^{++}, Co^{++}, or Fe^{++} demonstrated stronger adhesion with bacterial cells than loam ones treated with Na^{+}, and the complexes were stable in alkaline medium but labile in acidic medium (Hattori, 1970).

Three hypotheses have been proposed concerning mechanisms of the adsorption of the mineral's molecules on the surface of bacterial cells (Marshall, 1971):

(a) Adsorption of the molecules could proceed through on the surfaces of bacteria and mineral particles ("face-to-face adsorption").
(b) Adsorption of the molecules could proceed through on their edges ("edge adsorption").
(c) Adsorption could result from both mentioned mechanisms ("mixed adsorption").

Adsorption of sodium bentonite was studied on *Bacillus subtilis cells* (Lahav, 1962). The effect of sodium bentonite (molecules smaller than the bacterial cells) on the electrophoretic mobility of *Bacillus subtilis* was tested in solutions of sodium chloride and of sodium phosphate with different concentrations of hydrogen ions and ionic force. It was noted that the adsorption of sodium bentonite on bacteria was a reversible process. Bacterial population consisted of two types of microorganisms. The addition of bentonite affected the electrophoretic mobility of one bacterial type, while the other one was not affected. The first type represented bacteria-adsorbing bentonite, whereas the second one included bacteria not adsorbing bentonite on their surface. Moreover, the presence of both bacterial types was found only in the presence of bentonite. The effect of bentonite on bacterial mobility depended on pH, ionic force, and contents of electrolytes. The lower were the pH values and the higher was the ionic force, the more effective was the effect of bentonite.

Among different types of bacteria, for instance, the influence of the bacterial biomass of *Arthrobacter* sp. on the formation and stabilization of water-stable macroaggregates in the soil was studied after the addition of plant residues, mineral fertilizers (NPK, Ca), and bentonite (Dąbek-Szreniawska, 1974). The introduction of the bacterial biomass of *Arthrobacter* sp. resulted in an increased amount of water-stable macroaggregates (>250 μm). The highest increase in the water-stable aggregation was induced by a combined influence of bacterial biomass and plant residues during a 3-month incubation. Application of bentonite generally increased the water stability of aggregates. Application of mineral NPK fertilizers caused a decrease in the water stability of aggregates as a result of changes in the activity and the composition of soil microbial community.

New quantitative approaches to the studies of interactions between mineral soil solid phase and microorganisms give an opportunity to get more detailed information about structure and function of soil microbial community in micro- and macroaggregates (Väisänen et al., 2005).

Conclusions

The distinct interactive mechanisms between soil minerals, especially clay minerals, which form complexes with microorganisms and organic substances are confirmed. They affect the stability and cycling of soil chemical components and have a positive effect on soil microstructure and aggregation.

Bibliography

Bossuyt, H., Denef, K., Six, J., Frey, S. D., Merckx, R., and Paustian, K., 2001. Influence of microbial population on aggregate stability. *Applied Soil Ecology*, **16**, 195–208.

Chenu, C., 1993. Clay- and sand-polysaccharide associations as models for the interface between microorganisms and soil: water-related properties and microstructure. *Geoderma*, **56**, 143–146.
Dąbek-Szreniawska, M., 1974. The influence of *Arthrobacter* sp. on the water stability of soil aggregates. *Polish Journal of Soil Science*, **7**, 169–179.
Emerson, W. W., 1959. The structure of soil crumbs. *Journal of Soil Science*, **10**, 235–244.
Golchin, A., Oades, J. M., Skjemstad, J. O., and Clarke, P., 1995. Structural and dynamical properties of soil organic matter as reflected by ^{13}C natural abundance, pyrolisis mass spectroscopy and solid-state ^{13}C NMR spectroscopy in density fractions of an oxisol under forest and pasture. *Australian Journal of Soil Research*, **33**, 59–76.
Guggenberger, G., Elliott, E. T., Frey, S. D., Six, J., and Paustian, K., 1999. Microbial contributions to the aggregation of a cultivated soil amended with starch. *Soil Biology and Biochemistry*, **31**, 407–419.
Harris, R. F., Chesters, G., and Allen, O. N., 1966. Dynamics of soil aggregation. *Advances in Agronomy*, **18**, 107–169.
Hassink, J., Bouwman, L. A., Zwart, K. B., Bloem, J., and Brussaard, L., 1993. Relationships between soil texture, physical protection of organic matter, soil biota and C and N mineralization in grassland soils. *Geoderma*, **57**, 105–128.
Hattori, T., 1970. Adhesion between cells of *E. coli* and clay particles. *Journal of General and Applied Microbiology*, **16**, 351–359.
Hattori, T., and Hattori, R., 1976. The physical environment in soil microbiology: an attempt to extent principles of microbiology to soil microorganisms. *CRC Critical Reviews in Microbiology*, **4**, 423–461.
Huang, P.-M., Wang, M.-K., and Chiu, Ch-Y, 2005. Soil mineral-organic matter-microbe interactions: Impact on biogeochemical processes and biodiversity in soils. *Pedobiologia*, **49**, 609–635.
Lahav, N., 1962. Adsorption of sodium bentonite particles on *Bacillus subtilis*. *Plant and Soil*, **17**, 191–208.
Marshall, K. C., 1971. Sorptive interactions between soil particles and microorganisms. *Soil Biochemistry*, **2**, 409–445.
Schnitzer, M., Ripmeester, J. A., and Kodama, H., 1988. Characterization of the organic matter associated with a soil clay. *Soil Science*, **145**, 448–454.
Six, J., Bossuyt, H., De Gryze, S., and Denef, K., 2004. A history of research on the link between (micro)aggregates, soil biota, and soil organic matter dynamics. *Soil and Tillage Research*, **79**, 7–31.
Väisänen, R. K., Roberts, M. S., Garland, J. L., Frey, S. D., and Dawson, L. A., 2005. Physiological and molecular characterisation of microbial communities associated with different water-stable aggregate size classes. *Soil Biology and Biochemistry*, **37**, 2007–2016.

Cross-references

Clay Minerals and Organo-Mineral Associates
Microbes and Soil Structure
Organic Matter, Effects on Soil Physical Properties and Processes
Soil Aggregates, Structure, and Stability

MIRE

See *Peats and Peatlands, Physical Properties*

MODELING THE THERMAL CONDUCTIVITY OF FROZEN FOODS

Vlodek R. Tarnawski[1], Wey H. Leong[2], Toshihiko Momose[3]
[1]Division of Engineering, Saint Mary's University, Halifax, NS, Canada
[2]Department of Mechanical and Industrial Engineering, Ryerson University, Toronto, ON, Canada
[3]Bavarian Environment Agency, Hof/Saale, Germany

Definition

Thermal conductivity of foods. The bulk property of food products describing their ability to conduct heat resulting from a gradient of temperature. It is measured in Watts per Kelvin per meter ($W\ K^{-1}\ m^{-1}$).
Frozen foods. Foods with their aqueous solutions converted into ice and then stored at a temperature below freezing point.
Thermal conductivity models. Equations describing the material ability to conduct heat.

Introduction

A large variety of foods (meat, fish, poultry, fruits, vegetables, bakery, dairy foods, etc.) require refrigeration (chilling and/or freezing) to maintain their high quality, edibility, and nutritive values. Solid foods are capillary, porous, colloidal materials consisting of water, solid constituents (e.g., carbohydrates, fats, proteins, vitamins, or minerals), and in some instances, air (bakery products, ice cream, cheese, etc.). The majority of fresh natural foods (meat, fish, fruits, vegetables) are fully saturated with aqueous solution (solid food components dissolved in water). During a freezing process, food water is converted into ice and the solution concentration increases; consequently, the food initial freezing point (T_f) decreases below 0°C. Good knowledge of frozen food thermophysical properties, particularly thermal conductivity (λ), is required in the design of freezing/thawing equipment and analysis of chilling, freezing, storage, and thawing processes. This property describes food's ability to distribute heat strictly by a conduction mode. It is very difficult to measure and also to estimate as it is influenced by numerous parameters such as initial water content, temperature (T), density, food composition, anisotropy, ice fraction, measuring techniques, etc. Available experimental data usually do not cover a full T range encountered during freezing, storing, and thawing processes; often λ data are contradictory and incomplete (missing measurement details, T, composition data, a sample preparation procedure, and uncertainty analysis). Therefore, there is a strong demand for the use of λ models in computer analysis of food freezing, storing, and thawing processes.

Thermal conductivity of food components

Water and ice are two main components of frozen foods. Thermal conductivity of water (λ_w) is approximately double that of other solid constituents, while with respect to ice it is approximately four times smaller. There is a weak λ_w dependence on T. On the contrary to water, the thermal conductivity of ice (λ_{ice}) increases considerably with decreasing T. As a result, ice has a dominant effect on the frozen food's ability to conduct heat. Several predictive equations, $\lambda_{ice}(T)$, λ_{ice} in W/m K and T in °C, have been published over the last 30 years (Sakazume and Seki, 1978; Yen, 1981; Choi and Okos, 1986; U.S. Army Corps of Engineers 1996).

$$\lambda_{Choi-Okos} = 2.2196 - 0.0062489 \cdot T + 0.00010154 \cdot T^2$$
$$\lambda_{Sakazume-Seki} = 2.2156 - 0.0100456 \cdot T + 0.00003445 \cdot T^2$$
$$\lambda_{Yen} = 6.727 \cdot \exp[-0.0041 \cdot (T + 273.15)]$$
$$\lambda_{US-Army} = 2.21 - 0.011 \cdot T \quad (1)$$

Fukusako (1990) reviewed available $\lambda_{ice}(T)$ data and fitting correlations and concluded that variations among the reported data were caused mainly by differences in sample purity, sample preparation, methods of measurement, and reproducibility of experimental data. The difference in predicted λ is on average below 0.05 W/m K (Figure 1). The predictive λ_{ice} equation by Choi and Okos (1986) is commonly used in food engineering for modeling λ of frozen foods within a range of T from −40°C to 0°C; λ_{ice} increases by about 18.6% as Tdecreases from −1°C to −40°C. Therefore, λ_{ice} dependence on T may strongly influence the λ of lean frozen foods that usually contain a large amount of ice. Thermal conductivities of remaining basic food components (including water) are also estimated from equations given by Choi and Okos (1986) and in comparison to ice, λ shows a weak dependence on T.

$$\lambda_{water} = 0.57109 - 0.0017625 \cdot T + 0.00000607036 \cdot T^2$$
$$\lambda_{protein} = 0.17881 - 0.0011958 \cdot T + 0.0000027178 \cdot T^2$$
$$\lambda_{fat} = 0.18071 - 0.00027604 \cdot T + 0.00000017749 \cdot T^2$$
$$\lambda_{ash} = 0.32962 - 0.0014011 \cdot T + 0.0000029069 \cdot T^2$$
$$\lambda_{carbohydrates} = 0.2014 - 0.0013874 \cdot T + 0.0000043312 \cdot T^2$$
$$\lambda_{fiber} = 0.18331 - 0.0012497 \cdot T + 0.0000031683 \cdot T^2 \quad (2)$$

Thermal conductivity of frozen foods

Two measuring techniques of λ are commonly used for frozen foods, namely: steady and transient state. The steady-state technique (a guarded hot plate) requires a long time to reach the equilibrium T of tested foods and therefore it is prone to moisture migration and spoilage. The transient state technique offers a smaller size of equipment, much shorter measuring times, smaller food samples and consequently, it is currently a preferable choice for λ measurement. Thermal conductivity probes, however, lack thorough verification at $T < T_f$ and latent heat of ice may considerably alter measured λ (Wang and Kolbe, 1990). Besides, thermal conductivity measurements are based on a highly simplified assumption that foods are homogeneous and isotropic materials. In fact, fibrous foods usually conduct different amount of heat in a perpendicular and parallel direction to fibers; this difference could be up to about 15% for frozen beef (Heldman, 2003). As a result, experimental data gathered may be burdened with errors of unknown magnitude. Fat has a very

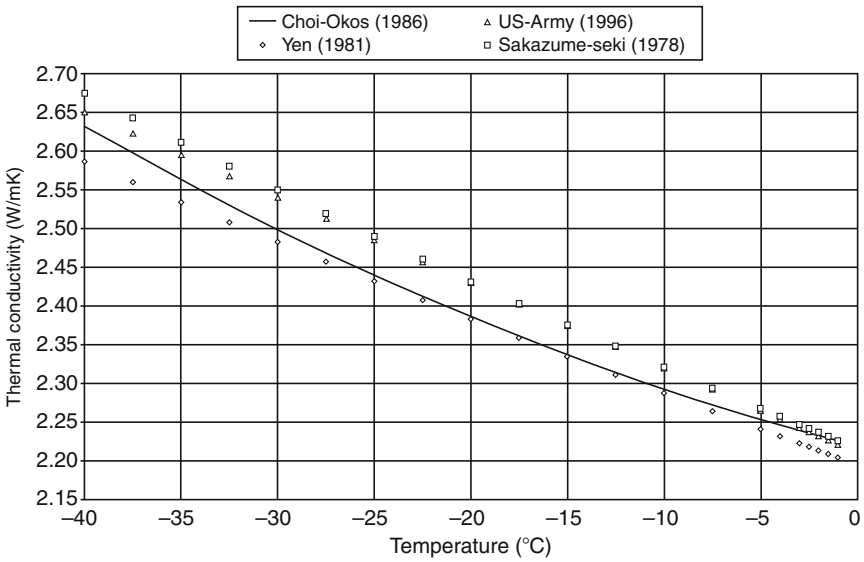

Modeling the Thermal Conductivity of Frozen Foods, Figure 1 Thermal conductivity of ice as a function of temperature.

low λ (0.2–0.5 W/m K) and therefore, its increasing content has a decreasing effect on the frozen food's λ. The majority of frozen foods show a strong λ dependence on decreasing T. Figure 2 displays experimental λ data of selected foods, by Pham and Willix (1989) and Willix et al. (1998), undergoing freezing from $-1°C$ to $-40°C$; within this T range λ increases by a factor of 2–3.

Predicting ice fraction in frozen foods

Thorough knowledge of ice fraction in frozen foods is crucial for obtaining good λ estimates. One of the most frequently used m_{ice} models was proposed by Schwartzberg (1976).

$$m_{ice} = (m_w - m_b) \cdot \left(1 - \frac{T_f}{T}\right), \quad (3)$$

where m_w = mass fraction of water at T_f in °C, m_b = mass fraction of bounded water, and T = temperature of frozen food in °C. For example, for meat products, $T_f \approx -0.9°C$ and $m_b = 0.4 \cdot m_{protein}$ (Pham and Willix, 1989).

The above equation gives good estimates for highly diluted solutions, i.e., T_f is close to 0°C.

Golovkin and Tchizov (1951) provided an empirical relation for ice fraction that follows closely experimental m_{ice} data of a variety of foods such as meat, fish, milk, eggs, fruits, and vegetables. Their experimental m_{ice}, from $-1°C$ to $-65°C$, was refitted and coefficients of the original empirical relation were slightly adjusted.

$$m_{ice} = \frac{1.133}{1 + \frac{0.339}{\log[1+|T-T_f|]}} \left(r^2 = 0.996\right). \quad (4)$$

The initial freezing point is a key parameter in the above Equations 3 and 4; its value, however, is difficult to predict or measure. In general, T_f for fish, meats, fruits, and vegetables varies from $-2°C$ to $-0.5°C$; a summary of T_f predictive models for a variety of foods was published by Sun (2006). A comprehensive summary of m_{ice} modeling approaches was given by Fikiin (1998) and Rahman (2001).

Models predicting thermal conductivity of frozen foods

For modeling purposes, solid foods are often subdivided into two groups, namely: fully saturated with water (fish, meat, fruits, vegetables, etc.) and partly saturated with water (bread, butter, ice cream, etc.), i.e., food pores are filled with water and/or moist air, respectively. Measuring λ of porous saturated/unsaturated materials undergoing freezing is difficult, error prone, time consuming, laborious, and equipment expensive. Therefore, several predictive models of λ for frozen fully saturated porous systems (e.g., food and soils) were proposed in the past. In the majority of cases, these models are based on a system composition data and λ of their components. The models for saturated solid foods consider that heat is being distributed by conduction only, while for unsaturated foods more complex modeling attempts are required to take into account simultaneous phenomena of water evaporation, condensation, and ice formation. A concise review of selective predictive models is given below.

Maxwell–Eucken (Maxwell–E) model

Maxwell (1873) published a model for predicting electrical conductivity of randomly distributed and noninteracting

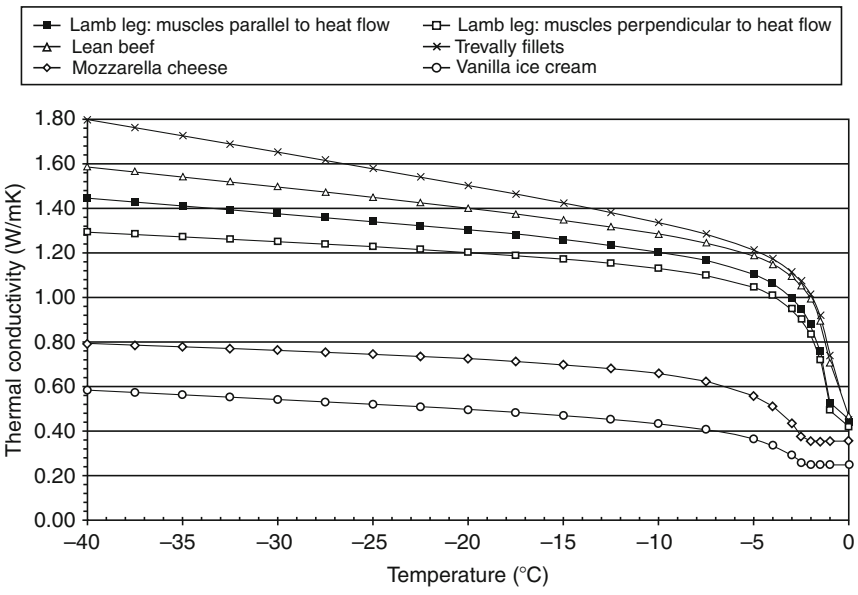

Modeling the Thermal Conductivity of Frozen Foods, Figure 2 Thermal conductivity of frozen foods vs. temperature.

homogeneously dispersed spheres (d) in a homogeneous continuous medium (con); and distances between spheres were assumed to be considerably larger than spheres' radii. Eucken (1932) extended this model to conduction heat flow in porous media and provided the following weighted average relation.

$$\lambda = \frac{k_{con} \cdot \theta_{con} \cdot \lambda_{con} + k_d \cdot \theta_d \cdot \lambda_d}{k_{con} \cdot \theta_{con} + k_d \cdot \theta_d}, \tag{5}$$

$$k_d = \frac{1}{3} \sum_{x=a,b,c} [1 + (\delta - 1) \cdot g_x]^{-1} \quad \delta = \frac{\lambda_d}{\lambda_{con}}, \tag{6}$$

where $k_{con} = 1$, θ are respective volume fractions, g_x is a shape factor for each particle's dimension in the dispersed phase. For solid spherical particles, $g_x = 1/3$ is applied to all three dimensions.

Levy model

Levy (1981) modified the Maxwell–E model by replacing the volume fraction of a dispersed phase, θ_d, by a new function F that eliminates a dilemma of phase designation.

$$F = \frac{1}{\sigma} - \frac{1}{2} + \theta_d - \frac{1}{2}\sqrt{\left(\frac{2}{\sigma} - 1 + 2 \cdot \theta_d\right)^2 - 8 \cdot \frac{\theta_d}{\sigma}}$$
$$\sigma = \frac{(\delta - 1)^2}{(\delta + 1)^2 + 0.5 \cdot \delta}. \tag{7}$$

In reality, porous media such as foods, however, are not necessarily composed of solid spheres and they may not be isolated from each other.

deVries model

Further modification of the Maxwell–E model was done by deVries (1963), who replaced a spherical shape of solid grains by rotated oblate ellipsoids dispersed in the continuous medium (water, air, ice), generating the following relation.

$$\lambda = \frac{k_{con} \cdot \theta_{con} \cdot \lambda_{con} + \sum_{j=1}^{N} k_j \cdot \theta_j \cdot \lambda_j}{k_{con} \cdot \theta_{con} + \sum_{j=1}^{N} k_j \cdot \theta_j}, \tag{8}$$

where N is the number of solid components; each solid grain component (j) has the same weighting factor k_j and the same thermal conductivity λ_j.

$$k_j = \frac{1}{3} \sum_{x=a,b,c} \left[1 + \left(\frac{\lambda_j}{\lambda_{con}} - 1\right) \cdot g_x\right]^{-1}, \tag{9}$$

where g_x is a solid particle ellipsoidal shape factor for each of three ellipsoid axes (a, b, c); $g_a + g_b + g_c = 1$, $a = b = p \cdot c$, where p is a shape value; thus, $g_a = g_b$, while $g_c = 1 - 2 \cdot g_a$.

The models by Maxwell–E, Levy (Equations 5–7), and deVries (Equations 8–9) are at first sight, identical in form, but in fact a different shape of solid particles (sphere vs. rotated ellipsoid) is used in these models. The shape value for spheres is known ($p = 1$), while for rotated ellipsoid the p is usually obtained by fitting the model to experimental data. Consequently, the model by deVries is rarely used in food engineering.

Mascheroni model

Mascheroni et al. (1977) assumed that solid frozen meats are made of partially dehydrated fibers (f), surrounded by ice and/or water randomly dispersed in a continuous matrix of the remaining food tissue. The first version of the model considers that heat flow is perpendicular ($\perp$) to meat fibers:

$$\lambda_\perp = \frac{\lambda_{ice} \cdot \lambda_f \cdot (1 - \xi_{ice})}{\xi_{ice} \cdot \lambda_f + \lambda_{ice} \cdot (1 - \xi_{ice})} + \lambda_{ice} \cdot \xi_{ice}, \tag{10}$$

where $\xi_{ice} = 1 - \sqrt{1 - \theta_{ice}}$, $\theta_{ice} = m_{ice} \cdot \frac{\rho_b}{\rho_{ice}}$, ρ_b = food bulk density, ρ_{ice} = density of ice.

The second model option assumes that heat flow is parallel (//) to the meat fibers:

$$\lambda_{//} = \lambda_{ice} \cdot \xi_{ice} + (1 - \xi_{ice}) \cdot \left[\lambda_{ice} \cdot \xi_{ice}^2 + \lambda_f \cdot (1 - \xi_{ice})^2 + \frac{4 \cdot \xi_{ice} \cdot (1 - \xi_{ice})}{\frac{1}{\lambda_f} + \frac{1}{\lambda_{ice}}}\right]. \tag{11}$$

Gori model

Gori (1983) assumed that frozen meats (also used for frozen soils) are composed of cubic cells, each having a concentrically located cubicle, representing all solid food components (s), surrounded with the continuous medium (unfrozen water [w], ice [i], or a mixture of both [wi]). The first version of the model considers the horizontal parallel isotherms in the cubic cell.

$$\frac{1}{\lambda} = \frac{\beta - 1}{\lambda_{wi} \cdot \beta} + \frac{\beta}{\lambda_{wi} \cdot (\beta^2 - 1) + \lambda_s} \quad \beta = \sqrt[3]{\frac{1}{1 - \theta_{wi}}} \tag{12}$$

The second version of the model takes into account a vertical parallel heat flux in the cubic cell.

$$\lambda = \frac{1}{\frac{\beta \cdot (\beta - 1)}{\lambda_{wi}} + \frac{\beta}{\lambda_s}} + \lambda_{wi} \cdot \frac{\beta^2 - 1}{\beta^2}. \tag{13}$$

Effective medium theory (EMT) model

The EMT model was adapted to predicting λ of vegetable foods by Mattea et al. (1986).

$$\sum_{1}^{n} \theta_j \cdot \frac{\lambda_j - \lambda}{\lambda_j + 2\lambda} = 0. \tag{14}$$

For frozen foods, three phases were considered:

$$\lambda_1 = \lambda_w \quad \theta_1 = \theta_w \quad \lambda_2 = \lambda_{ice} \quad \theta_2 = \theta_{ice}$$
$$\lambda_3 = \lambda_s \quad \theta_3 = 1 - \theta_w - \theta_{ice}$$

Modified resistor series model

Cleland and Valentas (1997) proposed a modified resistor series model for calculating λ of frozen foods, which may also contain bounded water (b).

$$\frac{\theta_w + \theta_b + \theta_s}{\lambda} = \frac{\theta_w + \theta_b}{\lambda_w} + \frac{\theta_s}{\sum_{j=1}^{n} \frac{\theta_j}{\theta_s} \cdot \lambda_j}. \tag{15}$$

Geometric mean model (GMM)

The GMM was successfully used in predicting λ of frozen soils by Johansen (1975).

$$\lambda = \lambda_s^{\theta_s} \cdot \lambda_{ice}^{\theta_{ice}} \cdot \lambda_w^{\theta_w}. \tag{16}$$

Parallel model (//)

It assumes parallel configuration of the system components in the direction of heat flow.

$$\lambda_{//} = \frac{\sum_{1}^{n} \theta_i \cdot \lambda_j}{\sum_{1}^{n} \theta_j}. \tag{17}$$

Series model (Σ)

It assumes series configuration of the system components in the direction of heat flow.

$$\lambda_{\Sigma} = \frac{\sum_{j=1}^{n} \theta_i}{\sum_{j=1}^{n} \frac{\theta_j}{\lambda_j}}. \tag{18}$$

Pham (1990) carried out a comprehensive analysis of seven physical predictive models and one set of empirical equations for λ of frozen foods and concluded that the model by Levy (1981) was the most accurate followed by the effective medium theory (EMT) model and the Maxwell–Eucken model. Tarnawski et al. (2005) analyzed and compared eight models (deVries, Levy, Mascheroni, Maxwell–Eucken, Gori, geometric mean, effective medium theory, modified resistor) and their 54 versions, developed for frozen foods and soils, against λ data of 13 meat products (Pham and Willix, 1989) in T ranging from -1°C to -40°C. The thermal conductivity of ice and other food components were assumed to be T independent; the fraction of ice was modeled using a relation given by Schwartzberg (1976). The models by deVries, Levy, and Mascheroni produced results very close to experimental data. In general, relatively small differences in predictions were observed, i.e., Relative Root Mean Squared-Error (RRMSE) was ranging from 5% to 7%; it was probably due to meat anisotropy, constant λ_{ice}, varying composition, measuring errors, and limitation of predictive models. A similar analysis carried out by Tarnawski et al. (2007) for T-dependent λ_{ice} showed that the models by Mascheroni et al. (1977) are marginally better than the other remaining models. Carson (2006) published a comprehensive review of models applied to unfrozen and frozen foods. Wang et al. (2006) verified 31 predictive models by comparing them with λ conductivity data for 22 meat and seafood products (Willix et al., 1998; Pham and Willix, 1989), with T ranging from -40°C to +40°C. The results obtained showed that the best 15 models had *RRMSE* varying from 11.5% to 16.4%. van der Sman (2008) modeled thermophysical properties of frozen meat products using their composition data, $\lambda(T)$ for water and ice, with the ice fraction estimated by a relation given by Schwartzberg (1976). The λ model by Torquato and Sen (1990) was extended to ternary systems (frozen meats) by modeling two existing phases (unfrozen water and muscle fiber) as one continuous medium and handling ice crystals as the dispersed phase. The model introduces a factor dependent on the structure and orientation of protein fibers. This modeling attempt was compared with experimental λ data by Pham and Willix (1989) and Willix et al. (1998), and predictions with an error of 10% were reported. In the past, comprehensive reviews on modeling λ of foods were also given by Sweat (1985) and Sanz et al. (1989).

In terms of frozen unsaturated food products (internal pores filled in with moist air), λ modeling is much more intricate as porosity of foods and filling mediums (water, air) have to be considered. Cogné et al. (2003) measured λ of ice creams using a hot-wire probe technique. The measured λ was affected by T and the ice cream's apparent density. For λ modeling, ice cream was considered as a heterogeneous and multiphase system composed of a frozen concentrated continuous liquid phase matrix (carbohydrates, proteins, lipids, and unfrozen water) filled in with ice and air. The dispersed phase (liquid water and solid components) λ was estimated by a parallel model and then together with $\lambda_{ice}(T)$ was applied to de Vries model for obtaining λ of a standard mix at different T; then, this λ with a value of λ_{air} was applied to Maxwell–Eucken model to obtain the overall λ. Jury et al. (2007) carried out λ measurements of bread with T ranging from -20°C to 80°C. Bread was assumed to be composed of dry fraction (proteins, carbohydrates, lipids, mineral salts, etc.) and pores containing moist air, both surrounded by water. When this system is exposed to $T < T_f$, very complex simultaneous heat and moisture transfer phenomena (evaporation–condensation effects, ice formation, etc.) take place (Hamdami et al., 2004). Consequently, measuring and estimating effective λ for unfrozen and frozen breads still remains a very complex issue (Hamdami et al., 2003).

Conclusions and recommendations

Accurate λ predictions for frozen foods are difficult due to a large number of modeling parameters involved, such as initial water content, temperature, density, food structure, anisotropy, initial freezing point, rate of ice formation, temperature-dependent thermal conductivity of ice, etc. Frozen foods are often considered as a mixture of homogeneous solid components being dispersed in continuous phase (*ice*, *water*, or *water+ice*). There are, however, still some dilemmas with a proper selection of a continuous medium and therefore, further studies are needed. A choice of *water+ice* as the continuous phase is promising as it improves λ predictions and eliminates discontinuity at the initial freezing point T_f, but nevertheless it requires further comprehensive testing. Temperature-dependent λ_{ice} has a strong influence on predicted λ of frozen lean meats; but, there are some unanswered concerns regarding the equations currently used for λ_{ice} estimation, as λ_{ice} also depends on ice structure and a freezing process for both water solution and pure water. Taking into account these issues and the enormous complexity of foods and the freezing process, developing an accurate mechanistic λ model for frozen foods is rather unrealistic. Review of frozen food literature reveals that Levy model and Mascheroni's equations produce very close results to experimental data (within approximately 10% error). The model by Mascheroni, however, is simpler in form, accounts for food fiber orientation, does not require any fitting, and it produces close predictions for low-fat meats. For high-fat meats, Levy's model gives better λ estimates, but the model structure is too complex and therefore it is not easy to use. Highly complex predictive models are difficult to handle when applied to food products of uncertain food structure, composition, and unknown thermal conductivity, because numerous rough assumptions have to be made. Besides, it is still unclear what the real impact of highly accurate λ predictions will have on the analysis of freezing processes and designing freezing/thawing equipment, due to a variety of foods having very diverse physical properties. It appears that, the demand for sophisticated and difficult to use λ models may not be fully justified and more attention should be paid to the use of simple models (e.g., geometric mean, series–parallel, etc.) applied to a wide variety of foods.

Bibliography

Carson, J. K., 2006. Review of effective thermal conductivity models for foods. *International Journal of Refrigeration*, **29**(6), 958–967.

Choi, Y., and Okos, M. R., 1986. Effects of temperature and composition on the thermal properties of foods. In Le Maguer, M., and Jelen, P. (eds.), *Food Engineering and Processes Applications, 1*. Amsterdam: Elsevier Applied Science, pp. 93–101.

Cleland, D. J., and Valentas, K. J., 1997. Prediction of freezing time and design of food freezers. In Singh, R. P., and Valentas, K. J. (eds.), *1997*. CRC Press: Handbook of Food Engineering Practice, pp. 71–124.

Cogné, C., Andrieu, J., Laurent, P., Besson, A., and Nocquet, J., 2003. Experimental data and modeling of thermal properties of ice creams. *Journal of Food Engineering*, **66**(4), 469–475.

DeVries, D. A., 1963. Thermal properties of soils. In van Wijk, W. R. (ed.), *Physics of Plant Environment*. New York: Wiley, pp. 210–235.

Eucken, A., 1932. Thermal conductivity of ceramics refractory materials. *Forsch. Geb. Ing., B-3, Forschungsheft*, **53**, 6–21.

Fikiin, K. A., 1998. Ice content prediction methods during food freezing: a survey of the eastern European literature. *Journal of Food Engineering*, **38**, 331–339.

Fukusako, F., 1990. Thermophysical properties of ice, snow, and sea ice. *International Journal of Thermophysics*, **11**(2), 353–372.

Golovkin, N. A., and Tchizov, G. B., 1951. Refrigeration technology of food products (in Russian). *Pischepromizdat*, **1951**, 232.

Gori, F., 1983. A theoretical model for predicting the effective thermal conductivity of unsaturated frozen soils. In *Proceedings of the Fourth International Conference on Permafrost, Fairbanks (Alaska)*. Washington: National Academy Press, pp. 363–368.

Hamdami, N., Monteau, J.-Y., and Le Bail, A., 2003. Effective thermal conductivity of a high porosity model at above and subfreezing. *International Journal of Refrigeration*, **7**, 809–816.

Hamdami, N., Monteau, J.-Y., and Le Bail, A., 2004. Thermophysical properties evolution of French partly baked bread during freezing. *Food Research International*, **37**, 703–713.

Heldman, D. R., 2003. Encyclopedia of Agricultural, Food, and Biological Engineering. Marcel Dekker.

Johansen, O., 1975. Thermal conductivity of soils. PhD Thesis, University of Trondheim, Norway, CRREL Translation 637.

Jury, V., Monteau, J.-Y., Comiti, J., and Le-Bail, A., 2007. Determination and prediction of thermal conductivity of frozen part baked bread during thawing and baking. *Food Research International*, **40**, 874–882.

Levy, F. L., 1981. A modified Maxwell–Eucken equation for calculating the thermal conductivity of two-component solutions or mixtures. *International Journal of Refrigeration*, **4**, 223–225.

Mascheroni, R. H., Ottino, J., and Calvelo, A., 1977. A model for the thermal conductivity of frozen meat. *Meat Science*, **1**, 235–243.

Mattea, M., Urbicain, M. J., and Rotstein, E., 1986. Prediction of thermal conductivity of vegetable foods by the effective medium theory. *Journal of Food Science*, **51**(1), 113–115.

Maxwell, J. C., 1873. *A Treatise on Electricity and Magnetism*, 1st edn. Oxford: The Calerdon Press, Vol. 1, p. 440.

Pham, Q. T., 1990. Prediction of thermal conductivity of meats and other animal products. In Spiess, W. E. L., and Schubert, H. (eds.), *Engineering and Food*, vol. 1st edn. London: Elsevier Applied Science, pp. 408–423.

Pham, Q. T., and Willix, J., 1989. Thermal conductivity of fresh lamb meat, offal and fat in the range –40 to + 30°C: measurements & correlations. *Journal of Food Science*, **54**(3), 508–515.

Rahman, M. S., 2001. Thermophysical properties of foods. In D-Wen Sun. (ed.), *Advances in Food Refrigeration*. Leatherhead Publishing: Surrey.

Sakazume, S., and Seki, N., 1978. Thermal properties of ice and snow at low temperature region. *Trans. JSME*, **44**(382), 2059–2069.

Sanz, P. D., Alonso, M. D., and Mascheroni, R. H., 1989. Equations for the prediction of thermophysical properties of meat products. *Latin American Applied Research*, **19**, 155–163.

Schwartzberg, H. G., 1976. Effective heat capacity for the freezing and thawing of food. *Journal of Food Science*, **41**, 152–156.

Sun, Da-Wen., 2006. *Handbook of Frozen Food Processing and Packaging*. Boca Raton: Taylor & Francis.

Sweat, V. E., 1985. Thermal conductivity of food: present state of the data. *Trans. American society of heating refrigerating and airconditioningEngineers*, **19**(part B), 299–311.
Tarnawski, V. R., Cleland, D. J., Corasaniti, S., Gori, F., and Mascheroni, R. H., 2005. Extension of soil thermal conductivity models to frozen meats with low and high fat content. *International Journal of Refrigeration*, **28**, 840–850.
Tarnawski, V. R., Bovesecchi, G., Coppa P., and Leong, W. H., 2007. Modeling thermal conductivity of frozen foods with temperature dependent thermal conductivity of ice. *The 22nd International Congress of Refrigeration*, August 21–26, 2007, Beijing, China.
Torquato, S., and Sen, A. K., 1990. Conductivity tensor of anisotropic composite media from microstructure. *Journal of Applied Physics*, **67**(3), 1145–1155.
U.S. Army Corps of Engineers, 1996. Engineering & Design –Ice Engineering: Manual No. 1110-2-1162, Washington D.C. p. 2.
van der Sman, R. G. M., 2008. Prediction of enthalpy and thermal conductivity of frozen meat and fish products from composition data. *Journal of Food Engineering*, **84**, 400–412.
Wang, D., and Kolbe, E., 1990. Thermal conductivity of surimi-measurement and modeling. *Journal of Food Science*, **50**(5), 1458–1462.
Wang, J. F., Carson, J. K., Cleland, D. J., and North, M. F., 2006. *A comparison of effective thermal conductivity models for frozen foods, in Innovative Equipment and Systems for Comfort and Food Preservation*, Proceedings, Auckland 2006, pp. 336–343.
Willix, J., Lovatt, S. J., and Amos, N. D., 1998. Additional thermal conductivity values of foods measured by a guarded hot plate. *Journal of Food Engineering*, **37**, 159–174.
Yen, Y. C., 1981. Review of thermal properties of snow, ice and sea ice. *CRREL Report*, **81**(10), 1–27.

Cross-references

Databases on Physical Properties of Plants and Agricultural Products

MODULUS OF ELASTICITY (YOUNG'S MODULUS)

The ratio of normal stress to corresponding strain below the proportional limit of a material (e.g., plant stalks and roots).

MODULUS OF RIGIDITY

The ratio of shear stress to the shear strain below the proportional limit of a material displacement per unit sample length.

MOHRE CIRCLE OF STRESS

A graphical representation of the components of stress acting across the various planes at a given point, drawn with reference to axes of normal stress and shear stress.

Bibliography

Glossary of Soil Science Terms. Soil Science Society of America. 2010. https://www.soils.org/publications/soils-glossary

Cross-references

Friction Phenomena in Soils

MONITORING PHYSICAL CONDITIONS IN AGRICULTURE AND ENVIRONMENT

Wojciech M. Skierucha
Department of Metrology and Modeling of Agrophysical Processes, Institute of Agrophysics, Polish Academy of Sciences, Lublin, Poland

Definition

Monitoring physical conditions in agriculture and environment is a collection and processing of data that allow to determine temporal and spatial variation of these conditions to make proper decisions in the future for the benefit of sustainable food production.

Introduction

Agriculture has both positive and negative influence on environment. Its primary function is meeting the growing demand for food. Agriculture creates habitats not only for humans but also for wildlife and plays an important role in sequestering carbon, managing watersheds, and preserving biodiversity. But agriculture degrades natural resources causing soil erosion, introducing unrecoverable hydrological changes, contributing in groundwater depletion, agrochemical pollution, loss of biodiversity, reducing carbon sequestration from deforestation, and carbon dioxide emissions from forest fires (Doran, 2002).

Physical conditions in agriculture and environment can be defined as physical properties and processes involved in mutual relation between the processes of food and fiber production and the impact of these processes on natural agro-environment. They include topography, surface water and groundwater distributions, heat-temperature distributions, wind direction changes, and intensity.

The measures of physical conditions in agriculture and environment should include a minimum number of measurable physical indicators, that can provide sufficient data not only for decision making in the production of food and fiber but also in ecosystem function and the maintenance of local, regional, and global environmental quality.

Agricultural sustainability and environmental quality are determined by the health of soil, which is a thin layer of the earth surface forming the interface between agriculture and environment. Soil quality, which can be described

by the combination of its physical, chemical, and biological properties and contamination by inorganic and organic chemicals is critical to environmental sustainability (Arshad and Martin, 2002). The physical properties of soils play a major role in controlling mass and energy transport in the subsurface environment.

The basic physical soil quality indicators recommended or used by soil researchers are as follows (Schoenholtz et al., 2000): texture (influence retention and transport of water and nutrients), soil depth and topsoil depth (major factor in total nutrient, water, and oxygen availability), bulk density (decides about root growth, rate of water movement, soil volume expression), soil water content, soil temperature, available water holding capacity (informs about plant available water, erosivity), soil roughness (erosivity, soil tilth), saturated hydraulic conductivity (water and air balance, hydrology regulation), resistance to penetration (root growth), porosity (water/air balance, water retention, root growth), and aggregate stability and size distribution (root growth, air/water balance).

The need for monitoring physical conditions in agriculture and environment is increasing, because of increasing pressure on natural resources, sustainability, and exhaustion of nonrenewable resources. Advances in sensors, computers, and communication devices result in great amounts of temporal and spatial information that should be processed in real-time (or near real-time) to produce unambiguous information for the decision-making stage.

Robust, low-cost, and preferably real-time sensing systems are needed for monitoring physical conditions in agriculture and environment. Commercial products have become available for some sensor types. Others are currently under development, especially in the field of precision agriculture.

Selection of the monitoring method

Monitoring is a series of measurements (or observations) done in a planned fashion in order to assemble a more complete view of existing conditions through time. Single observations or surveys are made at a point in time to record the current condition. Monitoring, in a formal sense, is a series of surveys.

The goals, applied sensors, data collection strategies, and methods of analysis used in monitoring must be defined in detail and in advance before taking further steps that sometimes require formal, technical, and financial arrangements. These elements and their relationship depend on the temporal and dimensional scale of planned observations. There are technical means to measure minute quantities of chemicals in the environment. At the other end of the dimensional scale, there are space-based satellite sensors routinely scanning and mapping the earth surface several times a day.

The choice of mass and volume of the sampled material, size of measurement probes, and temporal and spatial locations should be chosen for assuring the measured sample to be representative of the target component. This is especially important for soil because it is not homogeneous both in space and in time.

The investigation of the agricultural and environmental physical conditions sometimes requires physical removal of samples from the environment, for example, collecting soil cores in the vadose zone disrupt soil profiles and can create preferential flow paths. Measurements involving unrecoverable destruction of the measured medium are called destructive. Nondestructive measurements or monitoring is becoming increasingly important with the technological miniaturization as well as the development of sensors, electronics and telecommunication. The example of nondestructive monitoring is by means of satellite-based sensors to measure topography, plant cover, or topsoil temperature.

Selectivity

The key feature of the applied measurement method is its selectivity, that is, the lack of sensitivity of the conversion function (calibration) on the influence from the factors other than the measured one. Proper selectivity liberates the user from frequent, specific for each soil, in situ calibrations.

The solution to the problem of electric measurement of the physical quantity in selective way is to find such an electric property of the medium conditioning it, which is specific to the considered medium. For example, the specific property of molecular oxygen in electrolyte ("soil water") is small activation energy of electrode reaction of its reduction. It can be concluded that electric measurement of oxygenation may be based on the ammetric measurement of the current of electrode reaction of oxygen molecules reduction (Malicki and Bieganowski, 1999).

Concerning the problem of electric soil moisture measurement, the medium conditioning moisture is water and its specific property is the polar structure of water molecules. Polarity of water molecules is the reason that dielectric permittivity (dielectric constant) of water is much higher than permittivity of soil solid phase (the relative dielectric constant of water in the electric field of frequency below 18 GHz and at room temperature is about 81, while the relative dielectric constant of solid phase is 4–5 at the same conditions). The dielectric constant of soil strongly depends on its water content, therefore it may be concluded that electric measurement of soil moisture should be based on the measurement of its dielectric constant.

Similarly, concerning the issue of electric measurement of soil salinity, the media conditioning salinity are salts present in soils and the specific property is their ionic form. The ability to transport electric charge by the ions in "soil water" allows the soil to conduct electric current. Therefore, the electric measurement of soil salinity should be based on the measurement of its electric conductivity.

Status of water as significant issue of agrophysics

Increasing demands of water management result in the continuous development of its tools. One of the most important, besides the simulation models of water balance, is monitoring of water status in porous materials defined as a space-temporal recording of the water properties that stimulate the phenomena and processes observed in the soil–plant–atmosphere system.

Concerning agrophysics, water status in porous materials is the issue of first priority, because each phenomenon or process examined in its scope depends on water status.

Monitoring of water status is accomplished using digital systems. The digital data acquisition systems react only on electric signals and the applied sensors must convert the measured value into the proportional electric signal.

Water status of soil, as a porous material should be expressed by minimum five variables: amount of water in the soil (i.e., soil moisture), soil potential, salinity, oxygenation, and temperature (Malicki, 1999).

The most difficult are the electric measurement of soil water potential and soil water content (soil moisture); therefore, they are the subject of permanent research. It is assumed here, that the method successfully verified for soils will be also applicable for other porous agricultural materials because their structure is not as complex as soil.

Monitoring physical conditions in agriculture and environment is done by sampling, automatic ground measurement systems or remote sensing with the use of planes or satellites.

Sampling

There are several soil basic physical properties that cannot be measured automatically and the necessary information about their variability in time and/or space is gathered by means of traditional sampling. Soil mechanical properties, that is, soil texture and soil density or porosity, which is functionally dependent on soil density, do not change in time in uncultivated areas because they present the effect of long-term geological processes.

Sampling strategy in agro-environmental monitoring depends on the objectives, which include increase agriculture productivity (yield indicators), optimize water use in irrigation systems, or increase carbon sequestration. Also, it depends on observation scale from the geographical or administrative point of view: an experimental plot, field, landscape, watershed, farm, district, or whole country. Spatial and temporal variability must also be taken into account in constructing time schedule and sampling locations to be representative.

Sampling usually affects the environment, that is, this type of measurement maybe destructive to the tested object or its immediate vicinity. Drilling a deep well to collect groundwater does not affect the groundwater environment but the geological profile is irreversibly damaged. Soil cores collected in the vadose zone disrupt soil profiles and can create preferential flow paths.

Ground monitoring systems with automated data acquisition and processing

The technological progress in material science, electronics, telecommunication, and informatics effects in the development of new sensing devices that can be adopted in examining objects of agricultural and environmental studies. They include Time Domain Reflectometry (TDR) and Frequency Domain Reflectometry (FDR) probes for the simultaneous measurement of soil moisture, electrical conductivity, and temperature (Skierucha et al., 2006). There sensing devices include sensors and transducers, where the former detects the signal or stimulus and the latter converts input energy of one form into output energy of another form. An example of the sensor is thermistor giving the change of resistance as the function of temperature. This sensor associated with electrical circuitry forms an instrument, also called a transducer, that converts thermal energy into electrical energy.

Another important element of a ground monitoring system is a data acquisition and processing unit, which monitors the output signal of the transducer and processes the resulting data into a form that can be understood by the end user. The basic features of this unit include user-friendly interface for the operator, large storage memory, physical communication interfaces preferably with serial transmission from the instrument to the operator's notebook. Telemetry with the application of wireless networks is becoming popular especially for distant ground monitoring systems (Wang et al., 2006).

Monitoring stations must meet strong requirements concerning power consumption. The hardware designers should use low-power electronic circuits and apply sleep mode operations whenever possible. Also, charging the internal battery is accomplished with a solar panel.

Remote sensing

Remote sensing in agriculture and environment is the acquisition of biological and geochemical information about the condition and state of the land surface by sensors that are not in direct physical contact with it. The transmission of this information is in the form of electromagnetic waves reflected from the land surface either in passive mode – when the source of energy is the sun and/or the Earth, or in active mode – when the source energy is artificially generated. The analyzed signal reflected from the land surface is composed with different wavelengths over the electromagnetic spectrum (Artiola et al., 2004a). Today a large number of satellite sensors observe the Earth at wavelengths ranging from visible to microwave, at spatial resolutions ranging from submeters to kilometers and temporal frequencies ranging from minutes to weeks or months (Rosenqvist et al., 2003).

The remote sensed data provide information about ecosystem stability, land degradation and desertification (Artiola et al., 2004b), carbon cycling (Rosenqvist et al., 2003), erosion and sediment yield, soil moisture

(Wigneron et al., 1998; Kerr, 2007), and plant and weeds cover (Thorp and Tian, 2004).

Conclusion

Monitoring physical conditions in agriculture and environment can be done in various temporal and dimensional scales and with the application of numerous instruments and methods reflecting the current development of technology. The received and processed data increase our knowledge for the benefit of social, political, and economic sustainable development as well as for better understanding the nature.

Bibliography

Arshad, A. A., and Martin, S., 2002. Identifying limits for soil quality indicators in agro-ecosystems. *Agriculture, Ecosystems and Environment*, **88**, 152–160.
Artiola, J., Pepper, I. L., and Brusseau, M. L., 2004a. Monitoring and characterization of the environment (Chapter 11). In *Environmental Monitoring and Characterization*. Burlington: Elsevier, pp. 1–9.
Artiola, J., Pepper, I. L., and Brusseau, M. L., 2004b. Remote sensing for environmental monitoring (Chapter 11). In *Environmental Monitoring and Characterization*. Burlington: Elsevier, pp. 183–206.
Doran, J. W., 2002. Soil health and global sustainability: translating science into practice. *Agriculture, Ecosystems and Environment*, **88**, 119–127.
Kerr, Y. H., 2007. Soil moisture from space: where are we? *Hydrogeology Journal*, **15**, 117–120.
Malicki, M. A., 1999. Methodical aspects of water status monitoring in selected bio-materials. *Acta Agrophysica (Series Monographs)*, **19** (in Polish).
Malicki, M. A., and Bieganowski, A., 1999. Chronovoltammetric determination of oxygen flux density in the soil. *International Agrophysics*, **13**(3), 273–281.
Rosenqvist, Å., Milne, A., Lucas, R., Imhoff, M., and Dobson, C., 2003. A review of remote sensing technology in support of the Kyoto Protocol. *Environmental Science & Policy*, **6**, 441–455.
Schoenholtz, S. H., Van Miegroet, H., and Burger, J. A., 2000. A review of chemical and physical properties as indicators of forest soil quality: challenges and opportunities. *Forest Ecology and Management*, **138**, 335–356.
Skierucha, W., Wilczek, A., and Walczak, R. T., 2006. Recent software improvements in moisture (TDR method), matric pressure, electrical conductivity and temperature meters of porous media. *International Agrophysics*, **20**, 229–235.
Thorp, K. R., and Tian, L. F., 2004. A review on remote sensing of weeds in agriculture. *Precision Agriculture*, **5**, 477–508.
Wang, N., Zhang, N., and Wang, M., 2006. Wireless sensors in agriculture and food industry – recent development and future perspective. *Computers and Electronics in Agriculture*, **50**, 1–14.
Wigneron, J. P., Schmugge, T., Chanzy, A., Calvet, J. C., and Kerr, Y., 1998. Use of passive microwave remote sensing to monitor soil moisture. *Agronomie*, **18**, 27–43.

Cross-references

Climate Change: Environmental Effects
Nondestructive Measurements in Soil
Online Measurement of Selected Soil Physical Properties
Remote Sensing of Soils and Plants Imagery
Spatial Variability of Soil Physical Properties

MUALEM EQUATION

Model for predicting hydraulic conductivity of unsaturated porous media.

Bibliography

Mualem, Y., 1976. A new model for predicting hydraulic conductivity of unsaturated porous media. *Water Resources Research*, **12**:513–522.

Cross-references

Water Budget in Soil

MULCHING

See *Water Use Efficiency in Agriculture: Opportunities for Improvement*

MULCHING, EFFECTS ON SOIL PHYSICAL PROPERTIES

Antonio Jordán[1], Lorena M. Zavala[1],
Miriam Muñoz-Rojas[2]
[1]MED_Soil Research Group, Departamento de Cristalografía, Mineralogía y Química Agrícola, Universidad de Sevilla, Sevilla, Spain
[2]Instituto de Recursos Naturales y Agrobiología de Sevilla (CSIC), Sevilla, Spain

Definition

Mulch. Mulch is any material, other than soil, placed or left at the soil surface for soil and water management.
Mulching. In agriculture and gardening, mulching is the practice of leaving crop residues or other materials on the soil surface for soil and water conservation and keeping favorable and stable environments for plant growth.

Introduction

Mulching is a form of conservation tillage consisting of leaving a layer of crop residues (CR) or other materials on the soil surface. Mulch helps to preserve high and sustainable yields by increasing the soil organic matter (SOM) content and therefore improving soil physical quality. Mulch tilling is also a form of minimum tillage and a cost-efficient alternative for high-yield conservation agricultural practice.

Leaving CR or other substances on the soil surface is a traditional practice for protecting soil from erosion and enhancing fertility (Lal and Stewart, 1995). It has been reported that conventional agricultural practices, based

on intensive fertilization and chemical amendments, often lead to degradation processes, such as erosion (see entry *Tillage Erosion*), acidification, and the emission of greenhouse gases (see entry *Greenhouse Gases Sink in Soils*). Current global problems such as population growth, greenhouse effect, malnutrition, water quality, reduction of agricultural land, and soil degradation (see entry *Desertification: Indicators and Thresholds*) require the implementation of conservation tillage practices to address the problem of sustainability, food security, and environmental quality.

Materials used as mulch

A wide variety of materials can be used as mulch. Most of mulches are organic materials (e.g., CR, litter, straw, leaves, or weed biomass), but other inorganic or industry-derived materials can be also used (plastic film, gravels, or geotextiles). The election depends in both availability and objectives.

Organic mulches must be weed free, easy to apply, and readily available by farmers. The mulch decomposition time can vary greatly. Depending on the amount and type of mulch, varying quantities of nutrients and organic matter enter the soil during the decomposition process. In agriculture, the most commonly used organic mulches are crop/plant residues, produced on-site or off-site and left on the soil surface after cropping (e.g., wheat straw). A large quantity of residue is produced annually, so that it constitutes a renewable and easily available resource. Other mulches used in agriculture and gardening are wood chips, pine bark, and pine needles. Some wastes, such as shredded or composted clipped grass, litter, and small branches can also be used.

Inorganic materials such as geotextiles can be used as mulch. Some of the advantages of using geotextiles is the prevention of weed growth (at least in a great proportion), and the normal aeration and water exchange. Rock fragments and gravels can be used as inorganic mulch materials. They show low decomposition rates and do not require annual replacement, but cannot be suitable for all crops. Plastic films help control most weeds and contribute to water conservation. Plastic films are used predominantly in extensive crop areas, but show some problems: interruption of air, water, and nutrients flow between the topsoil and the atmosphere, as well as other environmental problems such as disposal of plastic materials.

Effects on soil physical properties

Soil structure and aggregate stability

Soil structure is extremely important for the maintenance of soil quality and productivity. Aggregate stability (AS) affects root density and elongation (see entry *Root Responses to Soil Physical Limitations*), air and water flow and erosion (Amézketa, 1999). Some of the main factors affecting soil aggregation are SOM content (see entry *Soil Aggregates, Structure, and Stability*), texture and moisture content, but external factors as crop type, tillage practices, or microfauna are also important. Long-term tillage affects AS (Angers et al., 1993; Unger et al., 1998; Álvaro-Fuentes et al., 2008), as tillage destroys aggregates leading to a decrease in aggregate size and pore clogging by fine particles. It has been reported that decomposition rates of SOM are lower with minimum tillage and residue retention, and consequently it increases over time (Loch and Coughlan, 1984; Dalal, 1989).

AS is determined by the cohesive forces between particles. Therefore, it can be used as an index of structure and physical soil stability. Soil texture, clay mineralogy, cations, and the quantity and quality of SOM are key factors controlling aggregation. Plant roots (see entry *Plant Roots and Soil Structure*), microorganisms (especially fungi), and organic substances are also involved in the formation of aggregates and AS. AS may vary seasonally (Hillel, 1998) or during tilling. After mulching, increased SOM content contributes to enhance aggregation, as it has been reported under a diversity of climate areas (Mulumba and Lal, 2008; Jordán et al., 2010) even in the short term (Hermawan and Bomke, 1997).

Inorganic mulches (e.g., plastic film) show limited or no effect on soil structure. Zhang et al. (2008), for example, reported that under no tillage, the increase in SOM content and AS in soils under straw cover was higher than under plastic film; in this case, soil quality under plastic mulch was similar or even lower than in non-covered soils. In contrast, geotextiles may increase SOM content, improving topsoil structure and AS (Bhattacharyya et al., 2010).

Bulk density and porosity

The effects of CR on soil bulk density (BD; see entry *Bulk Density of Soils and Impact on their Hydraulic Properties*) are highly variable. Although high BD has been observed under mulch relative to conventional tillage (Bottenberg et al., 1999), decreased bulk densities have also been reported by Oliveira and Merwin (2001) and Ghuman and Sur (2001). In other cases, there is no relationship between mulch rate and BD. This variability may be due to differences in management practices, soil type, and the type of mulch material used in the experiments. However, Mulumba and Lal (2008) found that BD increased for mulching rates between 0 and 5 Mg ha^{-1} wheat straw mulch, but strongly decreased for higher rates.

Pores of different size (see entry *Pore Size Distribution*), shape, and continuity are created by abiotic and biotic factors (Kay and VandenBygaart, 2002). Mulumba and Lal (2008) found that total porosity increased significantly with increase in mulch rate after an 11-year treatment in the USA. Increased porosity due to mulch application has been also reported after shorter periods (Oliveira and Merwin, 2001; Jordán et al., 2010).

Penetration resistance

Many studies have reported greater penetration resistance in soils under no-tillage practices than in other conventionally tilled soils in the upper centimeters, and, generally, penetration resistance is higher under reduced tillage systems with residue cover. Mulch application has a significant effect on penetration resistance but only at certain stages of the crop production. After an experiment with Polish Luvisols under reduced and no-tillage practices, penetration resistance increased in the growing season, causing reduced plant growth and crop yield (Pabin et al., 2003). In this case, straw mulch did not counteract the negative changes in the parameters of the soil strength. According to Bielders et al. (2002), differences in penetration resistance after different treatments are mostly due to differences in intrinsic soil properties (e.g., cohesion, BD).

Crusting and sealing

Plant residues on the soil surface protect it against crusting (Sumner and Stewart, 1992), improving AS and infiltration rates (see entry *Soil Surface Sealing and Crusting*). Le Bissonnais and Arrouays (1997) observed that increasing SOM content decreased soil surface sealing. After a study in western Niger, Bielders et al. (2002) observed low permeability erosion crusts and discontinuous structural crusts with partially exposed clay skins in soils under conventional tillage, in contrast to mulched soils. As it has been reported in stone-covered soils (Martínez-Zavala and Jordán, 2008; Zavala et al., 2010), gravel mulch helps to avoid soil sealing and crusting (Poesen and Lavee, 1994).

The use of plastic film mulches has spread considerably as a way to reverse the low crop yields (e.g., Zhang and Ma, 1994), increasing the risk of crust formation (Li et al., 2005).

Soil temperature

Temperature affects the rate of soil biological and chemical processes (see entry *Temperature Effects in Soil*). The amount of energy entering the soil depends strongly on soil color, aspect, and the vegetative cover. CR on the soil surface can affect or completely modify the soil temperature regime by reducing the amount of energy entering the soil by the interception of radiation, shading the soil surface, and buffering temperature variations.

Soil temperature range is usually narrower in mulched than unmulched soils. Wheat straw has a higher albedo and lower thermal conductivity than bare soil, and therefore it reduces the input of solar energy (Horton et al., 1996). On the other hand, during colder periods, wheat straw mulch on the soil surface insulates it from the colder atmosphere (Zhang et al., 2009).

Results after application of inorganic mulches vary depending on the mulch material. After field experiments in the UK, Cook et al. (2006) demonstrated that soil temperature reduced with higher mulching rates. In contrast, the use of inorganic mulches can increase soil temperature. Nachtergaele et al. (1998) reported that gravel mulch increased soil temperature and decreased evaporation (see entry *Evapotranspiration*) in vineyard soils in Switzerland. Organic geotextiles can also attenuate extreme temperature fluctuations, reducing water loss through evaporation. Inorganic materials such as plastic mulches are often used to increase soil temperature in horticulture, leading to high yields. Apart from other environmental problems, intensive use of plastic mulches for increasing soil temperature shows some limitations. Enhanced mineralization rates can lead to exhaustion of SOM, affecting long-term soil physical and chemical fertility (Li et al., 2004).

Soil water

Mulching has a great impact on soil water and surface water. Mulching decreases runoff by improving infiltration rate and increases water storage capacity by improving retention (see entry *Field Water Capacity*). In addition, reduced evaporation rates help to extend the period of time during which soil remains moist.

Mulching improves considerably soil water characteristics, although different results have been reported. Organic mulches on the soil surface induce optimal soil conditions for plant growth, enhancing soil water retention and availability, and increasing macroporosity (Martens and Frankenberger, 1992). Much research has shown that use of mulch can increase infiltration and decrease evaporation, resulting in more water stored and reduced runoff rates (e.g., Smika and Unger, 1986).

Wheat straw mulch is considered the best way of improving water retention in the soil and reducing soil evaporation. High available water capacities have been reported under high mulching rates and reduced or no till practices. Mulumba and Lal (2008) and Jordán et al. (2010) found that even low mulch rates have a strong impact on the available water content. Contrasting data have been reported by Głąb and Kulig (2008), who found no effect in available water content after applying mulch and different tillage systems. Results can also vary between the upper and lower layers of the soil profile.

Soil erosion risk

Many researchers have reported low or negligible soil losses in mulched soils in comparison with conventional soil tillage (see entry *Water Erosion: Environmental and Economical Hazard*). The hydrological/erosional response of mulched soils depends largely on the mulching rates applied during the crop period. It has been reported that the erosive consequences of moderate storms in the Mediterranean area could be strongly reduced by using just 5 Mg ha^{-1} $year^{-1}$ mulching rates (Jordán et al., 2010). A mulch layer increases the roughness and the interception of raindrops, delaying runoff flow and favoring infiltration (García-Orenes et al., 2009). Low erosive responses of mulched soils have been reported from diverse climate areas of the world. In contrast, Jin et al. (2009) suggested that the relation between mulching rate

and interrill soil detachment is not unique and can vary depending on rainfall intensity. Increasing cover rates reduce infiltration and lead to an increasing net flux, which becomes deeper and faster in its concentrated flow part. In this case, ponding is faster and deeper, thus the water column pressure is greater and thereafter infiltration takes place more quickly and penetrates more deeply. However, this response can be overridden under moderate rainfall intensity by a dense soil cover or thick mulch layers.

Plastic mulches substantially accelerate runoff generation in slopes (Wan and El-Swaify, 1999). According to Bhattacharyya et al. (2010), the use of geotextiles is an effective soil conservation practice, but its efficiency decreases in large areas. Despite synthetic geotextiles dominating the commercial market, geotextiles constructed from organic materials are highly effective in erosion control and vegetation establishment (Ogbobe et al., 1998) and can be an ecological alternative for farmers (Giménez-Morera et al., 2010). Anyway, experimental studies under natural and simulated rainfall have demonstrated that cotton geotextiles reduce soil losses but increase water losses, probably due to water repellency of cotton. Although soil erosion can be severely reduced by geotextiles at the pedon or meter scale, surface runoff may result in high erosion rates at slope and watershed scales as more runoff will be available (Giménez-Morera et al., 2010).

Summary

During the last decades, conservation tillage techniques have displaced conventional tillage in many areas of the world. The use of CR left on the soil surface improves soil quality and productivity through favorable effects on soil physical properties. Mulch farming is a form of conservation tillage that preserves soil quality and the environment. Mulch affects soil physical properties by improving SOM content, increasing soil porosity and AS. Indirectly, mulching also regulates soil temperature, and increases water retention capacity.

An organic mulch layer serves as a protecting layer against rainfall-induced soil erosion by reducing drop impacts and modifying the hydrological response of the exposed surface. CR and other organic mulches intercept rainfall and contribute to decrease runoff rates and enhance infiltration, protecting soil from erosion. Inorganic mulches as geotextiles, gravels, or plastic films show a range of erosional responses to rainfall.

Bibliography

Álvaro-Fuentes, J., Arrúe, J. L., Gracia, R., and López, M. V., 2008. Tillage and cropping intensification effects on soil aggregation: temporal dynamics and controlling factors under semiarid conditions. *Geoderma*, **145**, 390–396.

Amézketa, E., 1999. Soil aggregate stability: a review. *Journal of Sustainable Agriculture*, **14**, 83–151.

Angers, D. A., Samson, N., and Légère, A., 1993. Early changes in water-stable aggregation induced by rotation and tillage in a soil under barley production. *Canadian Journal of Soil Science*, **73**, 51–59.

Bhattacharyya, R., Smets, T., Fullen, M. A., Poesen, J., and Booth, C. A., 2010. Effectiveness of geotextiles in reducing runoff and soil loss: a synthesis. *Catena*, **81**, 184–195.

Bielders, C. L., Michels, K., and Bationo, A., 2002. On-farm evaluation of ridging and residue management options in a Sahelian millet-cowpea intercrop. 1. Soil quality changes. *Soil Use and Management*, **18**, 216–222.

Bottenberg, H., Masiunas, J., and Eastman, C., 1999. Strip tillage reduces yield loss of snapbean planted in rye mulch. *HortTechnology*, **9**, 235–240.

Cook, H. F., Valdes Gerardo, S. B., and Lee, H. C., 2006. Mulch effects on rainfall interception, soil physical characteristics and temperature under *Zea mays* L. *Soil and Tillage Research*, **91**, 227–235.

Dalal, R. C., 1989. Long-term effects of no-tillage, crop residue, and nitrogen application on properties of a Vertisol. *Soil Science Society of America Journal*, **53**, 1511–1515.

García-Orenes, F., Cerdà, A., Mataix-Solera, J., Guerrero, C., Bodí, M. B., Arcenegui, V., Zornoza, R., and Sempere, J. G., 2009. Effects of agricultural management on surface soil properties and soil-water losses in eastern Spain. *Soil and Tillage Research*, **106**, 117–123.

Ghuman, B. S., and Sur, H. S., 2001. Tillage and residue management effects on soil properties and yields of rainfed maize and wheat in a subhumid subtropical climate. *Soil and Tillage Research*, **58**, 1–10.

Giménez-Morera, A., Ruiz Sinoga, J. D., and Cerdà, A., 2010. The impact of cotton geotextiles on soil and water losses from Mediterranean rainfed agricultural land. *Land Degradation and Development*, **21**, 210–217.

Głąb, T., and Kulig, B., 2008. Effect of mulch and tillage system on soil porosity under wheat (*Triticum aestivum*). *Soil and Tillage Research*, **99**, 169–178.

Hermawan, B., and Bomke, A. A., 1997. Effects of winter cover crops and successive spring tillage on soil aggregation. *Soil and Tillage Research*, **44**, 109–120.

Hillel, D., 1998. *Environmental Soil Physics*. San Diego: Academic.

Horton, R., Bristow, K. L., Kluitenberg, G. J., and Sauer, T. J., 1996. Crop residue effects on surface radiation and energy balance – review. *Theoretical and Applied Climatology*, **54**, 27–37.

Jin, K., Cornelis, W. M., Gabriels, D., Baert, M., Wu, H. J., Schiettecatte, W., Cai, D. X., De Neve, S., Jin, J. Y., Hartmann, R., and Hofman, G., 2009. Residue cover and rainfall intensity effects on runoff soil organic carbon losses. *Catena*, **78**, 81–86.

Jordán, A., Zavala, L. M., and Gil, J., 2010. Effects of mulching on soil physical properties and runoff under semi-arid conditions in southern Spain. *Catena*, **81**, 77–85.

Kay, B. D., and VandenBygaart, A. J., 2002. Conservation tillage and depth stratification of porosity and soil organic matter. *Soil and Tillage Research*, **66**, 107–118.

Lal, R., and Stewart, B. A., 1995. *Soil Management – Experimental Basis for Sustainability and Environmental Quality*. Boca Raton: Lewis. Advances in Soil Science.

Le Bissonnais, Y., and Arrouays, D., 1997. Aggregate stability and assessment of soil crustability and erodibility. II. Application to humic loamy soils with various organic carbon contents. *European Journal of Soil Science*, **48**, 39–48.

Li, F. M., Wang, J., Xu, J. Z., and Xu, H. L., 2004. Productivity and soil response to plastic film mulching durations for spring wheat on entisols in the semiarid Loess Plateau of China. *Soil and Tillage Research*, **78**, 9–20.

Li, L. L., Huang, G. B., Zhang, R. Z., Jin, X. J., Li, G. D., and Chan, K. Y., 2005. Effects of conservation tillage on soil water regimes in rainfed areas. *Acta Ecologica Sinica*, **25**, 2326–2332.

Loch, R. J., and Coughlan, K. J., 1984. Effects of zero tillage and stubble retention on some properties of a cracking clay. *Australian Journal of Soil Research*, **22**, 91–98.
Martens, D. A., and Frankenberger, W. T., 1992. Modification of infiltration rates in an organic-amended irrigated soil. *Agronomy Journal*, **84**, 707–717.
Martínez-Zavala, L., and Jordán, A., 2008. Effect of rock fragment cover on interrill soil erosion from bare soils in Western Andalusia, Spain. *Soil Use and Management*, **24**, 108–117.
Mulumba, L. N., and Lal, R., 2008. Mulching effects on selected soil physical properties. *Soil and Tillage Research*, **98**, 106–111.
Nachtergaele, J., Poesen, J., and van Wesemael, B., 1998. Gravel mulching in vineyards of southern Switzerland. *Soil and Tillage Research*, **46**, 51–59.
Ogbobe, O., Essien, K. S., and Adebayo, A., 1998. A study of biodegradable geotextiles used for erosion control. *Geosynthetics International*, **5**, 545–553.
Oliveira, M. T., and Merwin, I. A., 2001. Soil physical conditions in a New York orchard after eight years under different groundcover management systems. *Plant and Soil*, **234**, 233–237.
Pabin, J., Lipiec, J., Włodek, S., and Biskupski, A., 2003. Effect of different tillage systems and straw management on some physical properties of soil and on the yield of winter rye in monoculture. *International Agrophysics*, **17**, 175–181.
Poesen, J. W. A., and Lavee, H., 1994. Rock fragments in top soils: significance and processes. *Catena*, **23**, 1–28.
Singh, B., Chanasyk, D. S., McGill, W. B., and Nyborg, M. P. K., 1994. Residue and tillage management effects on soil properties of a typic cryoboroll under continuous barley. *Soil and Tillage Research*, **32**, 117–133.
Smika, D. E., and Unger, P. W., 1986. Effect of surface residues on soil water storage. *Advanced Soil Science*, **5**, 111–138.
Sumner, M. E., and Stewart, B. A., 1992. *Soil Crusting – Chemical and Physical Processes*. Boca Raton: Lewis. Advances in Soil Science.
Unger, P. W., Jones, O. R., McClenagan, J. D., and Stewart, B. A., 1998. Aggregation of soil cropped to dryland wheat and grain sorghum. *Soil Science Society of America Journal*, **62**, 1659–1666.
Wan, Y., and El-Swaify, S. A., 1999. Runoff and soil erosion as affected by plastic mulch in a Hawaiian pineapple field. *Soil and Tillage Research*, **52**, 29–35.
Zavala, L. M., Jordán, A., Bellinfante, N., and Gil, J., 2010. Relationships between rock fragment cover and soil hydrological response in a Mediterranean environment. *Soil Science and Plant Nutrition*, **56**, 95–104.
Zhang, S. F., and Ma, T. L., 1994. Yield components and cultivation technology of corn with high grain yield through plastic film cover in West Yellow River area. *Gansu Agricultural Science and Technology*, **1**, 16–17.
Zhang, Z., Zhang, S., Yang, J., and Zhang, J., 2008. Yield, grain quality and water use efficiency of rice under non-flooded mulching cultivation. *Field Crops Research*, **108**, 71–81.
Zhang, S., Lövdahl, L., Grip, H., Tong, Y., Yang, X., and Wang, Q., 2009. Effects of mulching and catch cropping on soil temperature, soil moisture and wheat yield on the Loess Plateau of China. *Soil and Tillage Research*, **102**, 78–86.

Cross-references

Bulk Density of Soils and Impact on their Hydraulic Properties
Desertification: Indicators and Thresholds
Evapotranspiration
Field Water Capacity
Greenhouse Gases Sink in Soils
Plant Roots and Soil Structure
Pore Size Distribution
Root Responses to Soil Physical Limitations
Soil Aggregates, Structure, and Stability
Soil Surface Sealing and Crusting
Temperature Effects in Soil
Tillage Erosion
Water Erosion: Environmental and Economical Hazard

MUNSELL COLOR SYSTEM

A color designation system that specifies the relative degrees of the three simple variables of color: hue, value, and chroma.

Cross-references

Color in Food Evaluation
Color Indices, Relationship with Soil Characteristics

MYCORRHIZAL SYMBIOSIS AND OSMOTIC STRESS

Juan M. Ruiz-Lozano
Departamento de Microbiología del Suelo y Sistemas Simbióticos, Estación Experimental del Zaidín (CSIC), Granada, Andalucía, Spain

Definition

The term Mycorrhiza comes from the Greek words "mycos," meaning fungus and "rhiza," meaning root and applies to a mutualystic symbiosis between roots of most higher plants and a group of soil fungi belonging to the phyla Glomeromycota, Basidiomycota or Ascomycota. By this mutualystic association, the plant receives soil nutrients (especially phosphorus) and water, while the fungus receives a protected ecological niche and plant-derived carbon compounds for its nutrition (Varma, 2008).

The term Osmotic Stress refers to all the environmental conditions that induce a water deficit in the plant tissues, limiting plant growth and development. It generally includes drought, cold and salinity, which directly decreases the plant water content due to an also low soil water content (drought) or which difficult the right uptake of water from soil due to the diminution of soil water potential (cold and salinity).

Eco-physiological studies investigating the role of the mycorrhizal symbiosis against osmotic stresses have demonstrated that the symbiosis often results in altered rates of water movement into, through, and out of the host plants, with consequent effects on tissue hydration and plant physiology (Augé, 2001). Thus, it is accepted that the mycorrhizal symbiosis protects host plants against the detrimental effects of water deficit, and that this protection results from a combination of physical, nutritional and

cellular effects. Several mechanisms have been proposed to explain these effects. The most important are: direct uptake and transfer of water through the fungal hyphae to the host plant, better osmotic adjustment of host plants, enhancement of plant gas exchange through hormonal changes, and protection against the oxidative damage generated by drought. Modulation by the mycorrhizal symbiosis of plant genes involved in the response of plants to water deficit have also been described, with special emphasis on the role of aquaporins (Ruiz-Lozano et al., 2006). Results obtained so far show that the mycorrhizal symbiosis up- or down-regulates aquaporin genes depending on the own intrinsic properties of the osmotic stress. In any case, the induction or inhibition of particular aquaporins by mycorrhizal symbiosis results in a better regulation of plant water status and contribute to the global plant resistance to the stressful conditions, as evidenced by the better growth and water status of mycorrhizal plants under conditions of water deficit (Ruiz-Lozano and Aroca, 2009).

Bibliography

Augé, R. M., 2001. Water relations, drought and vesicular-arbuscular mycorrhizal symbiosis. *Mycorrhiza*, **11**, 3–42.

Ruiz-Lozano, J. M., and Aroca, R., 2009. Modulation of aquaporin genes by the arbuscular mycorrhizal symbiosis in relation to osmotic stress tolerance. In Sechback, J., and Grube, M. (eds.), *Symbiosis and Stress*. Germany: Springer. ISBN 978-90-481-9448-3 in press.

Ruiz-Lozano, J. M., Porcel, R., and Aroca, R., 2006. Does the enhanced tolerance of arbuscular mycorrhizal plants to water deficit involve modulation of drought-induced plant genes? *The New Phytologist*, **171**, 693–698.

Varma, A., 2008. *Mycorrhiza. State of the Art, Genetics and Molecular Biology, Eco-Function, Biotechnology, Eco-Physiology, Structure and Systematics*, 3rd edn. Berlin: Springer.

http://www.springer.com/978-90-481-3584-4

Encyclopedia of Agrophysics
Gliński, J.; Horabik, J.; Lipiec, J. (Eds.)
2011, XLVI, 1028 p. 421 illus., 168 illus. in color.,
Hardcover
ISBN: 978-90-481-3584-4